SOLVENT THERMODYNAMIC, SURFACE ACTIVITY AND COMPRESSIBILITY BEHAVIOR OF FUSED QUARTERNARY AMMONIUM SALTS IN SOLVENTS OF DIFFERENT DIELECTRIC CONSTANTS

A THESIS

SUBMITTED TO THE

UNIVERSITY OF PUNE

FOR THE DEGREE OF

DOCTOR OF PHILOSOPHY

IN

CHEMISTRY

BY

PRAMOD D. SONAWANE

PHYSICAL CHEMISTRY DIVISION

NATIONAL CHEMICAL LABORATORY

PUNE - 411008

DECEMBER 2002

Dedicated to

MOTHER

&

MEMORY OF MY FATHER

ACKNOWLEDGEMENTS

I take this opportunity to express a deep sense of gratitude to my guide Dr. Anil Kumar for his guidance and keen interest during the course of this investigation. He has always insisted on his students being trained well and their efforts presented in a good manner. His immense interest in science and ever- enthusiastic attitude will be cherished by me throughout all walks of my life. His constructive criticism not only motivated me but also instilled a sense of confidence in me. His considerate nature and parental care has helped me in overcoming many hurdles during the course of this investigation. It is his insistence and support that has made me complete this investigation. The present thesis would have not been completed without his positive attitude, unfailing attention, and relentless adherence towards the accomplishment.

My sincere thanks are due to Dr. B.D. Kulkarni, Dy. Director, NCL, Dr. S. S. Tambe, and Mr. Somnath Nandi for their help in analyzing the vapor pressure data using Artificial Neural Network.

I am extremely grateful to Dr. A. S. Inamdar, Principal of my college (Abasaheb Garware College, Pune) and to Dr. H. G. Damle, (the present Head, Chemistry Department) and to Dr. M.V. Paradkar and Dr. R. S. Pande (the former Heads of Chemistry Department) for their kind permission to carry out this investigation and to Dr. M. J. Pujari, Vice-Principal for his moral support.

I also wish to express my sincere gratitude towards my colleagues, Dr. M. S. Kirtiwar, Prof. D. B. Satpute, and Dr. R. C. Chikate, for their constant encouragement, support and co-operation. I also sincerely thank the teaching and non-teaching staff of my college for their co-operation and help.

I sincerely acknowledge my labmates, Sanjay Pawar, Rohini Badarayani, and Suvarna Deshpande for their support, help, and encouragement during my research work. During my work, the friendly and

healthy environment created by my labmates made working in the lab enjoyable.

I express my sincere gratitude towards my friends Sandeep, Sunil, Avinash, Mayur, Ajay, Vijay, Vidnyan, and Pradeep for their constant encouragement help and support that they have given me during the time of crisis and throughout my life.

I wish to express my indebtedness to my family members. My mother and the memories of my father have always guided me to achieve my ambitions. I am obliged to my brother, Nitin and his wife Shubdha, my sisters and brother-in laws for their constant encouragement and support. It is the sacrifice and prayers of this people, which made me to complete this work successfully.

I take this opportunity to extend my heartfelt thanks to my beloved wife, Pramita, for her sacrifice, patience, encouragement, and her moral support during the compilation of this thesis, which made it easy for me to concentrate more on this compilation.

I also wish to thank Mr. T. Koshy and Mr. S. F. Punekar for their day to day help in the office. I also extend my sincere thanks to the library staff of NCL for their co-operation and help during the tenure of this work.

Finally, I acknowledge, the Director, NCL, and the Head, Physical Chemistry Division for allowing me to carry out this work and permitting to use the required facilities.

CERTIFICATE

It is certified that the work incorporated in this thesis "**Solvent Thermodynamic, Surface Activity And Compressibility Behavior Of Fused Quaternary Ammonium Salts In Solvents Of Different Dielectric Constants**" submitted by Mr. Sonawane Pramod Dattatraya, for the degree of **Doctor of Philosophy in Chemistry**, was carried out by the candidate under my supervision, in Physical Chemistry Division, National Chemical Laboratory, Pune, India. Materials obtained from other sources have been duly acknowledged in the thesis.

Dr. Anil Kumar

Research Guide

Candidate's Statement

I hereby declare that the work incorporated in the present thesis "**Solvent Thermodynamic, Surface Activity And Compressibility Behavior Of Fused Quaternary Ammonium Salts In Solvents Of Different Dielectric Constants.**" is original and is not been submitted to any other University / Institution for the award of a Diploma or Degree. I further declare that the results presented in the thesis and considerations made therein contribute in general to the advancement of knowledge in Chemistry and particularly to the field of Thermodynamics.

(P. D. Sonawane)

CONTENTS

1. INTRODUCTION

Studies of solute–solvent interactions in salt solutions have been the subject of considerable interest among the physical chemists for decades. Many researchers have attempted to study ion-solvent interactions in system comprising an electrolyte as a solute in water or non-aqueous solvent in dilute concentrations.

Conventionally two methods can be used to understand ion-solvent interactions in salt solutions: (a) addition of a solid salt in water to reach its saturation limit and (b) addition of a solvent in a saturated salt solution for the purpose of its dilution. Both these methods add to our understanding of ion-solvent interactions in solutions.

However, there exists a class of systems, in which a salt in its molten state exhibits continuous miscibility in a solvent. This situation is different from the conventional method mentioned above. In the conventional method, there is a serious limitation imposed by the restricted solubility of a salt in a particular solvent. If one tries to overcome the solubility limit, the system becomes biphasic and remains no more in a continuous liquid phase.

An alternate method to study the ion-solvent interactions could be to melt a given salt in its solid state and make its solutions just above its melting point. One of the advantages of studying fused salts is that a salt in its molten state when dissolved in a liquid, forms a continuously miscible system with a single liquid phase present throughout, unlike in the earlier case where a biphasic system is observed upon saturation.

The requirement of such continuously miscible system is fulfilled by the use of organic salts, which in general, have low melting points, and therefore becomes very easy to handle. They also offer easy experimental conditions as compared to the inorganic salts, the melting points of which are very high and thus posing difficulties in carrying out the experimental measurements.

Another interesting category of systems of thermodynamic investigation is where salt shows incomplete dissociation at room temperature. An example of such system is acetic acid-water, where acetic acid is not a fused salt but is a polar molecular liquid showing some self-dissociation. In the dilute aqueous range, there is a strong ion-association and no redissociation. This class of system can be recognized as a special system with complex chemical equilibria operating in the liquid phase.

It should be mentioned here that a salt can act as a fully ionized solute in dilute solution but exists as a molecular liquid in the molten state. Some relevant examples in this category are $HClO_4$, HNO_3 and HCl under high pressures.

The plots of Walden products, $\eta\lambda$ for some salt systems are shown in **Figure 1.1** where it is possible to observe the roles of ion pairing, dissociation and molecular association in different systems.

A thorough literature survey has revealed that numerous articles have been published in the salt water systems prepared by the conventional method, it is though, quite surprising that a very few experimental data are available on the fused salts and their solutions in water and organic solvents

in full miscibility range. The classical work on the properties of such system has been done by Kraus and his group[1]. An examination of his experimental data has revealed some interesting features of these systems. They are:

(a) anomalous viscosity behavior

(b) presence of ion-pairing and

(c) short-range interaction forces are seen to be playing a very important and predominant role in determining thermodynamic behavior of these systems.

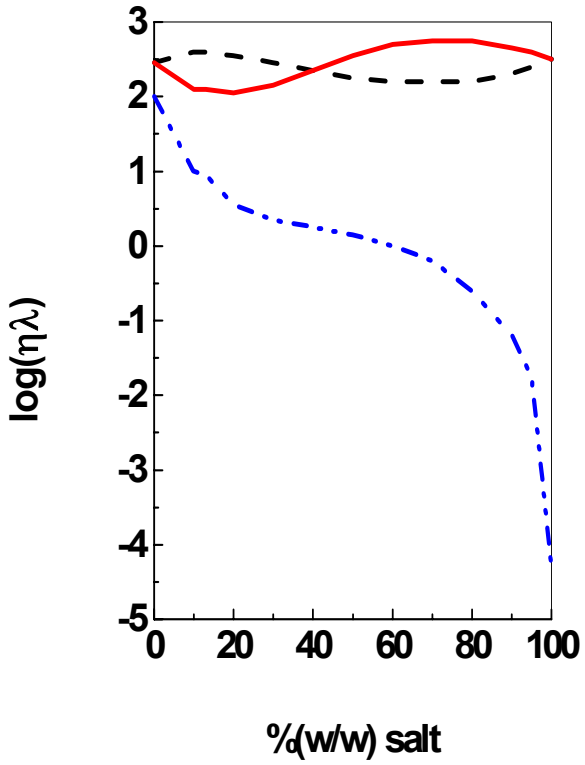

Figure 1.1: Plots of log (Walden product = viscosity x conductance product, $\eta\lambda$) versus solute composition %(w/w); anisole-terabutylammonium picrate (soild line); water-$LiClO_3$ (dashed line); water-acetic acid (dash dot dot dash).

In 1923, Debye and Huckel in their classical work first time studied the ionic interactions taking place in very dilute solutions.[2] The Debye-Huckel (D-H) model describes ion-ion interactions in a electrolytic solution consisting of solvated ion and water molecules. Their approach is based on:

(a) an ion is selected arbitrarily and is called as a central reference ion of a specific charge. This is represented as a point charge,

(b) this central ion is considered to be residing in a dielectric continuum formed by the water molecules and is surrounded by a cloud of smeared charge contributed by all the other ions except the central one,

(c) the electrostatic potential field in the solution is described by the linearized Poisson-Boltzmann equation,

(d) ion-ion interactions other than the electrostatic interactions are ignored, and

(e) since the solvent acts as a dielectric continuum, bulk permittivity of the solvent is considered ignoring the ion-solvent interactions.

Since the development of the D-H theory a large number of experimental data on the thermodynamic and transport properties of aqueous salt solutions have been gathered by researchers with a view to verifying this theory.[3] Application of the D-H model to these data brought out some serious limitations of this theory, which necessitated its modification. Several empirical, semi-empirical and theoretical treatments have been developed over the years. Their applications however, were limited to the systems of moderate concentrations of ionic solutes in aqueous and non-aqueous media.

A few operational approaches have been found successful in describing the thermodynamic properties of nearly concentrated solutions in the last two decades. In the past, many researchers have been attracted to describe the thermodynamic properties of such systems due to the importance of the role that a solvent played on a solute.[3d] In **Table 1.1** are listed several empirical and semi-empirical models that have been used in the past not only to test the D-H theory but also to handle the thermodynamic data of salt solutions of practical applications.

Table 1.1: Summary of the available models to describe equilibrium thermodynamic properties of aqueous electrolytes after the D-H theory (for detailed information, see ref. 3 (d))

Name of the model	No. of parameters	Comments
Guggenheim	One	Mole fraction based equation, later modified on ionic strength scale. Applicable up to 0.1 molar ionic strength.
Bromley	One	Applicable to strong electrolytes showing complete dissociation. Recommending the ion-ion interactions, particularly at high concentrations.
Meissner	One	Based on graphical method. A graph of reduced activity coefficient vs. ionic strength gives a family of curves. The mean activity coefficient can be predicted

		from this plot.
Pitzer	Three	Combination of D-H terms and additional terms are added to account for short – range interaction forces.
Chen	Two	Local composition model based equations accounting for ionic and molecular interactions.
Wilson	Two or Three	Essentially an equation for non-electrolytes. Prediction capability of multicomponent properties without any additional parameter.
NRTL	Two	Local composition is used for representing excess Gibbs energies. The non-randomness factor renders its applicability to a large variety of liquid mixtures.
UNIQUAC	Two	Uses local area fraction as the primary concentration available. Gives good representation of both vapor-liquid and liquid-liquid equilibria. Applicable to liquids participating in hydrogen bonding.
UNIFAC	Two	A group contribution method. Useful when experimental data on activity

	coefficient are not available; can also be used for extrapolation of the existing data.

A careful survey of the above listed models shows that the Pitzer equations have been the most successful in describing the thermodynamic properties like vapor pressures, activity coefficients, enthalpies, heat capacities, volumes, compressibilities and expansibilties of both single and mixed salt solutions up to elevated temperatures and pressures.

A mention should also be made regarding efforts put forward to model salt solutions in non-aqueous solvents and their mixtures. Some noteworthy efforts in this direction are the use of equations basically applicable to non-electrolyte solvents coupled with the Debye-Huckel theory.[4] A summary of the useful models is given below:

Table 1.2: Useful models to analyze the salt effect on thermodynamic activities. (for detailed information, see ref. 4)

Name of the Model	**Comments**
Long and McDevit	The ratio of the relative volatilities of a binary system with and without salt related to the salt concentration.
Furter and Johnson	The equation derived from the difference in effects of the salt on the chemical potentials of the two volatile components.
Special binary	Proposed by Jaques and Furter. In this pseudo-binary approach

approach	two volatile solvents and a salt treated as special binaries rather than as ternaries.
Vapor pressure depression model of Lu	An empirical method based on the information of the depression of vapor pressure by salt on each solvent and used to calculate the salt effect. Applicable to systems showing small deviations from ideality.
Ohe model	Based on the preferential solvation method proposed by Gross and Halpern, who assumed that addition of salt to solvent mixture reduces the activity of one component. Application of this model to experimental data showed an error of 11% in the vapor phase composition.
Schmitt-Vogelpohl model	A pseudo binary approach, based on the assumption that a salt forms a pseudo binary complex preferentially with the more volatile component. The degree of complexation is proportional to the salt solubilities in the pure solvent. Binary experimental data used for the representation of ternary data. The model fails in the dilute range.
Modified Schmitt-Vogelpohl model	Modified model of Schmitt-Vogelpohl by incorporating the concept of preferential solvation. Formation of a complex depends on the solubility of a salt and that a salt will preferentially associate with the component in which it is more soluble. The incorporation of the concept of preferential solvation increased the predictive capability of the model.

Kumar model	Based on pseudo complex formation. Used the dielectric constant data of pure solvents and their mixtures to account for the complex formation by using a new term inverse relative solubility coefficient. The mole fraction of the pseudocomplex directly related to the activity coefficient of a more volatile component with which the salt is complexed. A fascinating feature of this model is that the parameters can be calculated *a priori*. Several systems analyzed by this method showed that the vapor-phase composition, pressure, and temperature could be estimated to $\pm$ 0.015, $\pm$ 0.76 kPa and $\pm$ 0.30 K, respectively
Schuberth model	Expressions based on excess free energy function. Margules equation was used. One ternary and six binary parameters are used.
Hala model	Combines the 3–suffix Margules equation with one ternary parameter.
Boone model	Based on the concept of the pseudobinary approach. Wilson equation used to calculate activity coefficients. Parameters for the Wilson equation determined from infinite dilution activity coefficients. A good degree of success on five salt systems in water-methanol observed.
Bekerman and Tassios model	NRTL equation based model. Binary data can be estimated successfully. For ternary systems, the estimates are less reliable.

Rastogi model	Excess free energy is expressed as the combination of extended Debye-Huckel equation and NRTL equation. Exhaustive testing of this model is required.
Rousseau and Boone model	Modified form of Boone model. Wilson equation is replaced by the UNIQUAC equation. Binary solvent-salt system is treated as psuedobinary mixtures. The average deviation was 0.5 K and 0.011 in the temperature and vapor phase composition for 7 systems.
Glugla and Sax model	UNIQUAC equation based model. Extended the correlation for multicomponent solutions. Equation was found to be successful up to salt concentration < 2 M. Serious predictive problems for acetone-methanol-LiCl system is observed.
Sander model	Combination of Debye-Huckel term and a modified UNIQUAC equation with concentration dependent parameters. The parameters are ion-specific. No ternary parameters are required. Large deviations in the activity coefficients are noted. The vapor phase composition can be estimated to 0.012.
Dahl and Macedo model	A modified Huron-Vidal second order model used to describe the salt effect on VLE. A group combination model combining Soave-Redlich-Kwong equation of state with a modified UNIFAC model. The salt is assumed to be a single component and not dissociated into ions. Excellent predictions of the salt effect on VLE are obtained.

Kick model	Combination of modified Debye-Huckel term as proposed by Macedo et.al. and concentration independent UNIFAC terms. Model is capable of representing VLE for solvent-water-salt mixtures with accuracy of around 9% for the total pressure and of 4% vapor-phase composition.

A class of system, which has not attracted attention of researchers, is the system comprising salt and solvent both present in the liquid phase. Since both the components are in the liquid state, it is possible to form a system with a single liquid phase existing throughout the composition range. Such systems primarily comprise salts of organic compounds and a few nitrates in non-aqueous solvent and water. In a broader sense, salt may or may not be fully ionized in the solvent depending upon the relative permittivity of the solvent. Such territory of the systems is of considerable theoretical interest, particularly, if the relative permittivity of the solvent is too low, in which the process of ion pairing occurs. A full miscibility still exists in the range starting from an organic liquid to organic ionic melt. A systematic investigation of these systems is expected to be useful in obtaining deeper understanding of the interactions present between a pure organic liquid and a fused salt.

Viscosity and conductance are important tools to identify the characteristics of such fused salt in solvent systems. In the case of an organic salt dissolved in organic solvent, ion pairing is identified by the conductance, viscosity and the walden product ($\eta\lambda$). A survey of literature shows

measurement of walden product of such systems is carried out by many researchers.[5] They studied the $\eta\lambda$ for the aqueous $LiNO_3$ and $LiClO_3$ systems. The dilute aqueous solutions of these system showed a reduction in conductance from its limiting value as explained by Debye, Huckel and Onsager that the reduction in conductance is due to the electrostatic effect.[2,6] Application of the theoretical equations for a fully ionized solute to these system was found to be valid. This led Kraus to believe that complete ionization of salt at higher concentration takes place.

Conductance measurements of organic systems over the full concentration range from dilute electrolyte solution to fused salt have also been reported in the literature.[7,8] Kraus studied the conductance of tetraisoamylammonium thiocyanate in benzene at 298 K from dilute to concentrated solutions.[1e] Seward measured the conductance of tetra-n-butylammonium picrate in 1-butanol, anisole, nitrobenzene and ethyl carbonate from dilute solution to fused salt.[8] These data showed that the equivalent conductance λ had a minimum or maximum when plotted against the salt concentration in solvents of low relative permittivities, whereas in the case of polar solvents, λ is seen to be linearly decreasing with concentration. The walden product usually shows only a minimum. The concentration at which the minimum occurs increases with increasing relative permittivity. Similar behavior is also seen in the concentrated aqueous solutions.[9-12]

Seward also showed that the walden product at infinite dilution ($\eta_0\lambda_0$) was approximately equal to that of the molten salt, $(\eta\lambda)_0$, which prompted

Kraus to state that tetraisoamylammonmium picrate was completely ionized in its molten state.[7,8,13] Further Kenausis, Evers and Kraus (KEK) hypothesized that the $\eta\lambda$ / $(\eta\lambda)_0$ values in the concentrated region might be the high-concentration analog of the Arrhenius fraction of dissociation α and termed $\eta\lambda/ (\eta\lambda)_0 = F_i$, the ion fraction in concentrated solutions.[14,15] Kenausis, Evers and Kraus also proposed an equilibrium mechanism between ions and ion-pairs. The hypothesis and the proposed mechanism were challenged by Longo et.al. who actually observed a maximum in the $\eta\lambda$ product for tetraisoamylammonium thiocyanate in nitrobenzene.[16] This indicates that the KEK hypothesis of ion fraction and ion-pair equilibrium must be reexamined particularly in polar solvents.

A fascinating situation has been witnessed in the viscosity behavior of these systems. The increase in $\eta\lambda$ value near fused salt is striking. Addition of little water to the fused salt, the viscosity decreases faster than the increase in conductance. This is the most significant observation made so far and requires a thorough investigation. The viscosity of the solution reduces dramatically about 100 times, when a small amount of solvent is added to the fused salt. This anomalous behavior of viscosity cannot be accounted for by the equations representing normal viscosity behavior. Furthermore, no theoretical analysis exists for such a drop in viscosity. Experimental data for other system in this laboratory have confirmed this observation.[17] A modified 3- parameters equation based upon the expression of Mahiuddin and Ismail

was been applied successfully to account for the viscosity of such system.[18] The viscosity data were fitted to within 1.6%.

Another important property that can give us some structural information on the solute- solvent interactions is surface tension of the system. No peculiar behavior is observed in the surface tension data of these systems. However, the data on surface tension at different temperature is useful in calculating the entropy and enthalpy of the surface. The activity of solvent in the surface phase is calculated using vapor pressure data. A literature scan shows that there exists a good number of reliable surface tension data in aqueous phase. The work from the schools of Campbell and of Abraham deserves special mention here.[19,20] The experimental data collected by Campbell and coworkers in the aqueous fused salts and their mixtures are of high accuracy and reproducible to $\pm$ 0.5 x 10^{-3} N $m.^{-1}$

The school of Abraham has enormously contributed to the determination of surface tension of pure and mixed fused salts in aqueous systems. The reproducibility of surface tension determination was better than 1%. These authors have also computed the Gibbs - adsorption parameter with the help of solvent activities. The Gibbs adsorption parameter in turn has been employed to estimate number of solvent molecules adsorbed at the surface of fused salts.

Thermodynamics of a system can be discussed in terms of vapor pressures and activity coefficients. The plots of vapor pressure against the salt mole fraction of such systems are analogous to those observed for the

solutions of non-electrolytes. Strong positive and negative deviations from the Raoult's law have been observed. Despite of the simple nature of some systems, it has been possible to take into account the non-ideality by simple equations like van Laar, Margules etc.[21,22] Literature survey shows that equations comprising long-range and short-range combinations can be used to account for the shapes of the curve obtained by plotting solvent activity, a as a function of mole fraction. Another important method based on the Brunauer-Emmett-Teller (BET) adsorption isotherm was proposed by Stokes and Robinson in the literature.[23] An application of this model shows that it fails to reproduce the solvent activity above the mole fraction of solvent = 0.65. Unfortunately the Stokes- Robinson method fails in the high concentrations even in the simple salt systems. In their method, a Debye – Huckel term is combined with the hydration term. The hydration term is independent of concentration of salt and thus fails to account for thermodynamic changes taking place in the high salt concentrations. It is noted that many salts like quaternary ammonium salts are generally fully ionized in several organic solvents, but some of them do exhibit strong ion-pairing in the dilute region.[1c,7,8, 17,24-26] Because of the importance of volumetric properties in recognizing the solute-solute, solute-solvent and solvent-solvent interactions, it was thought worthwhile to explore this possibility to further our understanding in the case of the fused salt solutions. Unfortunately, systematic data on volumetric properties of these systems are not reported in the literature. Very recently some studies have been carried out for the fused

sodium thiocyanate and lithium nitrate in aqueous methanol and the isentropic compressibility calculated therefrom.[27,28] The results are explained in terms of hydration phenomena. In an earlier paper, Rahman and Mahiuddin have discussed the temperature and concentration dependence of the sound velocity in aqueous sodium nitrate and sodium thiosulphate solutions.[29]

A careful survey of the above-described literature indicates that both the experimental and modeling studies are required in this area. The main theme of this dissertation is therefore to delineate the nature and magnitude of ion- solvent and ion-ion interactions in these fused salt solutions made in organic solvents with a single liquid phase. The objectives of this dissertation are described in the next chapter.

Literature cited:

1. a) Kraus, C. A.; Fuoss, R. M. “Properties of Electrolytic Solutions. 1. Conductance as Influenced by the Dielectric Constant of the Solvent Medium.” *J. Am. Chem. Soc*. **1933**, 55, 21.

b) Fuoss, R. M.; Kraus, C. A. “Properties of Electrolytic Solutions. IX. Conductance of Some Salts in Benzene.” *J. Am. Chem. Soc*. **1933**, 55, 3614.

c) Bien, G. S.; Kraus, C. A.; Fuoss, R. M. “Properties of Electrolytic Solutions. XII. The Influence of Temperature on the Conductance of Electrolytes in Anisole.” *J. Am. Chem. Soc*. **1934**, 56, 1860.

d) Kraus, C. A. “The Present State of Electrolyte Problem.” *J. Chem. Educ*. **1958**, 35, 324.

e) Strong, L. E.; Kraus, C. A. “Properties of Electrolytic Solutions. XLV. Conductance of Some Salts in Benzene at Higher Concentrations.” *J. Am. Chem. Soc*. **1950**, 72, 166.

2. Debye, P.; Huckel, E. “ Zur Theorie des Elektrolyte.” *Phys. Z*. **1923**, 24, 185.

3. For summary see: (a) Robinson, R. A.; Stokes, R. H. “*Electrolyte Solutions*” 2nd ed. **1965**, Butterworths, London.

b) Harned, H. S.; Owen, B. B. “*The physical Chemistry of Electrolytic Solution*, **1943**, Reinhold, New York.

c) Horvath, A. L. “*Handbook of Aqueous Electrolyte Solution*” **1985**, John Wiley, New York.

d) Zemaitis, J. F. Jr.; Clark, D. M.; Rafal, M.; Scrivner, N. C. "*Handbook of Aqueous Electrolyte Thermodynamics, American Institute of Chemical Engineers*. **1986**, New York.

4. For example see: Kumar, A. "Salt Effect on Vapor – Liquid Equilibria: A Review of Correlations and Predictive Models." *Separation Science and Technology*. **1993**, 28, 1799.
5. Campbell, A. N.; Patterson, W. G. "The Conductance of Aqueous Solutions of Lithium Chlorate at 25^0C and 131.8^0C." *Can. J. Chem*. **1958**, 36, 1004.
6. Onsager, L. " The Theory of Electrolytes." *Phys. Z*. **1927**, 28, 27.
7. Seward, R. P. "Electrical Conductance and Viscosity in the System Tetra-n-butylammonium Picrate- n-Butyl Alcohol at 91^0C." *J. Am. Chem. Soc*. **1951**, 73, 515.
8. Seward, R. P. "The Electrical Conductance and Viscosity of Solutions of Tetra-n-butylammonium Picrate in Anisole, Nitrobenzene and Ethylene Carbonate." *J. Phys. Chem*. **1958**, 62, 758.
9. Campbell, A. N.; Gray, A. P.; Kartzmark, E. M. "Conductances, Densities, and Fluidities of Solutions of Silver Nitrate and of Ammonium Nitrate 35^0C." *Can. J. Chem*. **1953**, 31, 617.
10. Seward, R. P. "The Conductance and Viscosity of Highly concentrated Aqueous Solutions of Hydrazinium Chloride and Hydrazinium Nitrate." *J. Am. Chem. Soc*. **1955**, 77, 905.

11. Chambers, J. F.; Stokes, J. M.; Stokes, R. H.; Seward, R. P. “Conductances of Concentrated Sodium and Potassium Chloride Solutions at 25^0C.” *J. Phys. Chem*. **1956**, 60, 985.
12. Miller, M. L. “Concentrated Salt Solutions III. Electrical Conductance of Solutions of Sodium Thiocyanate, Sodium Iodide and Sodium Perchlorate.” *J. Phys. Chem*., **1956**, 60, 189.
13. Kraus, C. A. “Electrolytes from Dilute Solutions to Fused Salt.” *J. Phys. Chem*. **1954**, 58, 673.
14. Kenausis, L. C.; Evers, E. C.; Kraus, C. A. “Mechanisms underlying the Equilibrium Reactions between Ions and Ion-Pairs in Solutions of Electrolytes. I. Solutions in p-Xylene at 52^0C and Benzene at 25^0C.” *Proc. Nat. Acad. Sci., U. S*., **1962**, 48, 121.
15. Kenausis, L. C.; Evers, E. C.; Kraus, C. A. “Mechanisms underlying the Equilibrium Reactions between Ions and Ion-Pairs in Solutions of Electrolytes, II. The Effect of Temperature.” *Proc. Nat. Acad. Sci., U. S.* **1963**, 49, 141.
16. Longo, F. R.; Daum, P. H.; Chapman, R. Thomas, G.; “The Anomalous Behavior of $\eta\lambda$ Product in Solution of Tetra-n-pentylammonium Thiocyanate in Nitrobenzene at 52^0C.” *J. Phys. Chem*. **1967**, 71, 2755.
17. Kumar, A. “Surface Tension, Viscosity, Vapor Pressure, Density, and Sound Velocity for a System Miscible Continuously from a Pure Fused Electrolyte to a Nonaqueous Liquid With a Low Dielectric Constant:

Anisole with Tetra-n-butylammonium Picrate." *J. Am. Chem. Soc*. **1993**, 115, 9243.

18. Mahiuddin, S.; Ismail, K. "Concentration Dependance of the Viscosity of Aqueous Electrolytes. A Probe into Higher Concentration." *J. Phys. Chem.* **1983**, 87, 5241.
19. Campbell, A. N.; Williams, D. F. " Studies on the Thermodynamics and Conductances of Molten Salts and their Mixtures. Part III. Densities, Molar Volumes, Viscosities and Surface tensions of Molten Lithium Chlorate, with Small Additions of Water, and other Substances." *Can. J. Chem*. **1964**, 42, 1778.
20. Abraham, M.; Abraham, M-C.; Ziogas, I. "Surface Tension of Liquids From Molten Nitrate Mixtures to Water." *J. Am. Chem. Soc*., **1991**, 113, 8583 and references cited therein.
21. van Laar, J. J. "Sechs Vortrage Uber Das Thermodynamische Potential." *Vieweg-Verlag*, 1906.

    See also *Z. Phys. Chem*. (Leipzig) **1919**, 72, 723.
22. Prausnitz, J. M. "*Molecular Thermodynamics of Fluid-Phase Equilibria*." **1969**, Prentice-Hall, Englewoods Cliffs. N. J.; and the literature cited therein.
23. Stokes, R. H.; Robinson, R. A. "Ionic Hydration and Activity in Electrolyte Solutions." *J. Am. Chem. Soc*. **1948**, 70, 1870.
24. Yao, N. P.; Bennion, D. N. "Transport Behavior in Dimethyl Sulfoxide. 111. Conductance-Viscosity Behavior of Tetra-n-amylammonium Thiocyanate

from Infinite Dilution to molten Salt at 55^0C." *J. Phys. Chem.* **1971**, 75, 3586.

25. Davies, C. W.; "*Ion Association*". Chapter 10, **1962**, Butterworths, London.
26. Pitzer, K S.; Simonson, J. M. "Ion-Pairing in a System Continuously Miscible from the Fused Salt to Dilute Solution." *J. Am. Chem. Soc*. **1984**, 106, 1973.
27. Rahman, N.; Dass, N. N.; Mahiuddin, S. " Isentropic Compressibility of Aqueous and Methanolic Sodium Thiocyanate Solutions." *J. Chem. Eng. Data*. **1999**, 44, 465.
28. Rahman, N.; Mahiuddin, S.; Dass, N. N. "Speed of Sound in Aqueous and Methanolic Lithium Nitrate Solutions." *J. Chem. Eng. Data*. **1999**, 44, 473.
29. Rahman, N.; Mahiuddin, S. " Concentration and Temperature Dependence of Ultrasonic Velocity and Isentropic Compressibility in Aqueous Sodium Nitrate and Sodium Thiosulphate Solutions." *J. Chem. Soc. Faraday Trans*. **1997**, 93, 2053.

2. OBJECTIVES

From the contents described in the preceding chapter, it is apparent that three zones i.e. the solvent-rich, solvent poor and solute-solvent middle segments require systematic investigation for the ion-solvent and ion-ion interactions in the fused salts completely miscible in organic solvents. This dissertation therefore is aimed to resolve the following issues:

(1) What is the thermodynamic behavior of a fused salt from its highly concentrated solutions to very dilute solutions?

(2) To propose a thermodynamic model for describing vapor pressure of a solvent in the fused salt solution showing positive, negative and zero deviations from the Raoult's law.

(3) Can Artificial Neural Network be applicable to such complicated systems where many simple models fail to rationalize the vapor pressure data?

(4) How can one predict the surface tension-composition correlation for solution of fused salt in solvent? There are no simple methods to analyse the surface tension data of organic fused salt solutions.

(5) To measure and model volumetric properties of a fused salt in different solvents of varying relative permittivity in a single liquid phase.

In order to address the above objectives, the systems chosen for studying the fused salt solutions are: a quaternary ammonium salt, tetra-n-butylammonium picrate (abbreviated hence forth as TP) (m.p.= 362.5 K) with solvents of varying relative permittivity viz. anisole, (ε = 3.60), 1-butanol (ε = 9.40) and nitrobenzene (ε = 24.80). Several properties have been studied for

these systems and analyzed in terms of different models for obtaining the interaction parameters for vapor pressure, volume, compressibility and thermal expansion. The non-idealities noted in these systems have been discussed in terms of ion-ion and ion-solvent interaction parameters.

3. EXPERIMENTAL SECTION:

3.1 Materials: A summary of chemicals used during the experiments is given below:

Chemicals	Assay	Impurities	Supplier
tetra-n- butyl ammonium hydroxide 40% and 20% (v/v) solution in water	Extrapure	(Cl = 0.02%)	Aldrich Chem. Co.
picric acid, saturated aqueous solutions	Synthesis grade	-	Loba Chemie.
anisole, anhydrous	ACS reagent, 99.7%,	Water $\leq$ 0.005 Evaporation residue < 0.0003%	Aldrich Chem. Co.
1- butanol	A.R. grade 99.5%	passes test for water insoluble matter, acidity = 0.003%, non-volatile matter = 0.003% , water = 0.1%	S.D. Fine-Chem Ltd.
nitrobenzene	ACS reagent, 99.0%,	Cl^- $\leq$ 5 ppm Water soluble titr. acid $\leq$ 0.0005 meq / g	Aldrich Chem. Co.

3.2 Synthesis of tetra-n-butylammonium picrate:

Tetra-n-butylammonium picrate (TP) was synthesized in our laboratory by very slow neutralization of picric acid with tetra-n-butylammonium hydroxide solution (4% aqueous solution, v / v TBAH).[1-4] The aqueous solution of TBAH was added in drops at regular intervals to the reaction flask containing picric acid. The neutralization was monitored by checking the pH of the test sample by graded pH paper. A complete neutralization of the acid was assumed when the pH switched over from acidic to basic side as indicated by the pH paper. The precipitate was filtered after allowing it to settle for a couple of days. During filtration care was taken to wash the precipitate with water in order to remove the excess of TBAH. The salt thus formed was collected and recrystallized three times using A. R grade methanol. The pure crystals obtained after the third crystallization were filtered over a 4A sintered disc funnel, collected and dried under vacuum at 80^0C and were stored over silica in a desiccator. The melting point of the dried salt was noted to be 362.5 ± 1 K from batch to batch. Prior to the making of solutions the salt was again dried for 1/2 h under vacuum to ensure the removal of moisture if any, absorbed by the salt on storage.

3.3 Composition of solutions:

All the solutions were made on the weight basis. The samples were weighed on a CONTECH CB-series electronic balance with an accuracy of ±0.001 g. The mole fractions of the components calculated from these weights were accurate to ±0.001. The assumed molar masses for TP, anisole,

1-butanol and nitrobenzene were 470.60, 108.14, 74.12 and 123.11 g mol^{-1}, respectively.

3.4 Measurement of density:

Densities were measured with a pycnometer having a volume of 50 x 10^{-6} m^3 with a precision of ±0.05%. The pycometer was calibrated against densities of aniline, water, and aqueous sodium chloride with an accuracy of 0.1%.[5,6]

3.5 Measurement of speed of sound:

There are, in general, two methods for measuring the speed of ultrasonic waves through a liquid (i) diffraction method, and (ii) interference method.

3.5.1 Diffraction method:

This method, was first suggested by Brillouin, and later developed by Debye and Sears.[7,8] It is based on the principle that when an ultrasonic wave passes through a liquid, it gives rise to a periodic variation of density in a liquid and the structure of the liquid thus agitated can be simulated to that of a light diffraction grating. If a beam of monochromatic light is made incident on such simulated grating, a diffraction pattern must be observed in the transmitted light. However, the complete theory of this method present many difficulties.

3.5.2 Interference method:

This method was developed by Pierce.[9] The schematic diagram of the apparatus is shown in **Figure 3.1**. The source of ultrasonic waves is a quartz

crystal excited by a radio frequency oscillator. The dimension of the crystal plate is large as compared to the wavelength of the sound in the liquid. The crystal plate is placed at the bottom of the metallic container either of rectangular or clyindrical cross-section. At the end of the container a metallic piston moves with the help of micrometer screw. Due to reflection from this reflector a system of stationary waves is formed with nodes and antinodes. The prime criterion for the experiment is that the two surfaces, that of the reflector and of the crystal should be optically parallel to each other and the parallelism should be within 1 or 2 fringe widths with a monochromatic source of light. The reflected waves react on the quartz source and thereby change the plate current or the tank current of the oscillator supplying the voltage to the quartz crystal. The plate current or the tank current depends upon the amplitude of vibration of the crystal. Depending on the position of the reflector, the reflected vibrations will arrive at the crystal. If the vibrations after reflections are out of phase it will damp the vibrations of the crystal or if the reflections are in phase it will augment the vibrations of the crystal. This will be seen in the change of either plate or tank current of the oscillator. Consequently, the plate or tank current will go through a cycle of values as the reflector plate is moved through half a wavelength. The speed of sound can be determined by two ways: i) by plotting a graph between the change of plate or tank current and the position of the piston as noted in the micrometer screw. From the positions of successive maxima or minima, the value of $\lambda/2$ can be obtained and the speed ν determined from the relation $\nu = f \lambda$ where f

is the frequency of the wave or ii) by taking the average of the difference between two successive readings as the position of successive maxima or minima then determining the speed by the same equations as discussed above.

The speeds of sound were measured with a single – crystal interferometer supplied by M/S Mittal Enterprises. The calibration of the interferometer was done against the literature data on water and aqueous sodium chloride solutions.[10-12] A 4 MHz cell was used throughout for the measurement of speed of sound. The cell was filled with the desired solution and was kept for ½ h to equilibriate at constant temperature. Once the systems attained equilibrium, the cell was mounted on the base plate and the system was closed by placing the piston over the cell. Readings were taken by rotating the micrometer screw in one direction i.e anticlockwise direction. The average of ten or eleven readings was used to calculate the speeds of sound. The accuracy of the instrument as obtained by the calibration is ± 0.05%. The speed of sound was precise to ±0.02%.

3.6 Measurement of Vapor Pressures

Solutions were prepared by dissolving measured amounts of the dry picrate salt, with heating when necessary to insure complete dissolution, in sufficient solvent to result in a solution of approximately the composition desired. The solution was transferred into a Pyrex sample cell, degassed, and then was employed for vapor pressure measurement and final composition determination were carried out.

The following experimental assembly was set up for collecting the required data.

3.6.1. Apparatus:

The apparatus used in these experiments was designed to allow measurement of vapor pressure to 13 bars at temperatures to 373 K. The apparatus is represented schematically in **Figure 3.2**. Vapor pressures over the solutions were measured directly using a thermostatted capacitance manometer differential pressure transducer in conjunction with temperature control and signal conditioning electronics. The pressure transducer and the inlet line from the sample cell thermostat were maintained at approximately ten degrees above the temperature of the sample cell thermostat to prevent solvent condensation.

The samples were contained in Pyrex cells as illustrated in **Figure 3.3**. These cells included a main sample chamber of approximately 10 cm^3 internal volume and a small overflow trap to protect the system from inadvertent bumping of the hot solution. Solutions were stirred magnetically using a teflon coated stirring bar in the main sample chamber. Low vapor pressure epoxy was used as a glass-to-metal seal to connect the sample cell to a stainless steel manifold assembly through a Nupro stainless steel bellows-seal packless valve. The total dead volume over the solution was less than 15 cm^3.

A Pyrex bulb containing pure solvent was attached to the manifold through another bellows valve to allow pre-pressurization of the system dead volume to approximately the expected vapor pressure of the experimental

solution, both to minimize the solution composition change due to evaporation into the evacuated deal volume and to guard against flashing of the salt solution into the manifold system on opening of the sample cell.

A third bellows valve on the manifold system served to connect the assembly to a vacuum line. This line was used to degas the solutions to be studied and the pre-pressurizing solvent, and to reset zero on the differential pressure transducer before each run. The reference side of the transducer was maintained under vacuum, insuring that all pressures measured were absolute vapor pressures relative to vacuum reference.

The valve manifold assembly, including both the sample and pre-pressurization cells, was maintained at the temperature desired in a double walled cylindrical aluminium stirred air-oven, using a contact-thermometer temperature regulator. The oven was wrapped with a three inch layer of spun fiberglass insulation. The sample cell only was immersed in a stirred mineral oil bath inside this oven to smooth out short term temperature variations.

The temperature of the oil bath was measured using a 1000 ohm platinum resistance thermometer in a four-lead resistance measuring circuit, which included a potentiometer in conjunction with a Resistance Thermometer Potentiometer Adapter. A microvolt amplifier and chart recorder tandem served as the potentiometer balance detector. The temperature measurement system was calibrated against a platinum resistance temperature standard Reproduction of temperature values though the calibration process was better than 0.01 K.

For experiments at 373 K, in which all vapor pressures measured were below ambient, the less complicated apparatus diagrammed in **Figure 3.4** was used. A 10 cm^3 round bottom Pyrex flask with ground glass fitting was used as the sample cell. The sample cell and a small (ca. 2 cm^3) Pyrex pre-pressurization bulb were attached to a ground-glass three-way stopcock through 7 mm O.D. Pyrex tubing. This assembly was connected to the capacitance manometer through a length of 7 mm glass tubing and a short length of 0.125 in O.D. stainless steel tubing connected by an epoxy glass-to-metal seal. The system was connected to a vacuum line through a two-way ground-glass stopcock to allow for system degassing and re-zeroing of the pressure transducer.

The system was thermostatted in a 2 L stirred mineral oil bath held at the desired temperature. The portion of the manometer inlet line not immersed in the oil bath and the pressure transducer were maintained at a temperature approximately 5^o above that of the oil bath. The temperature of the sample cell bath was measured using a four-lead platinum resistance thermometer circuit as described above.

3.6.2 Measurements:

Vapor pressures of solutions were measured by a differential capacitance manometer.[26] The reference side of the manometer was kept evacuated, so that all the pressures measured were absolute nitrobenzene vapor pressures. Pyrex cells containing solutions were maintained approximately at 373K using an oil bath. Repeated evacuation of the sample cell vapor space was done in order to degas the solutions. The compositions

of the solutions were determined by weight after each experiment. Each experiment was repeated twice and an average was treated as a final value.

In view of our primary interest in the organic components, we measured the vapor pressure of nitrobenzene + tetra-n–butylammonium picrate (TP) at 373 K. Note that TP is in molten state at 373 K and forms a complete miscible solution with nitrobenzene at this temperature.

In general, the accuracy of the vapor pressure measurement based upon the 1- butanol- TP system was better than 1%. The vapor pressure were, however precise to ± 0.3%. The uncertainty in composition was estimated to be ± 0.0005.

3.6.3 Maintenance of Temperature:

The temperature for the measurements of vapor pressure was kept constant to within ± 0.1 K, by a temperature bath supplied by Tronac.

To maintain the temperature for the measurement of speeds of sound at different temperature a Julabo F 25 water bath, supplied by Julabo, Germany was used. Distilled water was used as the circulating fluid between the temperature range 273 to 303 K. A 1:1 mixture of distilled water and ethylene glycol was used as the circulating liquid above 303 K. Addition of ethylene glycol prevents the loss of water by evaporation. Temperature variation from 303 to 373 K can be very easily had by using this mixture of water and ethylene glycol. Enough care was taken to prevent the loss of heat from the tubing's connecting the bath and the cell containing the solution the speed of sound was to be determined, by proper insulation of the tubings. The

temperature was maintained constant to ± 0.01 K by the temperature bath for the volumetric measurements.

Literature cited:

1. Narayanan, T. P.; Pitzer, K. S. "Critical Behavior of Ionic Fluids" *J. Phys. Chem*. **1994**, 98, 9170.
2. Narayanan, T. P.; Pitzer, K. S. "Mean-Field to Ising Crossover in Ionic Fluids." *Phys. Rev. Lett*. **1994**, 73, 3002.
3. Narayanan, T. P.; Pitzer, K. S. "Critical Phenomena in Ionic Fluids: A Systematic Investigation of Cross Over Behavior. J. Chem. Phys. **1995**, 102, 8118.
4. Narayanan, T. P.; Pitzer, K. S. "The Liquid-Liquid Phase transition in Ionic solutions: coexistence curves of tetra-n-butylammonium picrate in alkyl alcohols. *J. Chem. Phys*. **1999**, 110, 3085.
5. Timmermans, J. The Physicochemical Constants of Binary Systems in Concentrated Solutions. 1959. Interscience. New York.
6. Kestin, J.; Khalifa,H. E.; Abe, Y.; Grimes, C. E.; Sookiaian, H.; Wakeham, W. A. "Effect of Pressure on the Viscosity of Aqueous NaCl Solutions in the Temperature Range 20-150 ^{0}C. *J. Chem. Eng. Data*., **1978**, 23, 328.
7. Brillouin, L. "Diffusion of Light and X-rays by a Transparent Body. The Influence of Thermal Agitation." *Ann. Phys*. **1922**, 17, 88.
8. Debye, P.; Sears, F. W. " On the Scattering of Light By Supersonic Waves." *Proc. Nat. Acad. Sci.* U. S **1932**, 18, 410.
9. Pierce, G. W. *Proc. Am. Acad. Sci*. **1925**, 60, 271.
10. Gucker, F. T.; Chernik, C. L.; Roy-Chowdhary. P. "A Frequency Modulated Ultrasonic Interferometer: Adiabatic Compressibilities of

Aqueous solutions of NaCl and KCl at 25^0C" *Proc. Nat. Acad. Sci*. U. S **1966**, 55, 12.

11. Gucker, F. T.; Stubley, D.; Hill, D. J. "The isentropic Compressibilities of Aqueous Solutions of Some Alkali Halides at 298.15 K." *J. Chem. Thermodyn*. **1975**, 7, 865.
12. Millero, F. J.; Ricco, J.; Schreiber, D. R. "PVT Properties of Concentrated Aqueous Electrolytes. II. Compressibilities and Apparent Molar Compressibilities of Aqueous NaCl, Na_2SO_4, $MgCl_2$, and $MgSO_4$ from Dilute Solution to Saturation and from 0 to 50^0C." *J. Soln. Chem.*, **1982**, 11, 671.

4. Vapor Pressure and Surface Tension

A. VAPOR PRESSURE

4A.1 Background:

The accurate measurement of vapor pressure of a system enables us to calculate the solvent activity and other thermodynamic quantities. In the system of our interest with a fused salt and organic solvent with continuous miscibility (e.g. anisole + TP) a plot of solvent activity, a_1 against the solvent mole fraction, x_1, of this system and of various other systems reported in the literature, like aqueous and non-aqueous electrolytes, reveals that the curves obtained are very similar to those obtained for non-electrolyte mixtures.[1,2] In these systems positive and negative deviations from the Raoult's law are observed. In view of the analogy in the shapes of the vapor pressure curves with those generally found in non-electrolytic mixtures, it seems worthwhile to explore the possibility of treating these systems with the simple expressions used for the treatment of non-electrolytes. These equations are briefly reviewed here in the present context. One of the simplest and the most successful model is that proposed by van Laar and has been used widely since.[3] The details of this model as well as other related equations along with other important contributions of Margules, Hildebrand, Scatchard, Guggenheim etc. are discussed by Prausnitz.[4]

According to the van Laar theory the solvent activity is given by a simple equation:

$$\ln a_1 = \ln x_1 + w_1 z_2^2 \qquad (1)$$

where, $z_1 = n_1 / [n_1 + \nu n_2 (b_2 / b_1)]$, $z_2 = 1 - z_1$, and $w_2 = (b_2 / b_1) w_1$. In these equations x_1 and x_2 are the mole fractions of solvent and salt, respectively and a_1 is the activity of the component 1. The parameter w indicates the non-ideality of the system arising from the differences between the intermolecular attractions for pairs of unlike species as compared to the mean of the intermolecular attraction for pairs of like species. z is a van Laar parameter varying with compositions of the mixtures. The ratio (b_2 / b_1) is the volume ratio of components and ν is the number of cation and anion.

Scatchard and Hildebrand later greatly improved the theory of van Laar by freeing it from the limitations of van der Wall's equation of state by defining a parameter 'c' called as the cohesive-energy density. Further they assumed that a) for molecules, whose forces of attraction are primarily due to dispersion forces there exists simple relation between c_{11}, c_{12}, and c_{13} as suggested by London's formula, b) at constant T and P the excess entropy of mixing vanishes. The activity coefficients are then given by:

$$R T \ln \gamma_1 = v_1 \phi_2^2 [\delta_1 - \delta_2]^2 \qquad (2)$$

and

$$R T \ln \gamma_2 = v_2 \phi_1^2 [\delta_1 - \delta_2]^2 \qquad (3)$$

where δ is called as the solubility parameter, ϕ_1 and ϕ_2 are the volume fractions of components 1 and 2, respectively. The above equations are called as the regular solutions equations. The parameters δ_1 and δ_2 are

temperature dependent, but their difference is not a function of temperature. This difference in the solubility parameter is a measure of non-ideality. Since the above equations always predict $\gamma_i \geq 1$; it states that regular solution equation can exhibit only positive deviations from Raoult's law. The advantage of the regular solution equation is its simplicity, and the simplicity is retained even when the model is extended to multicomponent systems.

Numerous equations of excess Gibbs energy have been suggested based on the consideration of interactions of unlike molecules in groups of various sizes. The contribution of a kind of interaction is considered to be proportional to the relative frequency of formation of the grouping and an intensity factor that reflect the nature of grouping. Wohl expressed these concepts in a general form as follows:

$$G^E / R\,T\,(\Sigma_i\, q_i\, x_I\,) = \sum_{i,j} z_i\, z_j\, a_{i\,j} + \sum_{i,j,k} z_i\, z_j\, z_k\, a_{i\,j\,k} + \ldots\ldots. \qquad (4)$$

where q_i is the effective molal volume of component I, and $z_i = x_i\, q_i / \sum_k x_k\, q_k$.

In the above a's are the constant intensity factors that are characteristics of the different groupings. For binary mixtures equation (4) reduces to:

$$G^E / R\,T\,(q_1\, x_1 + q_2\, x_2\,) = 2\, z_1\, z_2\, a_{12} + 3\, z_1^2\, z_2\, a_{112} + 3\, z_1\, z_2^2\, a_{122} \ldots\ldots (5)$$

The activity coefficients of the component 1 is then deduced from the above equation:

$$\ln \gamma_1 = z_2^2\, [A + 2\,(B\, q_1 / q_2 - A\,)\, z_1] \qquad (6)$$

The new parameters A and B may be directly derived from data.

By assuming $q_1 = q_2$ for the binary solutions whose molecular sizes are not much different, the commonly used Margules equation can be obtained as:

$$\ln \gamma_1 = x_2^2 [A + 2 (B - A) x_1] \quad (7)$$

The above equation is called as the 3 suffix Margules equation containing two parameters. Although the assumption $q_1 = q_2$ suggests that the Margules equation should be used only for mixtures, whose components have similar molar volumes, but it is used for all sorts of liquid mixtures, regardless of the relative sizes of the different molecules. The advantage of Margules and van Laar equations are that they can serve as simple empirical equations for representing experimentally determined activity coefficients with only few constants. If the data are scattered or scarce these equations can be used as an efficient tool to interpolate or extrapolate with respect to composition. When the data are precise and plentiful the wohl's expansion is truncated after the quartic term and then a four suffix Margules equation with three parameters can be obtained.

The equations described above are very simple and are seen to applicable for the systems, where the molecular sizes of the components do not vary much. In order to represent adequately the excess Gibbs energy of complex mixtures, a series of expansion was put forward by Redlich and Kister known as the Redlich-Kister expansion:

$$G^E / RT = x_1 x_2 [A + B (x_1 - x_2) + C (x_1 - x_2)^2 + D (x_1 - x_2)^3 + \ldots.] \quad (8)$$

where B, C, D are additional temperature-dependent parameters which must be determined from the experimental data. The equation for the activity coefficients is obtained from equation 8. The number of parameters A, B, C, ….used to represent the experimental data depends on the molecular complexity of the solution, the quality of data, and the number of data points available.

4A.2 Data and Analysis

As a part of the research program to study these infrequently available systems for theoretical purposes, the vapor pressures were measured on nitrobenzene with TP at a temperature above the melting point of TP and the solvent activities calculated therefrom. Experimental activity data on nitrobenzene with TP were analyzed in terms of empirical and semi-empirical thermodynamic models.

In **Table 4A.1** are listed the values of vapor pressures, p, of nitrobenzene (1) + TP (2) solutions at different mole fractions, x_1 of nitrobenzene at 373 K.

Table 4A.1 : Vapor pressures, p / kPa and activities, a_1 of nitrobenzene in Nitrobenzene + TP Solution at 373 K

x_1	p/ (kPa)	a_1	x_1	p/ (kPa)	a_1
0.0920	0.412	0.145	0.7093	2.269	0.800
0.1883	0.795	0.280	0.8125	2.522	0.889
0.3058	1.201	0.423	0.8826	2.642	0.931
0.4122	1.515	0.534	0.9655	2.789	0.982

0.5059	1.765	0.623	1	2.837	1
0.6114	2.038	0.715			

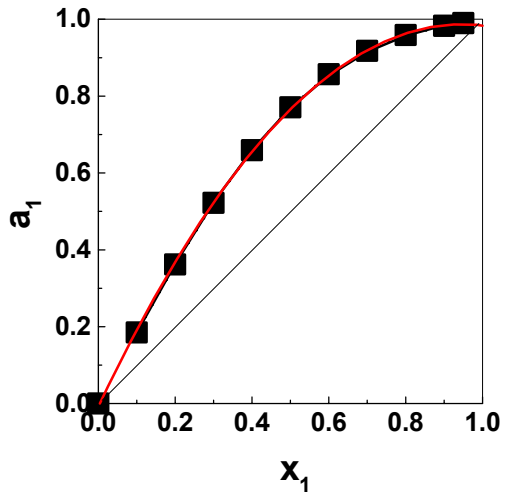

Figure 4A.1: Solvent activity, a_1 of nitrobenzene in nitrobenzene + tetrabutylammonium picrate at 373 K

The p - x_1 values can be represented using a polynomial equation:

$$p / kPa = 0.0645 + 4.06\ x_1 - 1.29\ x_1^2 \qquad (9)$$

with σ = 0.017 kPa

These vapor pressures were converted into activities of nitrobenzene, a_1 using a value of second virial coefficient , B as - 2.8742 x 10^{-3} m^3 mol^{-1} at 373 K. The plot of a_1 vs. x_1 (**Figure 4A.1**) shows positive deviations from Raoult's law. Value of B was calculated from the corresponding states correlations described in detail by Prausnitz employing the reduced temperature, T_r and reduced pressure P_r data given elsewhere.[4,5] The B value

calculated from this method agrees well with the method proposed by Hayden and O'Connell.[6]

In order to analyze the p - x_1 data for the system, we have attempted to undertake three different models as: Stokes-Robinson hydration model, Pitzer - Simonson model, and a local composition model of Chen et al. Chen and Evans.[7-10] The Stokes-Robinson hydration model was chosen for examining its validity in describing the vapor pressures of non-aqueous solvent - molten organic salt systems. This model has been used earlier in the case of aqueous systems. The semi-empirical models proposed by Pitzer and Simonson and Chen et al and Chen and Evans describe the short-range forces by the use of simple non-electrolytic and local composition terms, respectively. It was, therefore thought worthwhile to analyze the data by using these models. The non-electrolytic term in the Chen model has more rigorous theoretical basis as compared to that in the Pitzer-Simonson model.

4A.3 The Robinson-Stokes Model

The Stokes-Robinson model is based on the concept of hydration of ionic species in water and has been applied for analyzing the vapor pressure data of several concentrated salt solutions. The model uses two adjustable parameters. The Brunauer-Emmett-Teller (BET) adsorption isotherm is used in this model. The central idea is that the molten salt can attract solvent molecules, presumably to the surfaces of cations, much as water is attracted to the surface of a crystal. As more water is added, the binding energy per molecule decreases gradually to that of pure water in a dilute solution or with

a multilayer film. According to Braunstein and Braunstein and Trudelle et al. the operational equation is:[11-13]

$$a_1 (1 - x_1) / x_1 (1 - a_1) = 1 / c\,r + (c - 1)\, a_1 / c\,r \qquad (10)$$

with c and r being adjustable parameters.

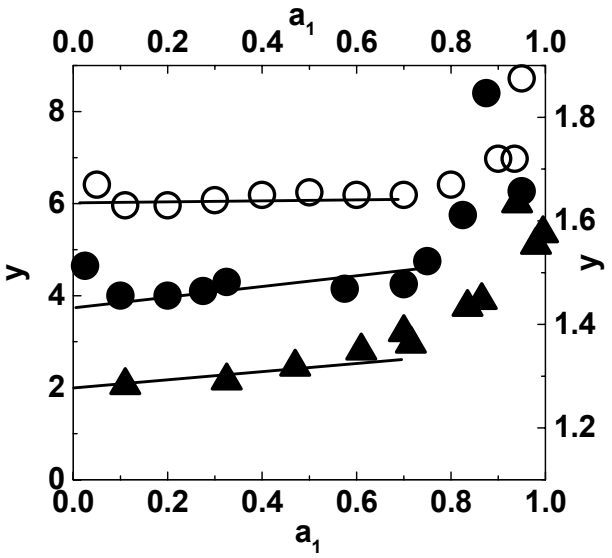

Figure 4A.2: Plots of the Stokes and Robinson Model; y (=$a_1 (1 - x_1) / x_1 (1 - a_1)$) against a_1; O TP + nitrobenzene, ● TP + anisole and ▲ TP + 1-butanol

Accordingly, a plot between the values calculated from the left hand side of the above equation and a_1 is expected to yield a straight line with 1 / c r and (c - r) / c r as intercept and slope, respectively. The resultant adjustable parameters c and r for our molten system, as obtained by the use of eq 10 are c = 1.044 and r = 0.595. For the purpose of comparison, the left hand side of eq 10 has been plotted against a_1 in **Figure 4A.2** for two other systems i.e. anisole and 1-butanol involving TP as a common salt.[1,8] An examination of

Figure 4A.2 reveals that the experimental a_1 values begin to deviate from linearity at x_1 > 0.84, 0.9 and 0.7 for nitrobenzene + TP, + anisole and + 1-butanol, respectively. The SRM represents the activity data for these systems with standard deviations σ = 0.007, 0.009 and 0.001 up to the point of deviation from linearity while compared to experimental data of TP + nitrobenzene, + anisole and 1-butanol, respectively.[1,8] This limitation of the Stokes - Robinson model in describing the activity data of aqueous systems in entire concentration range is documented elsewhere.[11,12]

4A.4 The Pitzer-Simonson Model

Considering the success of the Pitzer - Simonson model in the cases of systems comprising TP + anisole and + 1-butanol, the experimental a_1 data on nitrobenzene + TP were analyzed by this model. The Pitzer - Simonson model employs a combination of "electrostatic long-range term" expressed by the Debye - Huckel Component (DHC) with "non-electrostatic short range component" (NEC), like van Laar or Margules having two adjustable parameters. This model is based both on the full dissociation of salt throughout the composition and incomplete dissociation due to ion-pair formation in the low-salt region. Ion pairing, as calculated from conductance data, allows the revised calculations of mole fractions of cation, anion, and ion pair and solvent. The relevant details of PSM are described below:[8]

The Gibbs free energy of mixing (dimensionless), Δ_m G / RT is given by:

$$\Delta_m G / RT = n_1 \ln x_1 + 2 n_2 \ln x_2 + w_1 n_1 z_2$$
$$+ 4 n_2 (A_x / \rho) \ln [(1+ \rho I^{0.5}) / (1 + \rho / 2^{0.5})] \quad (11)$$

where n indicate the number of moles with subscripts 1 and 2 for nitrobenzene and TP, respectively. Quantities w_1 and z_2 are non-ideality and composition parameters, respectively contributing to NEC. Parameter z_2 is defined in terms of volume ratio and composition as $z_2 = x_2 / (q\, x_1 + x_2)$ with q being ratio of molar volumes given by b_1 / b_2. The last term in the above expression is a DHC written on the mole fraction basis. Both A_x, Debye-Huckel slope and ρ, a parameter related to hard-core diameter used in this study at 373 K are 12.25 and 9.66, respectively. Ionic strength, I_x is calculated on the mole fractions basis as $I_x = 0.5 \sum x_i z_i^2$.

The a_1 values were obtained from:

$$\ln a_1 = \ln x_1 + w_1 z_2^2 + 2 A_x I_x^{1.5} / (1 + \rho I_x^{0.5}) \quad (12)$$

Because of ion-pairing, the mole fractions of cation, anion and solvent species are recalculated using the ion association constant, K_x being obtained from conductance data of Seward.[14] The revised mole fractions of cation, anion, ion-pair (ip) as described below are inserted in eq 12 for calculating the solvent activities. Thus, the revised mole fractions for the species are:

$$x_i = (1 - \alpha) n_2 / F = I_x \quad (13a)$$

$$x_p = n_2 / F \quad (13b)$$

$$x_{ip} = n_1 / F \qquad (13c)$$

with $F = [\, n_1 + (2 - \alpha) n_2 \,]$ and subscripts i , p and ip indicate free ions (cation T^+ or anion P^-), ion-pairs and nitrobenzene with ion-pairing, respectively. The degree of ion-pair formation is given by α.

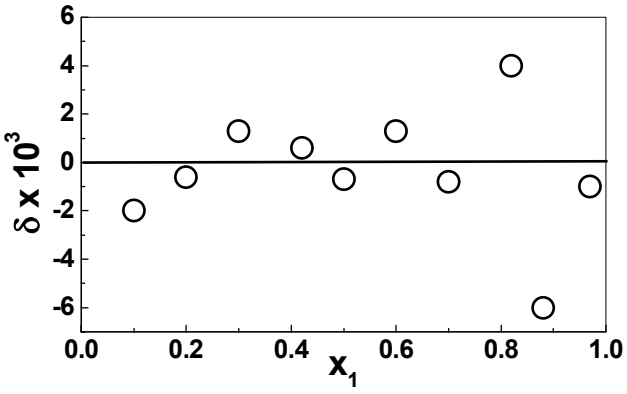

Figure 4A.3: δ (difference between experimental and calculated a_1) by PSM with $\alpha \neq 0$ as a function of x_1 for nitrobenzene + TP at 373 K

Eq 12 was applied to the vapor pressure data of nitrobenzene + TP listed in Table 1. Input quantities for the treatment were relative permittivity = 24.80; A_x = 12.25 and ρ = 9.66. In the case of complete ionization of TP in nitrobenzene (α = 0), the values of parameters i.e. w_1 = -0.565 and q = 0.341 along with $\sigma = 0.004_6$ were obtained using eq 12. However, when the same equation with the revised mole fractions (eq 13) accounting for ion-pairing was employed to fit the p-x data, resultant parameters were noted to be as w_1

= -0.589 and q = 0.338 with σ = 0.0035. Though the improvement in the fitting of the activity data with ion-pairing is not highly remarkable, it is important to note that the equations involving ion- pairing should be preferred over those derived for full dissociation of salt. This is stated in view of conductance data on the system.[14]

The value of q obtained in the above calculation is close to the ratio of molar volumes of nitrobenzene and TP, 0.297. A similar observation was noted in the case of anisole + TP. Once the experimental data on a large number of systems are available, it may then be possible to determine if PSM can successfully fit the vapor pressure data with a single parameter w_1 with q being calculated *a priori*. In **Figure 4A.3** are shown the deviation δ obtained from the difference of experimental data and the PSM with $\alpha \neq 0$.

4A.5 The Chen Model:

We also examine our p - x data using the local composition model of Chen et.al. and Chen and Evans, who described the contribution due to short range interactions with the concept of local composition.[9,10] This model is based on the assumptions of like ion repulsion i.e. the local composition of cations around cation is zero and similarly for anions, which is equivalent to assuming that repulsive forces between ions of like charge are extremely large, and local electroneutrality, where the distribution of cations and anions around the central solvent molecule is such that the net local ionic charge is zero. The model is developed by using the extended Debye-Huckel formula as proposed by Pitzer to represent the long-range interactions and the local

composition concept is developed to represent the short-range interactions.[2] The local composition concept and the Debye-Huckel equations are consistent in the sense that they both account for non-randomness by introducing local compositions through Boltzmann like factors. The local composition model is developed as the symmetric model, based on pure solvent and pure completely dissociated liquid electrolyte. The model is then normalized by infinite dilution activity coefficients in order to obtain an unsymmetric local composition model. Since in this model the interaction energies are considered to be symmetric, only two parameters salt-molecule parameter ($\Gamma_{ca,m}$) and molecule-salt parameter ($\Gamma_{m,ca}$) are obtained for a binary pair of single completely dissociated electrolyte and single solvent. The salt-molecule parameter, ($\Gamma_{ca,m}$) is the difference of the dimensionless interaction energies between the ion-molecule pair and the molecule-molecule pair. The molecule-salt parameter, ($\Gamma_{m,ca}$) is the difference of the dimensionless interaction energies between the molecule-ion pair and the cation-anion pair.

It is well known that local composition model binary parameters are not well determined for molecular system, even when the fit is very good. The fitted parameters generally have relatively large standard deviations and are very strongly correlated.

4A.6 Our Modified Treatment of the Chen Model

Our present treatment differs from that of Chen et al. as we have explicitly considered the ion pair formation in our treatment of short-range interactions. We retain the expression for long-range interactions of Pitzer as

such and modify the calculations for short-range interactions with ion pair formation. The equations are based on a simple system of nitrobenzene, T^+, P^- and $[TP]^0$. Different cells are assumed in this model: i) consisting of a central nitrobenzene molecule with other nitrobenzene molecules, T^+, P^-, and neutral ion pair $[TP]^0$ in its neighborhood. This type of cell follows the assumption of local neutrality; the surrounding T^+, $P^-$are such that the neighborhood of nitrobenzene is electrically neutral. The other kind of cell consists of either a central T^+ or P^- with nitrobenzene molecules and ions of opposite charge in its immediate neighborhood. These two cells follow the assumption of like ion repulsion: no ions of like charge exist near each other.

In short, the local mole fractions x_{ij} and x_{ii} of the species j and i, respectively are related in the immediate neighborhood of a central species i via interaction energies as:

$$x_{ji} / x_{ii} = (x_j / x_i) G_{ji} \quad (14)$$

where quantity G_{ji} is defined as:

$$G_{ji} = \exp (\alpha \iota_{ji}) \quad (15)$$

In eq 15, ι_{ji} is the difference of energies of interaction between ji (g_{ji}) and ii (g_{ii}) pairs of species shown below:

$$\iota_{ji} = (g_{ji} - g_{ii}) / R T \quad (16)$$

The terms g_{ji} and g_{ii} are inherently symmetric i.e. $g_{ji} = g_{ii}$. In the Chen model, parameter $\tau_{1,TP}$ is the difference of dimensionless interaction energies between the solvent - ion and the cation - anion pair, whereas parameter $\tau_{TP,1}$ is the difference of the dimensionless interaction energies between the ion-solvent pair and solvent-solvent pair.

A non-linear least squares program was employed to regress the vapor pressure data.[15] We obtained Chen parameters as $\tau_{1,TP} = 12.211 \pm 0.010$ and $\tau_{TP,1} = - 8.231 \pm 0.009$ with $\sigma = 0.006$ in a_1. It is noted that both the PSM and Chen models represent the activity data with reasonable accuracy.

In extremely dilute solutions, the interaction between the cation and anion in a solvent with a low relative permittivity is stronger than the interaction between the two solvent molecules. Our reported values for binary parameters have much larger difference than those for (Ag,Tl,Na)-NO_3-H_2O) system thus suggesting strong interactions between cation, anion and greater tendency for the ions to make ion-pair in very low concentration range.[9,10]

4A.7 Problems Associated with the Vapor Pressure Data Analysis

Thermodynamic properties like, vapor pressures of these systems and their modeling merit considerable theoretical attention. As such, equations for correlating the a_1 - x_1 data have numerous potential applications including many in chemical engineering and in atmospheric aerosol chemistry. Several models have been employed to analyze the vapor pressures or solvent activities of such systems as discussed above. The model of Stokes and Robinson has been noted to estimate the activities of water up to $a_1 < 0.65$,

the local composition model although bit cumbersome to use for the systems of current interest, it can reproduce the vapor pressure data of systems, like water – (Ag, Tl) NO_3 and nitrobenzene –TP with good accuracy. [7,13,16] However, application of Chen model to systems, like water- (Li,K)NO_3 results into the under-estimated water activities in high salt range.[9,17] The PSM has been shown to be applicable to the systems showing positive deviations from Raoult's law, but fails to predict the solvent activities in extremely dilute and extremely concentrated ranges, and the mole faction-based model of Clegg and Pitzer where they extended the Margules expansion to the four - suffix level to account for the short-range forces.[18] In order to account the properties in the dilute solutions; an additional term B_{TP} with an exponential dependence of ionic strength term was included to the Margules expansion. The solvent activity data for several single electrolytes like aqueous HCl, HNO_3, NaCl, KCl, $NaNO_3$ and KNO_3 were analyzed by the Clegg-Pitzer equation. The calculations were then extended to cover a model system comprising H^+, Na^+, K^+, Cl^- and NO_3^-.

After a careful study of the available literature data we realized that the PSM could predict the vapor pressures of those systems that show positive deviations from Raoult's law. In literature there exists accurate experimental p - x_1 data on several systems of current interest that show nearly zero to highly negative deviations from Raoult's law. For instance, the systems such as water - KNO_3 with nearly zero deviation from Raoult's law, water – Ca $(NO_3)_2$ and DMSO – $Ca(NO_3)_2$ with highly negative deviations from Raoult's law can

be examined. [12,19,20] Analysis of these systems and of others showed that the PSM did not generate accurate a_1 values in the limiting mole fraction range ($x_i \rightarrow 0$). The PSM equations were also be seen to compute incorrect slopes of the a_1 - x_1 curves. These limitations of PSM in the extreme x_i ranges are depicted in **Figure 4A.4 (a) to (d)** for several systems. In **Figure 4A.4(a)** and **(b)** are plotted the calculated a_1 (abbreviated as $a_{1,cal}$) values (dotted lines) by the PSM against experimental ($a_{1,exp}$) points for water – $LiNO_3$ and – $Ca(NO_3)_2$ in low and high x_i ranges, respectively systems.[12,20,21]

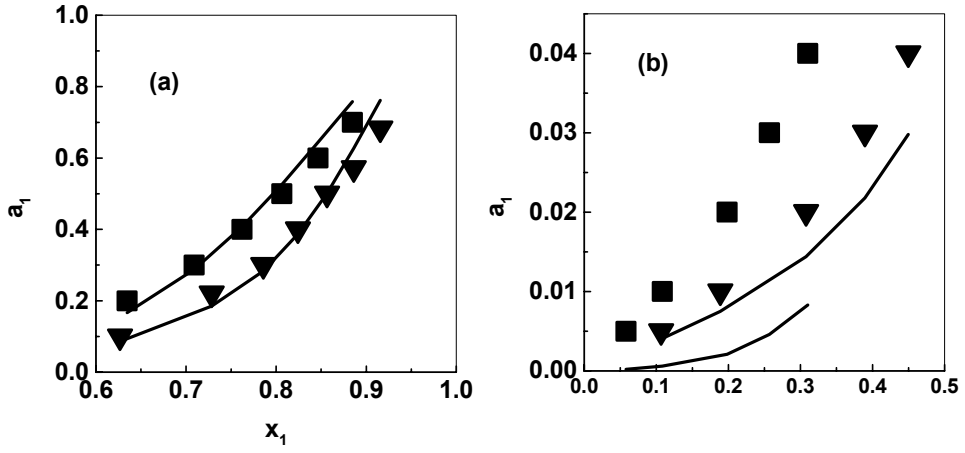

Figure 4A.4 (a) and (b): Solvent activities a_1 against x_1; symbols: experimental values; dotted lines: calculated by PSM **(a)** water – $LiNO_3$ ■; -$Ca(NO_3)_2$ ▼, in higher x_1 range; **(b)** in lower x_1 range , upper curve belongs to ■ , lower curve belongs to ▼; symbols have the same meaning as in Figure **4A.4 (a)**.

Examination of the above plots shows that the a_1 values for water - $LiNO_3$ and – Ca $(NO_3)_2$ can not be accurately computed by the PSM. For

instance, the maximum difference between $a_{1,exp}$ and $a_{1,cal}$ ($a_{1,exp}$-$a_{1,calc}$ = δ) at x_1 = 0.88 for water – $LiNO_3$ is 0.25, while for water – $Ca(NO_3)_2$, δ at x_1 exceeds 0.05. Very large values of δ are recorded by PSM in the water - $LiNO_3$. Analogous behavior of δ (**Figure 4A.4(c)**) as discussed is seen for DMSO – NH_4NO_3 and – KSCN.[22,23] Besides δ, the ($\partial a_1/\partial x$) values display incorrect slopes as compared to those obtained from experimental data. Similar anomalies exist in other systems with negative deviations from Raoult's law. This point has been ignored in the treatment of data by PSM and in the later modified versions of the Pitzer equations.[24] On the other hand, as indicated above, both the limiting a_1 values and the shape of slopes are correctly described by PSM in the cases of systems with positive deviations from the Rauolt's law.

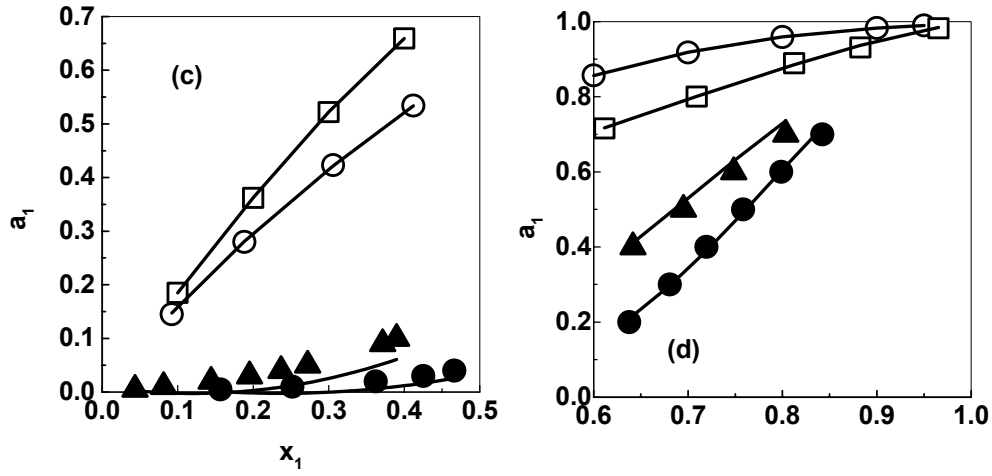

Figure 4A.4 (c) and (d) : Solvent activities a_1 against x_1; symbols: experimental values; dotted lines: calculated by PSM **(c)** DMSO–NH_4NO_3 ▲, -KSCN ●, 1-butanol–TP O, in lower x_1, nitrobenzene - TP ❒; **(d)** symbols and description are similar except plots are in higher x_1 range.

This observation is shown in **Figure 4A.4 (c) and (d)** for nitrobenzene - and 1-butanol with TP systems. Observations similar to those shown above are true for minor negative or positive deviations from Raoult's law. Later, PSM was modified to include one more adjustable parameter in the Debye-Huckel term, thus increasing the number of adjustable parameters to 4 or 5.[24] With the description of short-range forces by a Margules type of equation thermodynamic activities of water in different salt systems were described.

Prausnitz has summarized different forms of Margules-type equations.[4] Another question in applying the PSM model to the non-aqueous-salt systems is whether the Debye-Huckel term accounting for long-range interactions should be included in the treatment of thermodynamic data. If it is incorporated in the framework of equation, use of appropriate value of the parameter, ρ (a parameter calculated from the hard core diameters and solvent properties) should be examined.

4A.8 Our Proposal to Estimate Deviations from the Raoult's Law in the Present Systems

In view of the above we propose a simple equation for accurately correlating the solvent activity - composition data for the systems that are continuously miscible from pure fused salt to dilute solutions.

The free energy of mixing, $\Delta G_{m,}$ of a system containing a fused salt and a solvent can be written by combining the contributions due to long- and short-range interaction forces. If the solvent activity coefficient, is γ_1 given by γ_1 = DHT + NEC, where DHT and NEC account for the Debye- Huckel and

non-electrolytic terms, respectively, then one can write: NEC = γ_1 – DHT. The long-range interaction forces are calculated by the Debye – Huckel expression with certain modifications in the hard-core diameter based parameter as shown in the PSM.[8] It has been shown that it is the net effect of short-range forces that is primarily dominant in the full concentration range.[1,16] It is therefore, essential to optimize the most appropriate form of equation for calculating the contribution due to short-range interaction forces.

Starting with dimensionless free energy of mixing,(ΔG_m/ RT) = g, general equation for g can be written in terms of the above interactions as:

$$g = \sum_{j=1}^{m} x_j \ln x_j + \sum_{j=1}^{m} x_j f_j + \sum_{j=1}^{m} x_j (SR)_j \qquad (17)$$

In eq 17 first term on the right hand side are due to the ideal mixing, the second term the long-range interaction forces (f_j). The third term on the right hand side denotes short-range interaction forces (SR). x_j is mole fraction of j^{th} salt. Using the above expression for g, an operational equation for calculating the activity, a_1 of the solvent in a binary mixture can be given as:

$$\ln a_1 = \ln x_1 + f_1 + (SR)_1 \qquad (18)$$

In eq 18 f_1 denotes the contribution from the long-range interactions as described by the Debye-Huckel term as:

$$f_1 = 2 A_x I_x^{1.5} / \theta \qquad (19)$$

where, A_x is the Pitzer-Debye-Huckel slope calculated on the mole fraction basis as $A_x = 1/3(2 \pi N_A d_1 / M_1)^{0.5}(e^2 / \varepsilon k T)^{1.5}$. I_x, the mole fraction basis ionic strength is given by $I_x = 0.5 \sum x_i z_i^2$ with z being the ionic charge. The symbols e, N_A, d_1, M_1, ε, k and T are electronic charge, Avogadro number, the solvent density, the solvent molecular weight, relative permittivity, Boltzmann constant and temperature in K, respectively.

The term θ is:

$$\theta = 1 + \rho I_x^{0.5} \qquad (20)$$

In principle, the parameter $\rho = \sigma (8\pi e^2 N_A d_1 / M_1 \varepsilon k T)^{0.5}$ is calculated from the hard-core diameter, σ .

The short-range interaction forces for the systems showing deviations from Raoult's law indicated by $(SR)_1$ are given by:

$$(SR)_1 = x_2^{0.5} [q_{121} x_1 + q_{122} x_1^2 + q_{123} \exp(-x_1)] \qquad (21)$$

where, q_{121}, q_{122} and q_{123} are the adjustable parameters obtained from the least squares fitting of experimental data.

Substitution of eq 21 in eq 18 yields the working relationship for the a_1-x_1 data as:

$$\ln a_1 = \ln x_1 + f_1 + x_2^{0.5} [q_{121} x_1 + q_{122} x_1^2 + q_{123} \exp(-x_1)] \qquad (22)$$

Activity coefficient, ln $\gamma_{\pm}$ of salt, with fused salt as a reference state is then described by:

$$\ln \gamma_{\pm} = (SR)_2 - f_2 \qquad (23)$$

In the above equation $(SR)_2$ and f_2 are the terms indicating short-range and long-range interaction forces, respectively for a salt.

These terms are defined as:

$$(SR)_2 = x_1^{0.5} \{(-q_{121} - q_{123})\, x_2 + (2\, q_{121} + q_{122} + q_{123})\, x_2^2 + (q_{121} + q_{122} + q_{123})\, \exp \qquad (24)$$

and,

$$f_2 = A_x [\{ 2 / \rho \}\ \ln \{ \theta / (1 + \rho\ 2^{-0.5})\} + (I_x^{0.5} - 2\, I_x^{1.5} / \theta)] \qquad (25)$$

A simplified equation for calculation of g in the case of a binary mixture can therefore, be written as:

$$g = x_1 \ln x_1 + x_2 \ln x_2 + f^{\phi} + g^{\phi} \qquad (26)$$

In eq 26, f^{ϕ} and g^{ϕ}, the combined functions representing (LR) and (SR) terms for both the solvent and fused salt can be expressed as:

$$f^{\phi} = 2A_x\ [- I_x\ (2 / \rho)\ \ln (\theta / (1 + \rho / 2^{0.5}))] \qquad (27)$$

and

$$g^{\phi} = x_1^{0.5} x_2^{0.5}\{x_1^{0.5} [x_1^2 u_1 + q_{123} \exp (x_1)]$$

$$- x_2^{0.5} [x_2 (q_{121} - u_2 x_2 + q_{123} (1 - x_2^2)) - u_3 \exp (-x_2)]\} \quad (28)$$

with

$$u_1 = q_{121} + q_{122} x_1; \quad (29a)$$

$$u_2 = 2q_{121} + q_{122}; \quad (29b)$$

and

$$u_3 = q_{121} + q_{122} - q_{123} \quad (29c)$$

Equation 22 was tested against the $a_1 - x_1$ data at 373K for several systems. These systems are listed in **Table 4A.2**. First entry in **Table 4A.2** belongs to the systems showing negative deviations from Raoult's law. The compilation of the ionic species includes salts of 1:1 and 2:1 types; in which Li^+, K^+, NH_4, Ca^{2+} constitute the cations of the systems, whereas the anions includes halides, nitrates, thiocyanates, hydroxides, and organic species. In view of data available in limited solvents, only water and dimethylsulfoxide (DMSO) were used as solvents in the systems investigated in the present study. Value of A_x at 373K was estimated from the solvent properties as described by Pitzer and Li.[25] Second important parameter, ρ in the treatment was calculated from the hard-core diameter of the solute. In the treatment of data by Pitzer and coworkers, a fixed value of $\rho \cong 19$ has been used for most of the electrolyte solutions. [8,18] Initially, the $a_1 - x_1$ data were fitted with $\rho = 19$, however, it was noted that the use of a fixed value of ρ yielded high deviations

in experimental and calculated a_1. It should be noted that systems like water- LiCl, - LiBr and – Ca $(NO_3)_2$ exhibit very strong negative deviations from Raoult's law.

Application of a fixed value of ρ to these data generates unrealistic curves of calculated a_1 with x_1 values. It was therefore, decided that a value of ρ calculated directly from hard – core diameter and solvent properties would be more appropriate. This was verified by running a non- linear least squares fitting of $a_1 - x_1$ data of the above systems. It is further, noted that the calculation of ρ depends on the solvent relative permittivity.

Table 4A.2 : Analysis of solvent activities, a_1 using eq 22 together with resultant adjustable parameters and root mean squares deviation, rmsd. The systems are miscible throughout the composition; A_x for water = 3.44; for DMSO = 4.988 at 373K

Systems showing negative deviations from Raoult's law

Systems	q_{121}	q_{122}	q_{123}	q_{124}	rmsd	Data Source
water – LiCl	-8.667	9.656	0	-3.253	0.079	12
water – LiBr	-21.23	22.33	0	-1.039	0.126	12
water – $LiNO_3$	-4.009	4.942	0	-2.851	0.028	21
water – $Ca(NO_3)_2$	-7.133	7.911	0	-3.275	0.072	12, 21
∗water- NaOH	-2.403	2.688	0	-0.188	0.016	27
∗water-KOH	11.825	- 8.77	0	-9.217	0.026	27

∗water-AcNa	-0.337	0.676	0	-0.768	0.004	27
∗water-AcK	-0.210	0.960	0	-1.634	0.011	27
water – NH_4NO_3	-0.553	0.578	0	-0.548	0.006	21
DMSO - $LiNO_3$	-27.23	56.11	-28.41	-1.266	0.110	22
DMSO – KSCN	-17.83	37.86	-19.04	-2.449	0.094	23
DMSO – NH_4NO_3	-3.814	10.02	-5.283	-2.551	0.008	22
DMSO – $Ca(NO_3)_2$	-525.4	848.4	-380.5	153.1	0.131	20

Systems showing positive deviations from Raoult's law

1-butanol – TP	0.460	-0.320	0	-0.407	0.002	8
Anisole – TP	-2.469	2.762	0	-1.770	0.036	1
Nitrobenzene – TP	-0.572	0.749	0	-0.564	0.008	16
Water –KNO_3	-0.305	0.317	0	-0.517	0.002	19

Mixtures showing negative, positive or near ideal behavior from Raoult's law

Water - $(Li,K)NO_3$	0.944	-0.403	0	-1.447	0.001	17
Water -$(Li,NH_4)NO_3$	0.450	-0.159	0	-0.878	0.008	28
Water -$(K,NH_4)NO_3$	-0.298	0.269	0	0.0685	0.002	28
Water – (Ag,Tl) NO_3	0.720	-0.726	0	0.1425	0.001	13
∗Water-(NaOH,AcNa)	1.933	-1.254	0	-2.006	0.004	27
∗Water-(AcK,AcNa)	0.402	0.264	0	-1.609	0.005	27

∗Water – (KOH,NaOH)	6.653	-4.959	0	-5.208	0.016	27

∗ The solvent activities were measured at 690 K.

DMSO = dimethylsulfoxide AcNa = sodium acetate

AcK = potassium acetate NB= nitrobenzene

The results of regression for different systems with adjustable parameters $q_{12,i....}$ and root mean squares deviation, RMSD = $((a_{1,exp} - a_{1,cal})^2/N)^{0.5}$ are given in **Table 4A.2**, where N is number of data points. The correlation expressed in the form of eq 22 is noted to be highly accurate in estimating the solvent activities of all the systems with negative deviations from Raoult's law. Since water- LiCl and -LiBr systems show strong negative deviations from Raoult's law, it will be of interest to examine the performance of our equation in calculating their solvent activities. In **Figure 4A.5 (a)** are demonstrated the calculated a_1 values (solid line) obtained from the present work against experimental points for water-LiBr system. **Figure 4A.5 (b)** shows a plot of $a_{1,exp}$ against $a_{1,calc}$ by eq 22 for water-LiCl system. The calculated solvent activities by the present method agree very closely with those of experimental throughout the mole fractions. The activities of water of other systems with negative deviations from Rauolt's law, for instance water-$LiNO_3$, - NaOH and – KOH can also be accurately correlated with the correlation presented in the form of eq 22. Success of the correlation is demonstrated in **Figure 4A.6**, where the a_1 values are plotted against x_1 for water-$LiNO_3$, -NaOH and –KOH systems. Water- NH_4NO_3 shows very weak

negative deviations from Rauolt's law. Again use of eq 22 to these data offers accurate correlation of $a_{1,exp}$ with x_1 for water- NH_4NO_3, -CH_3COONa and – CH_3COOK systems with rmsd = 0.006, 0.005 and 0.012, respectively. Application of eq 22 for correlating the $a_1 – x_1$ data of systems containing 2:1 salt like Ca $(NO_3)_2$ in water is shown in **Figure 4A.7**, where the calculated a_1 values as lines in contrast with experimental data shown by symbols are plotted over full composition range. An examination of both rmsd and **Figure 4A.7** reveals that the solvent activity data for water- $Ca(NO_3)_2$ can be accurately correlated by the present equation over the full concentration range.

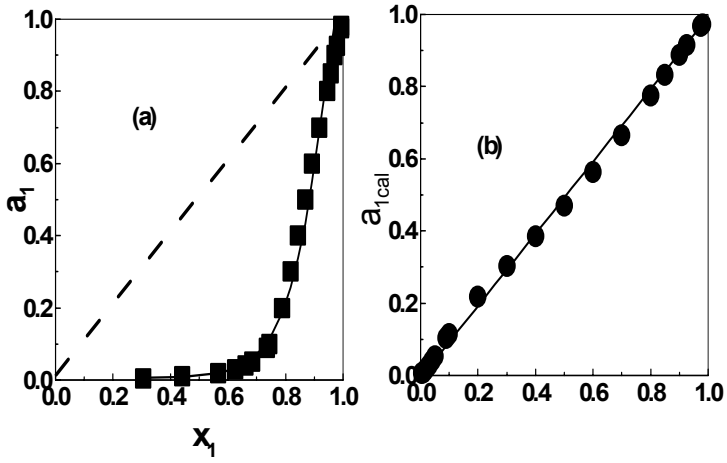

Figure 4A.5 (a): Solvent activities a_1 against x_1 for water–LiBr; points are experimental, solid lines are calculated by eq 22 **(b)** Experimental solvent activities $a_{1,exp}$ against $a_{1,calc}$ for water – LiCl

The validity of eq 22 was also examined for correlating solvent activities of other DMSO- containing salt systems showing strong deviations from Raoult's law. Such an exercise shows that the solvent activities for the DMSO - $LiNO_3$, –KSCN and $–NH_4NO_3$ systems can be correlated with good accuracy.

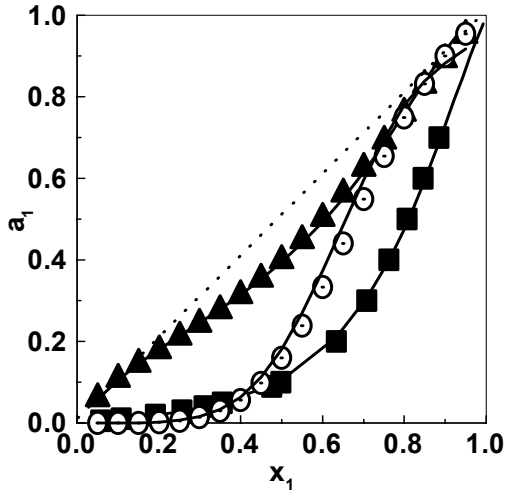

Figure 4A.6: Solvent activities a_1 against x_1; water- $LiNO_3$ ■; water- NaOH O; water- KOH ▲; points are experimental, lines are correlated values

An additional adjustable parameter, q_{123} required to fit activities of the DMSO- containing fused salt systems.

Figure 4A.8 demonstrates the composition dependence of deviation, δa_1 (= $a_{1,exp} – a_{1,calc}$) for the above three DMSO-containing systems. Random deviations seen in **Figure 4A.8** strengthen the use of eq 22 in correlating the composition dependence of a_1 in non-aqueous solvents. However, in the case of the DMSO–Ca $(NO_3)_2$ system (**Figure 4A.7**), the correlation is slightly poor in $x_1 > 0.84$. The reason for this is not known, though it appears that the (∂a_1

$/\partial\ x_1$) slope in the composition range $x_1 > 0.8$ is quite steep. As sufficient experimental activity data in non-aqueous solvents other than DMSO are not available over full mole fraction, it is not possible to examine the utility of the proposed equation in a variety of such solvents.

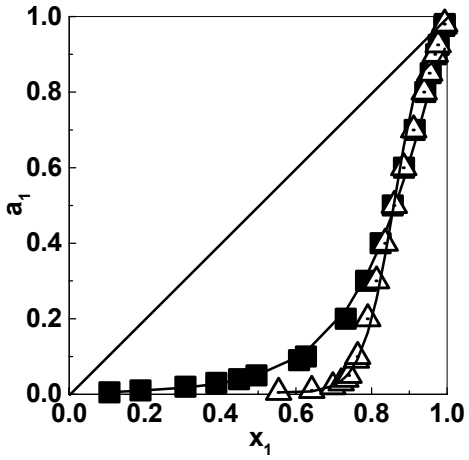

Figure 4A.7: Solvent activities a_1 against x_1; water- $Ca(NO_3)_2$ ■; DMSO-$Ca(NO_3)_2$ Δ; points exp., lines correlated values.

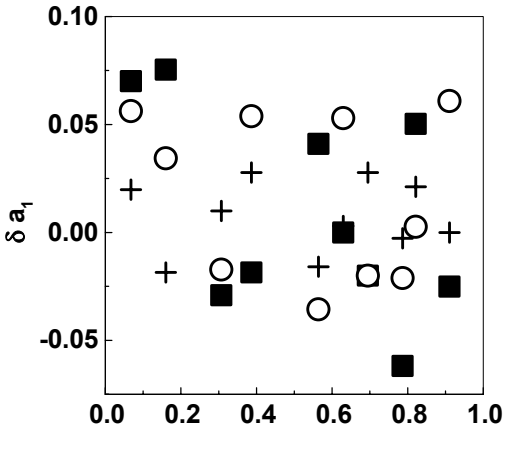

Figure 4A.8: Deviation, $\delta\ a_1$ as a function of x_1 for DMSO – $LiNO_3$ ■; DMSO – KSCN O; DMSO – NH_4NO_3 +

Having successfully examined the utility of eq 22 in analyzing the systems showing negative deviations from Raoult's law, it will be of interest to correlate the solvent activities, a_1 of the systems showing positive deviations from Raoult's law. Four systems, which were employed in such a test, are listed in **Table 4A.2**. Three systems out of four consist of a common organic salt i.e. TP, while the solvents (anisole, 1-butanol, nitrobenzene) are chosen according to their relative permittivities. The fourth system, namely water-KNO_3 shows weak positive deviations from Raoult's law.

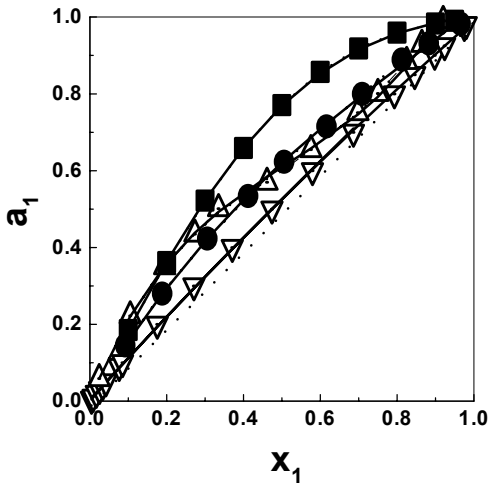

Figure 4A.9: Solvent activities a_1 against x_1, anisole - TP ∆, 1-butanol –TP ■; nitrobenzene – TP ●; water - KNO_3 ∇ points experimental, lines correlated values.

In **Figure 4A.9** are shown the plots of a_1 vs. x_1 for the above mentioned systems, where the correlated a_1 values are plotted in contrast to the experimental values for the TP - anisole, -1-butanol, -nitrobenzene and water-KNO_3 systems. A glance on the plots depicted in **Figure 4A.9** confirms the use of eq 22 in correlating the solvent activities for the systems showing positive deviations from Raoult's law.

Compared to binary systems the experimental data for ternary systems are rare. The proposed equation was applied to the mixtures of water - $(Li,K)NO_3$, -$(Li,NH_4)NO_3$, -$(K,NH_4)NO_3$ and -$(Ag,Tl)NO_3$. Results of the calculations for these systems are included in **Table 4A.2**. The ionic parameters were calculated using the composition of mixtures. Application of the proposed equation to the mixtures implies that these mixtures were

treated as pseudo-binary systems, and no information on the ternary mixtures was found necessary to predict the solvent activity data. Alternatively, the ternary data on the solvent activity can also be analyzed, if the averaging of the adjustable parameters of binary systems is taken over mole fractions. Thus, again no adjustable parameters were required to describe the solvent activity data on ternary systems. Results of such calculations are shown in **Figure 4A.10**, where the $a_{1,cal}$ data are plotted against the $a_{1,exp}$ values for the above systems. The water activities in the mixtures of fused salts can be with an average rmsd = 0.005 calculated for seven mixtures.

In the past PSM has been shown to accurately fit the solvent activity data for the systems which show positive deviations from Raoult's law.[8,16,26] An attempt was made to apply PSM to water-LiCl, DMSO-KSCN and $-LiNO_3$ systems, which show strong negative deviations from Rauolt's law. The composition dependence of δa_1 (= $a_{1,exp} - a_{1,calc}$ by PSM) values for these systems are plotted in **Figure 4A.11**.

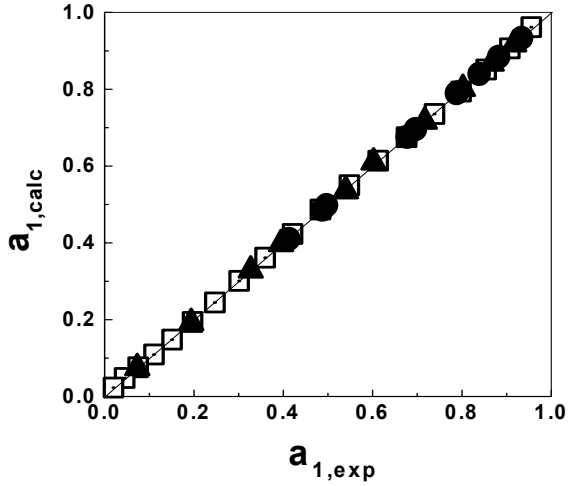

Figure 4A.10: $a_{1,cal}$ versus $_{a1,exp}$ for water – $(Li+K)NO_3$ (50.34 and 51.29 mole per cent $LiNO_3$) ❒; - $(K+NH_4)NO_3$ (equimolar) O; - ($Li+NH_4)NO_3$ (equimolar) ▲.

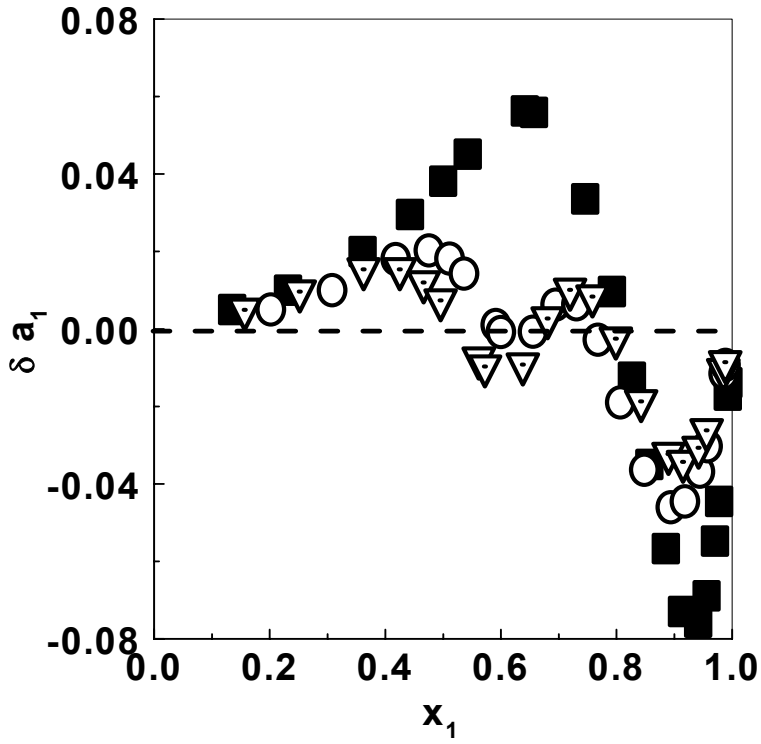

Figure 4A.11: Deviation, δa_1 obtained from the difference of experimental and calculated by PSM for water-LiCl ■, DMSO – $LiNO_3$ O, - KSCN ∇

It is clear from these plots that activities of water-LiCl system are underestimated up to $x_1 \approx 0.8$ by PSM. The negative δa_1 values in low salt composition range suggest overestimation of activities by the use of PSM. Similar conclusion can also be drawn for other two systems also, though magnitude of δa_1 is not very large.

4A.10 Comparison between our model and Clegg-Pitzer model:

It will be of interest to examine performance of the equation of Clegg and Pitzer for correlating the a_1-x_1 data for the systems of current interest.[18] Their equation for correlating the a_1 - x_1 data of single salt system is:

$$\ln a_1 = \ln x_1 + f_1 - x_M x_X B_{TP} \exp(-\alpha I_x^{0.5}) + x_1^2 (W_{1,TP} + (x_I - x_1) U_{1,TP}) + x_1 x_I^2 (2 - 3 x_1) V_{1,TP} \quad (30)$$

where B_{TP} ,$W_{1,TP}$, $U_{1,TP}$ and $V_{1,TP}$ are adjustable parameters. x_I, the mole fraction of ions is defined as $x_I = 1 - \sum x_n$.

Clegg and Pitzer introduced B_{TP} for accounting the differences in the solvent activities in the very dilute range. Secondly, they fixed a value of α = 13 on an arbitrary basis. They applied eq 30 to the solvent activity data with a maximum $x_1 \approx$ 0.5, 0.112 and 0.265 for water- HNO_3, - KNO_3 and - $NaNO_3$ solutions, respectively at 298.15K. For the purpose of comparison, the a_1 - x_1 data were fitted to eq 30 to water-LiBr, -$LiNO_3$, - $Ca(NO_3)_2$ and DMSO – NH_4NO_3 at 373 K. The parameters of eq 30 for these systems are listed in **Table 4A.3** together with their errors.

Table 4A.3: Parameters of eq 30 proposed by Clegg and Pitzer for a few sample systems at 373K. The source of experimental data is reported in **Table 4A.1**.

Systems	B_{TP}	$W_{1,TP}$	$U_{1,TP}$	$V_{1,TP}$	α
Water- LiBr	-22.466	-10.1283	-15.9531	5.9116	13
	$\pm$ 0.890	$\pm$ 0.3032	$\pm$ 0.6187	$\pm$ 0.3548	
Water-$LiNO_3$	-12.6498	-4.0002	-6.4008	2.4882	13
	$\pm$ 0.2226	$\pm$ 0.1830	$\pm$ 0.3972	$\pm$ 0.2629	
DMSO-NH_4NO_3	-11.7024	-1.8647	-3.5924	1.8719	13
	$\pm$ 0.2704	$\pm$ 0.2422	$\pm$ 0.5589	$\pm$ 0.4018	
Water-$Ca(NO_3)_2$	131.616	-3.5802	-4.9883	1.4269	1.90
	$\pm$ 24.283	$\pm$ 0.3717	$\pm$ 0.5612	$\pm$ 0.1951	$\pm$ 0.20

In **Figure 4A.12 (a)** are plotted the solvent activities ($a_{1,CP}$) calculated by Clegg and Pitzer equation as a function of x_1 together with the experimental a_1 values for water – LiBr, - $LiNO_3$ systems. It is clear from these curves that the equation of Clegg and Pitzer can reproduce the a_1 values in range of x_1 = 0.8 to 0.9 only. One observes overestimation of a_1 from $x_1 \approx 0.3$ to 0.8; the overestimation being too prominent in the lower x_1 range. The analysis of water-$LiNO_3$ gives rise to very poor correlation of the a_1 values throughout the composition range. Again the overestimation of the a_1 values is several times of magnitude when compared to the experimental ones. A similar trend in the estimated a_1 values can be witnessed in the DMSO –

NH_4NO_3 system shown in **Figure 4A.12(b)**, where δ a_1 values is plotted as a function of x_1.

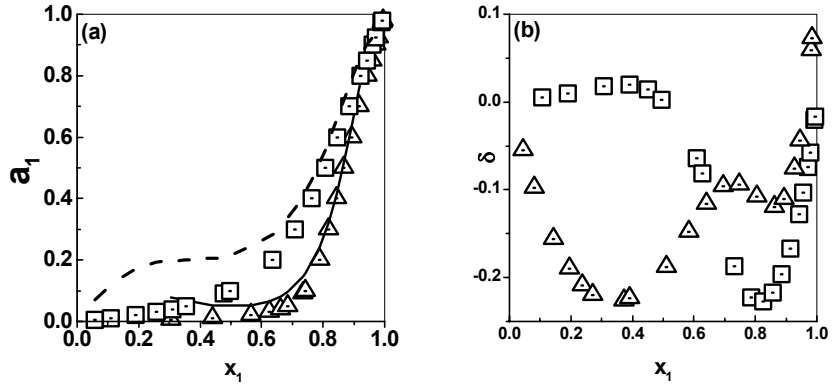

Figure 4A.12 (a): Plots of solvent activities a_1 against x_1, water-LiBr Δ, water-$LiNO_3$ ❒, points are experimental; lines are calculated by eq 30 of Clegg and Pitzer, **(b)** δ = (a_{1exp} – a_{1CP} by eq 30) plotted against x_1 for water - NH_4NO_3 □, DMSO-$Ca(NO_3)_2$ Δ

In this case though the δ a_1 values are close to zero deviation up to x_1 $\approx$ 0.5, but these deviations are too large in higher x_1 range. The severe limitations of the Clegg and Pitzer equation can further be seen in terms of δ a_1 for water- $Ca(NO_3)_2$ system plotted in **Figure 4A.12 (b)**. In this case a maximum of δ a_1 $\approx$ -0.24 is noted at x_1 $\approx$ 0.4. There is a clear systematic deviation of the calculated a_1 values from the experimental ones. Clegg and Pitzer used an additional parameter B_{TP} to deal with the activities in the higher x_1 or low-salt range. Another significant point in this regard is the estimation of

α parameter with B_{TP} term. Clegg and Pitzer argued to fix α = 13 for 1:1 symmetrical electrolytes. Though they did not present their results for aqueous $CaCl_2$, they suggested that their equation with more additional parameters could represent the solvent activities. What optimum values of ρ and α should be considered for 1:2 or 2:1 type of salts remains to be ascertained. In their equation, α = 13 for water- Ca $(NO_3)_2$ produces unrealistic estimates of a_1 values. If α s treated as a freely adjustable parameter, the fits of the a_1 - x_1 data are better than those obtaining with, α = 13. The adjusted value of α in this way is 1.90 $\pm$ 0.20 for aqueous Ca $(NO_3)_2$. On the other hand, arbitrary selection of ρ (Clegg and Pitzer adapted ρ = 13 for general purpose) does not bear any noticeable implications on the overall fits of the solvent activities.

In summary, solvent activities of systems showing deviations from Raoult's law can be correlated with composition with the help of the proposed equation. It is not the purpose of this work to present the comparative performance of several models applicable in these regards. It has been shown earlier that the BET isotherms represent the solvent activity data for the anisole- and nitrobenzene-TP systems in a limited solvent activity range.[16,26] In general, the BET isotherms are also not applicable to different types of deviations from Raoult's law.

4A.11 Exploring Artificial Neural Networks for Analysis of Vapor Pressure

In the thermodynamic models mentioned in the above, different sets of system-specific adjustable parameters are evaluated. The large number of adjustable parameters limit the extension of models to systems comprising a mixture of two or more components. Their application to such systems requires the knowledge of certain properties of mixtures necessitating additional experimental work. The other limitation of the above-stated models is that the shapes of a_1 - x_1 curve range from a very high positive to negative deviation from the linearity as suggested by the Raoult's law.[1,8,11,12,16,21,22] In essence, none of the prevailing models are capable of describing the shapes of such complex curves explicitly. Hence, a unified tool is required to model the shapes of complex curves.

Literature survey shows that Artificial Neural Networks (ANNs) are employed widely to solve a variety of engineering problems.[29,30] It is one of the most extensively employed nonlinear modeling tool in recent years. Usages of ANNs also include determining structure–activity relationships, PVT data analysis and fluid property predictions.[31] Recently, ANNs have been used in conjunction with a mixing rule based on the combination of the Wong-Sandler and Heron-Vidal order-1 concepts.[32,33] In these studies, ANNs have been successfully applied (with a maximum deviation of 0.8%) to the polar as well as non-polar systems at low pressure and systems consisting of compounds that are similar or dissimilar in size.

In here, we have explored ANNs to predict the solvent activities of different electrolyte solutions. The advantage of ANN-based models is that they can be easily used to build multiinput–multioutput nonlinear relationships without specifying the functional relationships explicitly (instead they use a universally applicable functional form).

In this section the *multi-layered-perceptron* (MLP) network, which is the most widely employed network paradigm–comprising input, hidden and output layers of neurons, has been utilized. For computing outputs of the hidden and output nodes the logistic sigmoid transfer function is used and the network training is conducted using the most popular *error-back-propagation* (EBP) algorithm.[34] Network training essentially aims at obtaining the optimal values of the weights of the connections that link neurons in the successive network layers. The EBP algorithm achieves this task by iteratively minimizing an error function (usually *root-mean-squared-error*, RMSE). Specifically, for each pattern in the training set, the prediction error (difference between the network-computed and actual output) is evaluated and it is used to modify the network weights using the EBP framework. Usually several training iterations are required to obtain a converged weight set. Obtaining an optimal weight set is of critical importance since it influences prediction accuracy of the ANN model. An ANN model with good prediction ability not only accurately predicts the outputs of the training set data but also those corresponding to a totally new input set. For obtaining an optimal weight set three adjustable ANN parameters, namely, number of hidden nodes, learning rate (β) and the

momentum coefficient (α) need to be judiciously selected. The details of selecting these parameters and the procedure for obtaining an optimal weight set, can be found elsewhere.[30]

Two MLP models (Model-I and Model-II) have been developed to predict the solvent activities: one for the systems at room temperature (298 K) and the other for systems at elevated temperatures (373 K and above). The three important parameters governing the activity values, namely (i) mole fraction of the solvent, (ii) closest approach diameter of the solute (ρ) and (iii) free energy of solvation, constitute the inputs to the network with the activity of the solvent as the sole network output. The second parameter ρ was calculated using the hard-core diameter of the solute, whereas the free energy of solvation was calculated by the Born equation.[8,35]

The solvent composition-activity data of electrolyte solutions belonging to 1:1, 1:2, 2:2, 2:1, and 3:1 types at different temperatures were modeled using ANNs. While the cations considered are alkali metals, alkali earth metal transition and other metals, and organic species like TP, the anions comprise halides, nitrates, acetates, hydroxides, and thiocyanates. The details of the systems studied are provided in **Tables 4A.4 and 4A.5**.

Table 4A.4: Systems at 298 K considered for the ANN-based modeling (Model-I)

Systems:

W-NaCl, W-NaOH, W-NH_4Cl, W-NH_4NO_3, W-CsI, W-$MgCl_2$, W-$MgBr_2$, W-MgI_2, W-CsBr, W-$Zn(NO_3)_2$, W-$ZnBr_2$, W-$Ca(NO_3)_2$, W-CsCl, W-LiBr, W-KCNS, W-$AlCl_3$, W-KI, W-ZnI_2, W-$ZnCl_2$, W-$CaBr_2$, W-$LiNO_3$, W-LiCl, W-KBr

W- KNO_3, W-KCl, W-$MnCl_2$, W-$CaCl_2$

Table 4A.5: Systems at higher temperatures considered for the ANN-based modeling (Model-II)

System	T (K)	Ref	System	T (K)	Ref
w-LiCl	373	12	w-$Ca(NO_3)_2$	373	12
w-LiBr	373	12	D-$LiNO_3$	373	22
w-$LiNO_3$	373	21	D-NH_4NO_3	373	22
w-NaOH	690	27	D-KSCN	373	23
w-NH_4NO_3	373	21	D-$Ca(NO_3)_2$	373	20
w-KOH	690	27	anisole-TP	373	1
w-KNO_3	373	19	1-butanol-TP	373	8
w-AcNa	690	27	nitrobenzene-TP	373	16
w-AcK	690	27			

w = water, D = dimethylsulfoxide, Ack = potassium acetate, AcNa = sodium acetate

For developing the two ANN models, the available data was partitioned into two sets i.e., *training* and *test* sets. While the training set was used for updating the network weights, the test set was used to gauge how well the net- work model is generalizing on new data. The model parameters, namely number of hidden nodes, β, and α were rigorously optimized to obtain the lowest possible RMSE for the test set. Details of the optimized model parameters are tabulated in **Table 4A.6**.

Table 4A.6: Optimized values of the ANN-specific parameters and statistical analysis of model predictions

Model	Hidden Nodes	Patterns		β	α	10^2 $rmse_{train}$	10^2 $rmse_{test}$	CC_{train}	CC_{test}
		Training	Test						
I	4	504	80	0.45	0.01	4.103	4.434	0.943	0.943
II	6	174	22	0.45	0.01	4.715	3.862	0.984	0.981

Upon analyzing the predictions made by Model-I, it is seen that: (i) 87% of the data points can be predicted with greater than 95% accuracy, (ii) 5% of the data with 90-95% accuracy, (iii) 4% data with 80-90% accuracy, and (iv) 4% of the data with accuracy less than 80%. The detailed statistical analysis of Model-I predictions is also presented in **Table 4A.6**, which shows that the correlation coefficient for both the training and test sets predictions is high (= 0.943). This indicates that the network model can be indeed used to predict the solvent activities of electrolyte systems. **Figure 4A.13** shows a comparison of the experimental and Model-I predicted solvent activities.

An analysis of Model-II predictions (also see **Table 4A.6**) shows that the model predicts : (i) 65% of the data points with an accuracy of 95% or higher, (ii) 19% points with 90-95% accuracy, (iii) 9% data with 80-90% accuracy and (iv) 7% points with less than 80% accuracy.

The correlation coefficient values for the training and test sets are 0.984 and 0.981, respectively. The tabulated statistical results (**Table 4A.6**) suggest the excellent capability of the model in predicting the solvent activity of electrolyte systems at 373 K or higher temperatures.

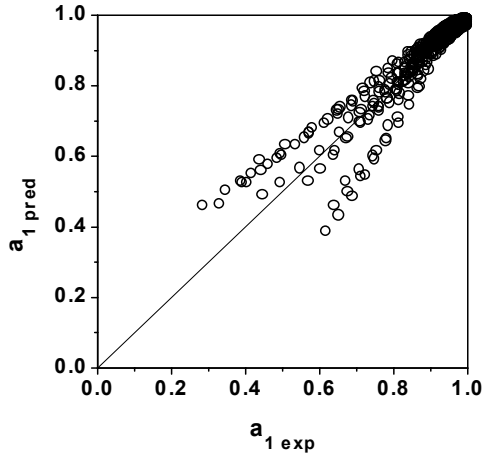

Figure 4A.13: Plot of Model- I predicted solvent activity as a function of experimental solvent activity (at 298 K)

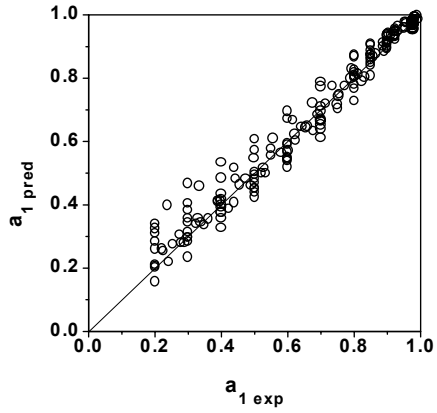

Figure 4A.14: Plot of Model-II predicted solvent activity as a function of experimental solvent activity (for higher temperature)

The plot of the Model-II predicted solvent activities as a function of experimental solvent activities are shown in **Figure 4A.14**.

It can be concluded from this study that ANNs can be used for predicting-with reasonable accuracy, the solvent activities of electrolyte solutions. Considering the fact that the experimental data used for the modeling purpose contain some amount of noise, the prediction accuracy for both the models developed here is sufficiently good to warrant the usage of ANNs in place of traditionally used thermodynamic models. Another important revelation of this study is that ANN can be a powerful tool to predict the vapor pressures of fused salt solutions. This aspect has not been tested before for such a powerful and versatile technique.

Literature Cited:

1. Kumar, A. "Surface Tension, Viscosity, Vapor Pressure, Density, and Sound Velocity for a System Miscible Continuously from a Pure Fused Electrolyte to a Nonaqueous Liquid with a Low Dielectric Constant: Anisole with Tetra-n-butylammonium Picrate." *J. Am. Chem. Soc.* **1993**, 115, 9243 and refs. cited therein.
2. Pitzer, K. S. "Electrolytes From Dilute Solutions to Fused Salts." *J. Am. Chem. Soc.* **1980,** 102:9, 2902.
3. van Laar, J. J. "Sechs Vortrage Uber Das Thermodynamische Potential." *Vieweg-Verlag*, **1906**.

   See also *Z. Phys. Chem*. (Leipzig) **1919**, 72, 723.
4. Prausnitz, J. M, *Molecular thermodynamics of fluid phase equilibria,* **1969**, Prentice Hall, Inc. Englewood Cliffs, NJ
5. Simmrock, K. H.; Janowsky, R.; Ohnsorge, *Critical Data of Pure Substances*; pt.2, Chemistry Data Series Vol. II, Pt. 2 **1986,** DECHEMA, Editors Behrens D, Eckermann, R.
6. Hayden, J.; O'Connell, J. A. "A Generalized Method for Predicting Second Virial Coefficients." *Ind. Eng. Chem. Proc. Des. Dev,* **1975**, 14, 209.
7. Stokes, R.H.; Robinson, R.A., "Ionic Hydration and Activity in Electrolyte Solutions." *J. Am. Chem. Soc.* **1948**, 70, 1870.
8. Pitzer, K.S.; Simonson, J.M. "Ion Pairing in a System Continuously Miscible from the Fused salt to Dilute Solution." *J. Am. Chem. Soc.* **1984**, 106, 1973.

9. Chen, C-C.; Britt, H. I.; Boston, J. F.; Evans, L. B. "Local Composition Model for Excess Gibbs Free Energy of Electrolyte Solutions. Part I Single Solvent, Single Completely Dissociated Electrolyte Systems." *AIChE J* **1982**, 28, 588.
10. Chen, C-C.; Evans, L. B. "A Local Composition Model for the Excess Gibbs Energy of Aqueous Electrolyte System." *AIChE J* **1986**, 32, 444.
11. Braunstein, J. *Ionic Interaction: From Dilute Solutions to Fused Salts*. Petrucci, S., Vol.1. Chapter 4. **1971**.Ed., Academic, New York.
12. Braunstein, H.; Braunstein, J. "Isopiestic studies of Very Concentrated Aqueous Electrolyte Solutions of LiCl, LiBr, $LiNO_3$, $Ca(NO_3)_2$, $LiNO_3$+KNO_3, $LiNO_3$+$CsNO_3$, and $Ca(NO_3)_2$ + $CsNO_3$ at 100 to 150^o C." *J. Chem. Thermodyn.* **1971**, 3, 419.
13. Trudelle, M.-C.; Abraham, M. Sangster, J. "Vapor Pressures of Aqueous Solutions of $AgNO_3$-$TiNO_3$ by the Static Method at 98.5^o C." C*an. J. Chem*. **1977**, 55, 1713.
14. Seward, R. P. "The Electrical Conductance and Viscosity of Solutions of tetra-n-butyl Ammonium Picrate in Anisole, Nitrobenzene and Ethylcarbonate." *J. Phys. Chem*. **1958,** 62, 758.
15. Chen, C -C.; Britt, H. I.; Boston, J. F. "Process Simulation Of Electrolyte Systems" *Proceedings of the 1984 Summer Computer Simulation Conference, Vol. 1, Soc. For Comp. Simulation*, **1984** 552.
16. Sonawane, P. D.; Kumar, A. "Vapor Pressures of Nitrobenzene + Tetrabutyammonium picrate at 373 K." *J. Chem. Eng. Data*. **1998**, 43, 97.

17. Simonson, J. M.; Pitzer, K. S. “Thermodynamics of Multicomponent, Miscible, Ionic Systems: The System $LiNO_3$ – KNO_3 –H_20.” *J. Phys. Chem*, **1986**, 90, 3009.

18. Clegg, S. L.; Pitzer, K. S. “Thermodynamics of Multicomponent, Miscible, Ionic Solutions: Generalized Equations for Symmetrical Electrolytes.” *J. Phys. Chem.* **1992**, 96, 3513; for errata see: Clegg, S. L.; Pitzer, K. S. *J. Phys. Chem.* **1994,** 98, 1368.

19. Sangster, J.; Abraham, M-C.; “ Vapor Pressures of {(1-x) (0.4888 Ag + 0.4612 Tl + 0.0500 KNO_3) + H_2O)} at 371.7 K.” *J. Chem. Thermodyn.* **1982**, 14, 599.

20. Sacchetto, G. A.; Kodejs, Z. “Vapor Pressures of Very Concentrated Electrolyte Solutions. II. Measurements on {(1-x) $(CH3)_2SO$ + x$(CaNO_3)_2$} by a dew point apparatus.” *J. Chem. Thermodyn.* **1983**, 15, 457.

21. Sacchetto, G. A.; Bombi, G. G.; Macca, C. “Vapor Pressures of Very Concentrated Electrolyte Solutions. I. Measurements on {(1-x) H_2O + x $LiNO_3$)} and {(1-x)H_2O + x NH_4NO_3)} by a dew point apparatus.” *J. Chem. Thermodyn.* **1981**, 13, 31.

22. Sacchetto, G. A.; Kodejs, Z. “Vapor Pressures of Very Concentrated Electrolyte Solutions. III. Measurements on {(1-x) $(CH_3)_2SO$ + x((1-y) NH_4NO_3 + y $LiNO_3$)} by a dew point apparatus.” *J. Chem. Thermodyn*, **1984**, 16, 15.

23. Sacchetto, G. A.; Kodejs, Z.; Spalkova, H. “Vapor Pressures of Very Concentrated Electrolyte Solutions. IV. Measurements on{(1-x) $(CH_3)_2SO$ + x KSCN} by a dew point apparatus.” *J. Chem. Thermodyn.* **1988**, 20, 363.

24. Petrenko, S. V.; Pitzer, K. S. "Thermodynamics of Aqueous NaOH Over the Complete Composition Range and to 523 K and 400 Mpa." *J. Phys. Chem.* **1997,** 101, 3589 and refs. Cited therein.
25. Pitzer, K. S.; Li, Yi-gui. "Thermodynamics of Aqueous Sodium Chloride to 823 K and 1 kbar (1000MPa)." *Proc. Natl. Acad. Sci*. U.S.A. **1983**, 80, 7689.
26. Kumar, A. "Experimental Surface Tension and Derived Surface Activities of the Nitrobenzene- Tetrabutylammonium System from 364.1 K at 393.1 K Over the Full Concentration Range."*Fluid Phase Equil*. **1999**, 165, 79.
27. Weres, O.; Tsao, L. "Activity of Water Mixed with Molten Salts at 317^0 C." *J. Phys. Chem*, **1986**, 90, 3014.
28. Pitzer, K. S, *personal communication,* **1996**, data are available to readers.
29. Tambe S. S., Kulkarni, B. D. and Deshpande, P. B., "*Elements of Artificial Neural Networks with Selected Applications in Chemical Engineering, and Chemical & Biological Sciences*." **1996**, Simulations and Advanced Controls, Louisville, KY.
30. Nandi S.; Ghosh S.; Tambe S. S.; Kulkarni, B. D. "Artificial Neural Network Assisted Stochastic Process Optimization Strategies." *AIChE J.*, **2001,** 47, 126.
31. Alvarez, E.; Riverol, C.; Correa, J. M.; Navaza, J. M. "Design of a Combined Mixing Rule for the Prediction of Vapor-Liquid Equilibria using Neural Networks." *Ind. Eng. Chem. Res*., **1999,** 38, 1706.
32. Sandler, S.; Wong, D., "A Theoretically Correct Mixing Rule for Cubic Equations of State." *AIChE J*., **1992,** 38, 671.
33. Michelsen, M. L.; Kistenmacher H. "On Composition Dependent Interaction Coefficient." *Fluid. Phase. Equilib*., **1990,** 58, 229.

34. Rumelhart, D.E.; Hinton, G. E.; Williams R. J. “Learning Representations by Backpropagating Errors.” *Nature*, **1986**, 323, 533.

35. Born, M., “Volumes and Heat of Hydration of Ions.” *Z. Physik.* **1920**, 1, 45.

B. SURFACE TENSION

4B.1 Background:

An important property that gives us information on the solute-solvent interactions in surface and bulk phases is surface tension of the system. The general trend of surface tension is:

a) addition of solute to solvent, in general, increases the surface tension of the solvent, although not to a considerable extent. In general, strong electrolytes show this type of behavior, b) addition of solute causes a gradual decrease in the surface tension of the pure solvent. Weak and non-electrolytes are often seen to show this type of behavior, and c) some very important types of substances are classified under this category and are called as surface active agents. This type of substances posses the ability to decrease the surface tension of water to a large extent even by addition of small amounts of it. Certain sulfonic acids, sulfonates and other types of organic compounds come under this category. Solutes, which decrease the surface tension, are said to exhibit positive surface activity, while those, which tend to increase the surface tension, are said to have a negative surface activity.

During our investigation on the surface and thermodynamic properties of continuously miscible systems consisting of a pure fused electrolyte and a solvent, it has been noted that no accurate expressions for calculating the surface tension of such systems are available in the literature. In addition, a literature survey further reveals that the same is true for liquid mixtures. In

the past, surface tension data of binary liquid mixtures have been analyzed using the Bertrand-Acree-Bruchfield, Acre and Bertrand and the Flory equations.[1-4] Other empirical, semi-empirical and statistical methods have been employed to quantify the surface tension of the mixtures.[5-9] It is, however, noted that the predictive accuracy of several of these methods is as poor as 4 per cent. Earlier, notable empirical contributions in this direction are by Sprow and Prausnitz and Guggenheim.[10,11] The scaled particle theory for the mixture when applied to molten systems partially accounts for their non-ideality.[12,13] Some of models that are noted above are briefly summarized below:

According to Gibbs the surface activity is due to unequal distribution of solute between the surface and the bulk of the solution.[14] On purely thermodynamic argument he deduced that, if a solute distributes itself so that the surface contains q moles of solute per 1 cm^2 of area in excess of that present in the body of the solution, then for dilute solutions q at equilibrium should be given by

$$q = -C / R T \, d\sigma / dC \quad \text{(Gibbs adsorption equation)}$$

where C is the concentration of the solute, T is the temperature in Kelvin, R is the universal gas constant and $d\sigma / dC$ is the concentration gradient of surface tension of the solution.

In contrast to the treatment of Gibbs, van der Walls and Bakker treated the surface as a layer of small but finite uniform thickness.[15] This treatment is applicable to a system of single component i.e. a surface separating a simple

liquid from its vapor. Another method was put forth by Verschaffelt, where he has treated surfaces between phases of several components, recognizing explicitly the finite thickness of the surface the surface layer.[16] Guggenheim while agreeing with the principle of Verschaffelt, extended the treatment for the surface between phases of several components.[17] In the Guggenheim model the thermodynamic properties of a plane interface are derived by treating the interface as having a finite thickness. Formulae are derived for the dependence of the interfacial tension on the temperature and composition of one of the two bounding phases; the pressure not being an independent variable is eliminated. His equation is given as:

$$-d\sigma = h^{\sigma}\, dT / T + \sum_{r}{}'(T_r - x_r^{\alpha}\, T_1 / x_1^{\alpha})\, R\, T\, D \log p_r^{\alpha}$$

where h^{σ} = heat absorbed when unit area of surface layer σ is formed reversibly at constant T and P , r = number of components, p_r^{α} = fugacities.

The derived formulae are found to be invariant with respect to the thickness arbitrarily assigned to the interfacial layer. It is seen that the formulae so derived for the plane interfaces can be safely applied to curved interfaces provided that the thickness of the inhomogeneous layer is negligibly small as compared to its radius of curvature. The surface tension of dilute solutions has been treated theoretically by Langmuir, Frumkin, and Butler but none of these involve the surface tension of the second component, and the equations are basically unsymmetrical.[18-20] Later Schuchowitzky,

Belton and Evans, and Guggenheim have formulated the surface tension of ideal and regular solutions in terms analogus to those used in the treatment of homogeneous liquid solutions.[11,21,22] Although the method of derivation is different, the assumptions and the final equation of these methods are identical.

The above equation is same as first proposed empirically by Szyszkowski and later discussed by Langmuir.[18,23] Application of this equation by Schuchowitzky to solutions of benzene in ether and benzene in nitrobenzene produced excellent results. A comparison of the experimental data on the surface tension of mixtures, which form ideal or nearly ideal solutions in the bulk phase by Belton and Evans was found to be in good agreement with the surface tension of mixture calculated by the above equation. The mixtures discussed above all were of non-polar nature and further the difference in the surface tension of two components were nearly equal and they behave as ideal solutions.

However, the above equation is found to be inaccurate to mixtures, which differ significantly in their molar surface areas; and to the mixture of solutions of polar + non polar types, such solutions can be thought as to be behaving non-ideally and showing deviations from ideal solutions.

Since the various models discussed above, cannot correlate the experimental surface tension data of systems showing deviations from ideal behavior, and also of the system differing widely in their molar surface area,

several models are suggested to take into account the non-ideality of the systems as well as the difference in the molar surface area.

In 1950 Prigogine and Sarolea put forth the first molecular theory for the surface tension of chain molecule mixtures[24]. In this model, the liquid is represented by a regular crystalline lattice (the quasi-crystalline model of a liquid), on which molecules of type I and II are distributed. Molecules of type I occupy one lattice site (monomers) while type II occupies r connected lattice sites (r-mers). Further the molecules of type II are supposed to be open, unbranched chain (rigid and flexible). The energies of interactions between various components are denoted as follows: Σ_{11}, between two nearest neighboring monomers, Σ_{12} between a monomer and a neighboring r-mer segment, and Σ_{22} between adjacent segments of r-mer. The surface tension can then be found out by differentiating the free energy with respect to the surface of the solution, given by

$$A = N^{\sigma} å,$$

where å is the area occupied by one lattice point. It was found that the surface tension calculated in this way differed from that obtained on the basis of the parallel layer model.

The parallel layer model is a simple model based on the division of the solution in successive layer, and it is assumed that only the first layer has a composition different from that of the bulk phase. The equation for the surface tension from the statistical thermodynamics comes out to be $\sigma = \sigma_A \varphi_A + \sigma_B \varphi_B$, where σ_A and σ_B are the surface tension of pure components, φ_A and φ_B are

the volume fractions. This model was later modified for the special case, in which rigid molecules only were considered and only those configurations in which all the r-mers are arranged parallel to the surface. This model was chiefly developed for athermal solutions. Gaines et. al. later modified this equation by adding an additional term β, the interaction parameter.[25] If $\beta = 0$ the equation reduces to the equations for the athermal solutions of Prigogine – Marcheal.

Application of this model by Aveyard, and Edmunds and McLure to the surface tension data of mixtures of several n-alkanes from C_6 to C_{16} and to the solutions of n-alkane + dimethylsiloxanes mixtures shows that the Prigogine model gave excellent agreement with the experimental values.[8,26] However, this theory cannot evaluate chemical potential of bulk mixtures, also it is seen to be inapplicable in calculating the surface tension where the relative adsorption is weak.

The model of regular solutions discussed above is a very simple, single parameter based model related to the difference between the interactions of various kinds. However, in real solutions the situation is not so simple, but there exists between two molecules a potential energy of interactions depending on the distance between the molecules and their orientation, which cannot be characterized by a single parameter. To over come the above limitations a more refined statistical model was developed based on the combination of cell model with the principle of corresponding states. Prigogine et al. describes the details of the model.[27] The experimental surface tension

data of the systems cyclohexane + carbontetrachloride, cyclohexane + neopentane, carbon tetra chloride + neopentane and benzene + neopentane were compared against the results of calculation obtained by using the above equation and it was seen that the calculated values were in good agreement with the experimental values considering the fact that no adjustable parameters were required.

Later on, Bellemans extended the above theory for the surface tension of mixtures of small molecules to mixtures of chain molecules.[28] The essential feature of this theory is that the surface tension of both the components of the mixture and of the mixture itself obey the same reduced surface equation of state. Application of this model to the solutions of n-alkane + dimethylsiloxanes at 303.2 K shows relatively poor agreement with the experimental values. However, the variation of σ^{E}_{φ} with chain length is well reproduced qualitatively.

Another important empirical method to estimate the surface tension based on the principles of corresponding states (PCS) is the Brock and Bird model.[29] This model is based on the modifications of the PCS. They define surface tension in terms of reduced surface tension. This equation was applied to 84 substances of widely differing characters for which surface tension and critical data were available. These substances include noble gases, diatomic, polyatomic inorganic substances, normal and branched paraffins, alkyl benzenes, unsaturated hydrocarbons, esters, organic compounds etc., over the range of available data. The average error was

found to be 6.2%. However, for the light atoms and molecules, molten metals, highly polar inorganic substances, highly associating substances and fused salts could not be correlated by this equations.

A model based on the assumption that the surface tension is a linear function of the surface layer mole fraction was put forward by Eberhart.[30] The condition for equilibrium between the surface layer and the bulk liquid phase provides a relation ship between the surface and the bulk compositions as:

$$\sigma = y_A \sigma_A + y_B \sigma_B$$

where, σ_A and σ_B are the surface tension of pure components, y_A and y_B are the surface phase mole fractions. A separation factor S, termed as the surface enrichment factor for the component having lower surface tension is defined as $S = (y_A / y_B) / (x_A / x_B)$ and the surface tension in terms of the bulk mole fractions can be expressed as:

$$\sigma = (S x_A \sigma_A + x_B \sigma_B / S x_A + x_B)$$

Surface tension data on a variety of alloys, fused salt, organic and inorganic liquid mixtures have been tested with the above equation and were found to be in good agreement with the experimental values. In addition to this the surface tension data of the fused salt $RbNO_3$- KNO_3 system at 350^0C reported by Bertozzi and Sternheim was fitted with this equation with a value of S = 1.43.[31] The surface tension data for isooctane + benzene system at 30^0 C were also fitted with good accuracy by using the value of S = 3.12.[32] The advantage of this model is that if the surface tension of a mixture A and B and another mixture of B and C at the same temperature is known, then the

surface tension for a mixture of A and C can be calculated at this temperature by using S (A,B) S (B,C) = S (A,C). This relation was tested for the surface tension data of fused-alkali nitrate systems with an precision of 3 % for the S values.

Another model proposed by Sanchez is based on a generalized square-gradient approximation for the free energy density of a non-uniform fluid.[33] It gives a relation between the surface tension and isothermal compressibility and mass density.

$\sigma\ (k / \rho)^{1/2}\ A_0^{1/2}$ = constant in the normal liquid range.

It is observed that except for water A_0 is temperature independent for a variety of organic, inorganic, and polymer liquids, including hydrogen-bonding liquids, $A_0^{1/2}$ appears to be invariant. Same is the case among diatomic elements (except hydrogen), among heavy noble elements, and also for the quantum noble elements helium and neon. The constant A_0 is shown proportional to a second moment of a direct correlation function. A semiempirical formula has been derived for A_0 relating it to parameters Σ_0 and σ_0 that characterize the pair interaction potential.

The model of Sprow and Prausnitz is based on a thermodynamic treatment, the fundamental assumption of this treatment is that the surface layer is represented by a physical region of constant and uniform composition, located between the bulk and vapor phases.[10] Thus we have:

$$A_i\ \sigma^M = -R\ T\ \ln a_i^B + \sigma_i\ A_i + R\ T\ \ln a_i^S$$

Where A_i is the partial molar surface area of component i, in the surface mixture, a_i^S and a_i^B are the activities in the surface and bulk liquid phase, respectively. The activity coefficient effects are introduced *via* a_i. This equation has been applied with good success to calculate the excess surface tension for the system nitrogen + carbon monoxide, argon + methane, and carbon monoxide + methane. Comparison of the surface tension data calculated using this equation is seen to be in good agreement with the experimental values for several simple systems. Similarly this equation in conjunction with Wilson equation has been successfully employed by Wilson to correlate the surface tension of several complex mixtures.[34] In all the cases the agreement is quite good and approaches the estimated experimental accuracy in most of the cases.

Another important theory, known as the scaled particle theory (SPT) put forward by Lebowitz, et.al. has been used to study variety of problems.[12] They extended the pure component theory of hard sphere system to calculate the surface tension of real systems. This theory is based on the consideration of an approximate expression for the work of adding an additional hard sphere to a mixture.

$$\sigma = W'' (O) / 8\pi$$

$$= (3 k T / 2 \pi) \{2 [\delta_1 / (1 - \delta_3)] + 3 [\delta_2 / (1 - \delta_3)^2]\}$$

W '' (O) arises out of cubic expression of W (R) i.e the change in the configuration part of the Helmholtz free energy upon adding the solute hard sphere particles of radius r to the system.

This theory was applied to compare the experimental excess surface tensions of N_2 - Ar, CH_4 – Ar, and CH_4 – N_2 with those calculated by the use of this equation. This theory fails to predict the asymmetry of the excess surface tension evident in the experiments. Whereas, a fairly good agreement with the experimental surface tension data of one- component liquids is observed.[35,36] The SPT has also been applied to a binary molten salt-solvent system.[13] It was observed that the excess surface tension was correctly represented qualitatively by SPT. The estimates were found to be in good agreement with the experimental quantities. However, an asymmetric parabola with a maximum value of $x_1 = 0.4$, (where x_1 is the mole fraction of the solvent) as indicated by the experiment is not correctly predicted by the SPT.

In their elaborate work Goldsack and Sarvas have derived explicit and implicit equations for the surface tension using both mole fraction and volume fraction statistics.[7] Their derivation is based on the same assumptions as assumed by Prigogine and Butler that the surface layer can be treated thermodynamically as a phase separate from the bulk phase. Starting with the Butler's equation they derive an explicit mole fraction based equation for the surface tension of binary mixtures given by:

$$\sigma = (\sigma_1 x_1 + \sigma_2 x_2) + R T x_1 x_2 \Delta [(A_2 - A_1) / A_1 A_2]$$

$$- \quad R T/ 2 \; x_1 x_2 \Delta^2 [A_1 x_1 + A_2 x_2 / A_1 A_2]$$

Similar equations were derived on volume fraction basis. A variety of binary mixtures with increasing (σ_2 - σ_1) values were chosen to the test the equations. It is seen that the equations based on the volume fraction statistics give better accuracy over the corresponding ideal mole fraction statistics. With increasing (σ_2 - σ_1) difference, there is an increasing deviation from ideal equations behavior no matter what form of ideal equations is used. Whereas, the resultant equations are able to account for the concentration dependence of the surface tension of binary solutions with a wide range of polarity (i.e. polar- polar, non-polar-non-polar, and non-polar-polar) within an average error of less than 1% using these equations. For some systems like 1, 2-dibromoethane + benzene; phenol - benzene the average error was substantially larger. This discrepancy was attributed to the surface orientation effects, which required molar area values A_i much different from those calculated using the assumption that the bulk density gives a good first estimate of these molar area values. Alternately, this deviation can be explained on the basis that the mixture does not form ideal solutions to a first approximation. Activity coefficient effects could be invoked to account for this, possibly by using regular solution behavior. For over 90% of the binary systems studied, however, the ideal solution approximation coupled with the use of bulk densities for calculating molar surface area values has been shown to be useful. However, these results are found in the cases where the difference in the surface tension of pure substances is less than 20×10^{-3} N m^{-1}. It is seen that with increasing (σ_2 - σ_1) values, substantial large errors

are obtained in the surface tension values calculated by the use of the above equations. This is due to the need for expansion of the logarithmic expression to its first order term in Δ in order to derive an explicit expression for Δ in terms of bulk parameters. Furthermore, the higher order expansion terms generally shows diverging values. To overcome this limitation an implicit equation with first or second order approximations to the implicit σ term on the right hand side is derived from the explicit Δ function approach. For such systems, where the (σ_2 - σ_1) values were large, use of implicit equations showed decrease in the errors. Furthermore, it was generally found that equations based on volume fraction statistics gave better results as compared to the mole fraction based equations.

For those systems where the explicit higher order terms in the equations for the surface tension showed divergence, it was found that the implicit forms of the surface tension equations gave excellent agreement with the experimental data with an average error less than 1%.

The resultant equations when applied to the system glycerin- ethanol, where the (σ_2 - σ_1) value is greater than 30 x 10^{-3} N m^{-1}, neither the explicit nor the implicit equations were able to account for the deviation in the surface tension values. This is particularly true for the aqueous systems. It seems that for such systems the assumption of ideal or near-ideal solutions is not valid and activity coefficients in the surface and bulk chemical potential would have to be taken into account in deriving surface tension equations for such mixtures.

The Goldsack - Sarvas equation has also been used to analyze the surface tensions of the molten binary and ternary component systems containing charged species of inorganic and organic types in aqueous and non-aqueous solvents. Fits of the surface tension vs. x by the Goldsack - Sarvas equation without adjustable parameters were noted to be satisfactory, but not highly accurate as desired considering the non-ideality of the systems.[13,37]

In view of the above, we set our goal to develop a suitable expression to estimate the surface tension of binary liquid mixtures. We then, intend to apply the proposed method to estimate the surface tension of the systems comprised of a fused organic salt dissolved in a polar or non-polar solvent.

4B.2 Our Proposal of Equations for Correlation of Surface Tension

We begin with a general Butler equation for correlating the surface tension of a binary mixture, σ with that of pure components, σ_1 and σ_2 as[20]

$$\sigma = \sigma_1 + (RT / A_1) \ln (x_{1,s} / x_{1,b}) \qquad (1a)$$

and

$$\sigma = \sigma_2 + (RT / A_2) \ln (x_{2,s} / x_{2,b}) \qquad (1b)$$

where, A_1 and A_2 are the molar surface areas of components 1 and 2, respectively. $x_{1,s}$ and $x_{1,b}$ denote mole fractions of component 1 in the surface and bulk phases, respectively with analogous definitions of $x_{2,s}$ and $x_{2,b}$. R and T have usual significance. Hansen and Soger have presented a critical description of the equations to correlate the surface tension of liquid mixtures using Raoult's law.[38]

Multiplication of Equations (1a) and (1b) by $x_{1,b}$ and $x_{2,b}$, respectively and the subsequent addition of the resultant equations yield:

$$\sigma = \sigma_{id} + RT [(1 / A_1)x_{1,b} \ln (x_{1,s} / x_{1,b}) + (1 / A_2)x_{2,b} \ln (x_{2,s} / x_{2,b})] \quad (2)$$

In Equation (2) $\sigma_{id} = \sigma_1 x_{1,b} + \sigma_2 x_{2,b}$ is the surface tension of mixture on the basis of ideal mixing.

In order to estimate σ from Equation (2), knowledge of the surface mole fractions, $x_{1,s}$ and $x_{2,s}$ is required. Relationship of $x_{1,s}$ with $x_{1,b}$ can be understood considering a dimensionless difference parameter δ, comprising of two components i.e. δ_p and δ_m under certain conditions as:

$$x_{1,s} = x_{1,b} + x_{1,b} x_{2,b} \delta_p + x_{1,b} x_{2,b}^2 \delta_m \quad (3)$$

and

$$x_{2,s} = x_{2,b} - x_{1,b}\ x_{2,b}\ \delta_p - x_{1,b}\ x^2_{2,b}\ \delta_m \qquad (4)$$

bearing in mind $x_{1,s} + x_{2,s} = 1$

This definition of surface mole fractions involving δ is different from the one proposed by Defay et al.[39] It will be seen later that the proposed definition is more accurate than the one suggested by these authors.

From Equations (3) and (4) we obtain the ratios of the mole fractions in surface and bulk phases as:

$$\ln (x_{1,s} / x_{1,b}) = \ln (1 + x_{2,b}\ \delta_p + x^2_{2,b}\ \delta_m)$$
$$= \ln (1 + x_{2,b}\ \delta) \qquad (5)$$

and

$$\ln (x_{2,s} / x_{2,b}) = \ln (1 - x_{1b}\ \delta_p - x_{1b}\ x_{2,b}\ \delta_m)$$
$$= \ln (1 - x_{1,b}\ \delta) \qquad (6)$$

where

$$\delta = \delta_p + \delta_m\ x_{2,b} \qquad (7)$$

Substitution of Equations (5) and (6) in Equation (2) yields:

$$\sigma = \sigma_{id} + RT\ [(x_{1,b} / A_1 \ln (1 + x_{2,b}\ \sigma)$$
$$+ (x_{2,b} / A_2) \ln (1 - x_{1,b}\sigma)] \qquad (8)$$

Since the product of mole fraction with δ is much less than unity, expansion of the logarithmic terms to their first term yields:

$$\sigma = \sigma_{id} + RT\, x_1\, x_2 \quad (1 / A_1 - 1 / A_2)\, \delta \qquad (9)$$

where for binary mixtures $x_{1,b} = x_1$ and $x_{2,b} = x_2$.

Thus, Equation (9) yields

$$\sigma = \sigma_{id} + RT\, x_1 x_2\, (1 / A_1 - 1 / A_2)\, [\delta_p + \delta_m\, x_2] \qquad (10)$$

Equation (10) is a complete working equation for correlating surface tension of a binary mixture and satisfies the limiting conditions. Two unknown parameters δ_p and δ_m can be evaluated from the experimental surface tension-composition data.

In order to examine the validity of Equation (10) for the estimation of the σ data of several binary liquid mixtures, we chose compounds of different nature i.e. aliphatic, aromatic hydrocarbons, their halide and other derivatives like alcohols, ketones, etc. The range of selection of binary solvents includes highly non-polar to highly polar molecules. In **Table 4B.1** the entry numbers of the components employed in the present study are listed. Before applying Equation (10) to the surface tension data, it is essential to note that the values of molar surface area, A, are calculated with high accuracy. There are

however, different methods for calculating the molar surface area values.[8,9] One such method assumes the surface layer to be strictly a monolayer where A is related to molar volume $V^{2/3}_1$ using a single constant.[10] Such an assumption for calculating A requires the molecules to be spherical. Molecules of the species used in general are not spherical in shape. Another useful method to calculate A is again based on the $V^{1/3}$ as:[40]

$$A = \pi [0.007225 - V^{1/3} (0.023171 - 0.01858 V^{1/3})] \quad (11)$$

In addition, Marcus has tabulated the molecular diameters for several solvents both from experimental data and from a correlation derived by Kim.[40,41] The tabulation is a useful compilation for calculating the molar surface area. Equation (10) was tested against the experimental σ data of several binary liquid mixtures. These systems are listed in **Table 4B.2** together with the source of data and the adjustable parameters, δ_p and δ_m obtained from a least squares fit of the σ data.

Table 4B.1: Entry names for the compounds used in **Table 4B.2**

Entry Name	Compound	Entry Name	Compound
ACET	Acetic acid	ACT	Acetone
ANIS	Anisole	BENZ	Benzene
CB	Chlorobenzene	CDS	Carbon disulfide
CF	Chloroform	CP	Cyclopentane

CT	Carbon tetra chloride	CX	Cyclohexane
D	di methyl sulphoxide	DMF	di methyl formamide
DOX	Dioxane	EGY	Ethylene glycol
GBL	γ -butyrolactone	GLY	Glycerol
MOL	Methanol	MXY	m- xylene
NB	Nitrobenzene	PHE	Phenol
POL	1- propanol	PROAC	Propionic acid
PXY	p- xylene	TP	Tetra-n-butylammonium picrate
TCE	Tetra chloro ethylene	THF	Tetrahydrofuran
TOU	Toluene	W	Water

In such a type of equation, it is essential to employ the appropriate values of the surface tension of the pure components, as the determination of δ_p and δ_m will depend upon the differences of the experimental σ of mixtures and those of the pure components. We have used the pure component σ values directly from the main source of data. It is noted that the Equation (10) can accurately describe the σ data for a variety of systems. Agreement between experimental, σ_{EXP} and the calculated σ_{CAL} surface tension values for several systems is shown in the form of average per cent error, APED, in **Table 4B.2**.

Table 4B.2: Results of calculations by Equation (10) for estimating surface tension, σ of mixtures together with adjustable parameters

System	$\delta p \times 10^{24}$	$\delta_M \times 10^{24}$	APED* %	T / (K)	Source of Data
	Binary	Liquid	Mixtures		
ACET-GLY	-5.887	-44.75	1.09	298	42
ACT-BENZ	-0.6532	3.101	0.42	298	43
BENZ-CB	-2.348	-0.7523	0.86	293	44
BENZ-CX	-1.686	-5.063	0.20	293	45
BENZ-D	15.72	-1.662	0.37	303	46
BENZ-DOX	1.038	-0.9697	0.16	293	45
BENZ-NB	-35.15	-62.35	0.29	293	45
BENZ-PHE	24.09	11.58	0.25	298	47
CB-D	2.726	1.367	0.44	303	46
CB-MXY	-0.5803	-0.3784	0.13	293	44
CB-PXY	0.8257	-15.58	0.37	293	44
CDS-BENZ	-8.644	7.851	0.91	298	43
CF-D	140.5	-14.07	0.78	303	46
CP-BENZ	-1.222	-0.9045	0.14	298	48
CP-CT	-38.01	36.84	0.05	298	48
CP-TCE	-7.981	-13.91	0.02	298	48
CP-TOU	-5.170	-3.407	0.05	298	48
CT-CB	-3.380	-9.192	0.20	293	49
CT-D	26.04	7.985	0.98	303	46

CX-CB	5.770	12.25	0.18	293	49
CX-DOX	-0.6093	4.018	0.45	293	45
CX-NB	35.02	43.63	1.00	293	45
CX-TCE	5.284	4.202	0.40	298	48
CX-TOU	7.283	1.904	0.10	298	48
D-GLY	149.8	-165.4	0.63	298	42
DOX-CB	-1.463	1.380	0.01	303	50
DOX-MXY	-9.780	9.902	0.15	303	50
DOX-NB	-1.697	1.254	1.10	293	45
DOX-TOU	3.156	-6.412	0.13	303	50
DMF-GLY	-88.5	325.	0.97	298	42
MOL-GLY	10.49	-41.55	2.19	298	42
POL-GLY	-48.38	1950	2.25	298	42
PROAC-GLY	-202.3	1593	4.19	298	42
THF-GBL	47.12	52.98	0.16	298	51
TOU-D	5.402	0.630	0.09	303	46
W-GBL	-5.110	3.917	0.35	303	51
W-EGY	-11.335	11.363	1.25	303	52
		Fused salt solutions			
W-(AgTl)NO_3	0.2022	-1.930	0.82	373	37
W-(AgTlCs)NO_3	-0.4382	-0.0856	0.61	373	37
W-(AgTlCd)NO_3	-0.5099	0.5352	0.62	373	37

W-(AgTlCa)NO_3	-0.0586	0.0420	0.59	373	37
ANIS-TP	1.163	5.422	0.20	373	13

Let us examine the performance of Equation (10) in correlating the σ data. In **Figure 4B.1(a) and (b)** a comparison of experimental data points with the calculated lines as a function of mole fraction is shown. An excellent agreement between the σ_{EXP} values with those of σ_{CAL} values is seen over the whole concentration range in **Figure 4B.1(a)**, where the data are plotted for the binary mixtures of cyclohexane with chlorobenzene (293K) and with dioxane (293K), chlorobenzene with DMSO (303K) and cyclopentane with tetrachloroethylene (298K). The APED values calculated by the use of Equation (10) and experimental data are 0.18, 0.45, 0.44 and 0.02 for the CX-CB, CX-DOX, CB-D and CP-TCE systems, respectively. Similarly, the σ_{CAL} of mixtures, for instance, benzene – dioxane (293K), benzene – phenol (298K), dioxane - toluene (303K) and toluene - DMSO (303K) shown in **Figure 4B.1(b)** depict excellent agreement (APED = 0.16, 0.25, 0.13 and 0.09, respectively) with the experimental values in the surface tension range from 0.022 to 0.042 Nm^{-1}.

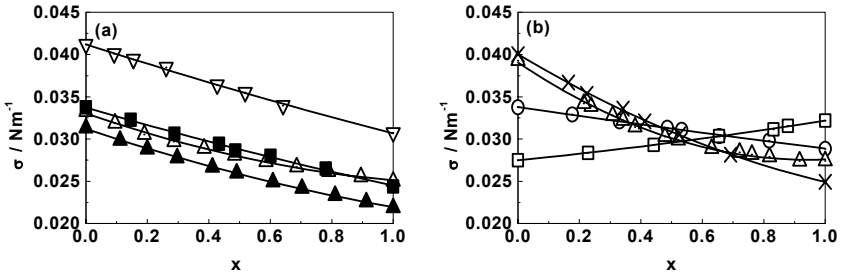

Figure 4B.1: Plots of surface tension, σ (Nm^{-1}) vs. mole fraction, x; points: experimental Solid lines calculated by Equation (10) **(a)** ▲ CX - CB, ■ CX - DOX, ∇ CB - D, Δ CP -TCE **(b)** o BENZ - DOX, Δ BENZ -PHE, □ DOX -TOU, X TOU – D

A stringent test of the surface tension equations lies in correlating the $\sigma^{ex} = (\sigma_{EXP} - \sigma_1 x_1 - \sigma_2 x_2)$ values. Results of such correlations are shown in terms of σ^{ex}_{EXP} versus σ^{ex}_{CAL} in **Figure 4B.2 (a) and (b)** for eight systems, i.e. dioxane - m-xylene, dioxane - chlorobenzene, cyclohexane – toluene, cyclopentane- carbontetrachloride, chlorobenzene - p xylene, chloroform – DMSO, cyclohexane- nitrobenzene and benzene - nitrobenzene. An interesting and powerful aspect of the proposed equation is its validity in the wide range of σ^{ex} ranging down to -5 x 10^{-3} N m^{-1}. In **Figure 4B.2 (a)**, a maximum deviation of -0.4 x 10^{-3} Nm^{-1} in σ^{ex} is seen only at one composition for the system chlorobenzene - p-xylene. Otherwise, the deviations between experimental and calculated values by Equation (10) are very small and at random. Further, our claim of success of Equation (10) is backed by the results of σ^{ex}_{EXP} versus σ^{ex}_{CAL} for other systems like, chloroform - DMSO, cyclohexane - nitrobenzene and benzene - nitrobenzene, where excellent

agreement between the calculated and experimental quantities is noted. This agreement is shown in **Figure 4B.2(b)**, where the range of σ^{ex} is down to - 5 x 10^{-3} Nm^{-1}. From these illustrations and analysis of other systems, one can again see that Equation (10) can be used with confidence to calculate the non-ideal component of the mixture surface tension data for different mixtures.

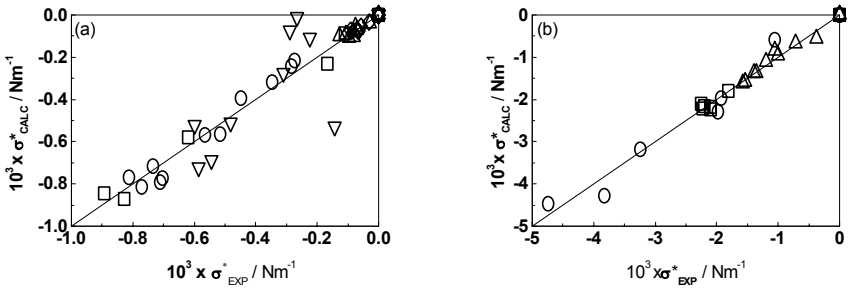

Figure 4B.2: Calculated excess surface tension, σ^{ex}_{CALC} (Nm^{-1}) = σ_{CALC} - σ_{id} ; vs. experimental excess surface tension σ^{ex}_{EXP} (Nm^{-1}) = σ_{EXP} - σ_{id} where $\sigma_{id} = \sigma_1 x_1 + \sigma_2 x_2$ **(a)** Systems: ❒ DOX - MXY, ◊ DOX - CB, o CX - TOU, Δ CP - CT, ∇ CB - PXY. **(b)** ❒ CF - D, o CX - NB, Δ BENZ - NB.

In the past, equations based on volume and mole fractions have been employed to calculate σ of binary mixtures.[7,21] In an elaborate work, Goldsack and Sarvas claimed that the surface tension data of mixtures could be estimated without using any adjustable parameters.[7] In **Figure 4B.3 (a) and (b)**, comparative plots are given showing the performance of our equation as compared to those obtained from the methods of Goldsack and Sarvas, Sanchez, and Brock and Bird for a few representative systems.[7,29,33] In the Sanchez method use is made of the adiabatic compressibility together

with the density of the pure components for calculating the mixture surface tension, while the Brock - Bird equation requires the critical constants of pure components as the input parameters. An examination of **Figure 4B.3 (a) and (b)**, where a few systems (cyclohexane –toluene, cyclohexane – chlorobenzene, and benzene – chlorobenzene, benzene – cyclohexane) are chosen for the sake of illustration, shows that our equation correlates the surface tension of these systems with excellent accuracy.

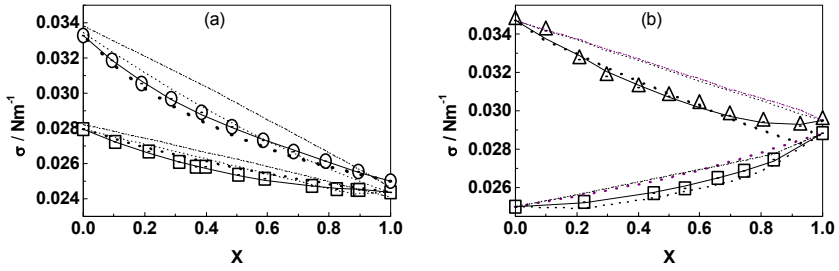

Figure 4B.3: Performance of the proposed Equation (10) in calculating σ (Nm^{-1}) as compared to other equations; Points are σ_{EXP} (Nm^{-1}). **(a)** ❒ CX - TOU, o CX - CB,: σ_{CALC} (Nm^{-1}); solid line σ_{CALC} (Nm^{-1}) by Equation (10), dots by Sanchez equation; dash by Goldsack-Sarvas equation, dash dot dot: σ_{CALC} (Nm^{-1}) by Brock-Bird equation. **(b)** Δ BENZ - CB, ❒ BENZ - CX, calculated lines are the same as in **(a)**

The prediction of surface tension by the Sanchez and the Brock - Bird methods is very poor and deviate strongly from the experimental data. The reasons for such poor predictions by these equations can be easily traced to the linear dependence of the input parameters on the mole or volume fractions. Thus, the predicted surface tensions by the Sanchez and the Brock-Bird method show a linear change with compositions contrary to the

experimental findings, where non-ideality is prominent. The Goldsack - Sarvas equation, based on the volume or mole fractions yield better results as compared to the Sanchez and the Brock - Bird equations. From the analysis of these data, APED as obtained by the Sanchez, Goldsack - Sarvas, and Brock - Bird equations is about 2 per cent. On the contrary, our equation demonstrates higher capability of correlating the surface tension data with APED to be about 0.27 per cent for these systems.

If the systems are chosen in which one component is common, one observes a strong correlation between the δ_p or δ_m values and the relative permittivity, ε, of the uncommon components. This is shown in **Figure 4B.4**, where the δ_p or δ_m values are plotted against ε for systems of glycerol with propanoic acid, 1-propanol, methanol, DMF and DMSO. It is seen from the plots of **Figure 4B.4** that an increase in ε leads to strong variation in δ_p or δ_m values. In the above series of glycerol containing mixture, a deviation from the smooth correlation is noted in the case of acetic acid, which can be attributed to the associative nature of the acid.

In **Figure 4B.4** the variation of δp or δm with increasing ε is also shown for the systems containing DMSO as a common component with chloroform, carbon tetrachloride, benzene, toluene and chlorobenzene. It is not certain why the increase in polarity of medium leads to a decrease in the δ_p or δ_m values. Factors like, specific interactions and their variations with the polarity appear to be responsible for such behavior. This subject is an ongoing study in our laboratory.

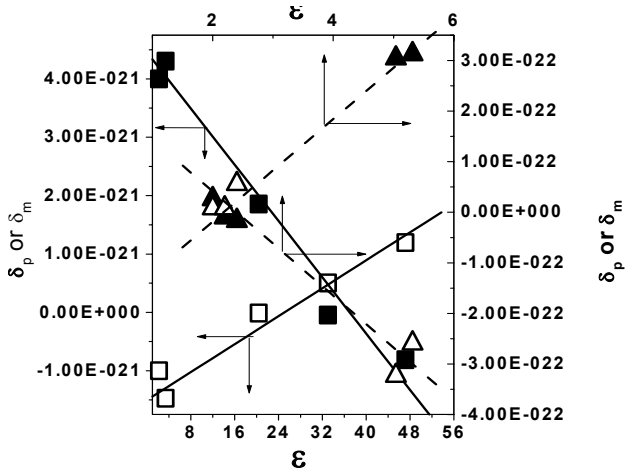

Figure 4B.4: Correlation of the system-specific parameter, δ_p and δ_m with relative permitivity, $\in$ of one of the components. ❒ (δ_p), ■ (δ_m) GLY - PROAC, - POL, - MOL, - DMF, - D. plots shown using solid line; ▲ (δ_p) Δ (δ_m) ; D - CF, -CT,- BENZ, - TOU, - CB. Plots shown using broken line

4B.3 Temperature Dependence of Surface Tension Data:

Equation (10) can be applied at different temperatures considering the δ_p and δ_m parameters varying with temperature as:

$$\delta_p \text{ or } \delta_m = a + b\,T + c\,T^2 \qquad (12)$$

Adjustable parameters obtained from Equation (12) are listed in **Table 4B.3** in order to conserve space only for three systems together with the APED. From the results, it is seen that Equation (10) in conjunction with Equation (12) can successfully describe the temperature dependence of surface tension of mixtures. It is important to note that constants for these systems are obtained in a temperature range from 278 to 423 K. In this

temperature range the δ_p and δ_m parameters are non-linear with temperature. A linear fit of δp and δm with T does not reproduce the surface tension data within experimental accuracy. The functional form of δp and δm in Equation (12) can further be revised with a large number of temperature dependant σ values.

Table 4B.3: Coefficients of Equation (12) for calculating temperature dependence of δ_p and δ_m to be used in Equation (10) for correlating the surface tension of mixtures

Systems	W-GBL		THF-GBL		W-EGY	
	δ_p	δ_m	δ_p	δ_m	δ_p	δ_m
a x 10^{22}	28.278	-43.014	0.232	0.197	-0.643	0.713
B x 10^{23}	-1.965	3.299	-0.022	-0.007	0.0289	-0.0397
C x 10^{27}	34.639	-61.234	0.394	0.064	-0.368	0.458
Range T	303-343 K		278-298 K		298-423 K	
Reference	[28]		[28]		[29]	
APED %	0.38		0.15		1.29	

4B.4 Extension to the Fused Salt Solutions

Fused organic or inorganic salts, which are continuously miscible in the solvents, occupy special place in the physical chemistry, as their study is likely to indicate about how the molecular and ionic interactions vary from pure solvent to fused salt. A survey of literature shows that the Goldsack -

Sarvas equation has been used to analyze the surface tensions of the molten binary and ternary component systems containing charged species of inorganic and organic types in aqueous and non-aqueous solvents.[13,37] Fits of the surface tension vs. x by the Goldsack - Sarvas equation without adjustable parameters were noted to be satisfactory, but not highly accurate as desired considering the non-ideality of the systems. Thus, Equation (10) was applied to the σ_{EXP} data both in binary, ternary and quaternary systems containing molten salts. It should be noted that x_2 in Equation (10) refers to the mole fraction of salt, which is applicable to a binary mixture. In the case of multicomponent systems, the input parameters are calculated based on their linear summations over the mole fractions of different ionic components. Thus, $x_2 = x_{salt1} + x_{salt2} + x\ salt_3 + ...$ These results are recorded in **Table 4B.2**. The values of σ_2 for the salt mixtures, like W- $(Ag,Tl)NO_3$, etc. were taken from Abraham et al.[37] For instance, Equation (10) can successfully analyze the σ_{EXP} data of ionic systems like water – $(Ag,Tl)NO_3$, in which the difference between surface tensions of the pure components is about 56 x 10^{-3} N m^{-1}. An average per cent error of 1.1 is recorded in this case. Further the differences in the pure σ_{EXP} values increase up to about 70 x 10^{-3} Nm^{-1} in the case of Water - $(Ag, Tl, Ca)NO_3$. Equation (10) can estimate the σ_{EXP} of several mixture compositions with high accuracy.

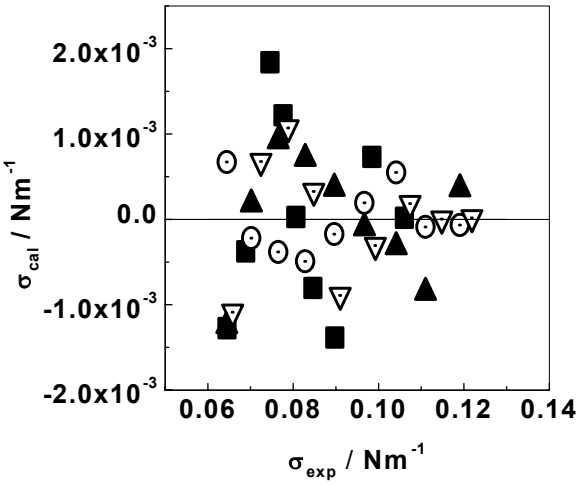

Figure 4B.5: Deviations ($\sigma_{exp.} - \sigma_{cal}$) versus $\sigma_{exp.}$ for different molten ionic systems: ■ W - $(Ag,Tl)NO_3$; O W- $(Ag,Tl,Cs)NO_3$; ▲ W- $(Ag,Tl,Cd)NO_3$; ∇ W- $Ag,Tl,Ca)NO_3$

Since surface tension data for these ionic systems are collected at high temperature i.e. 373 K, a successful application of our equation to such a temperature reinforces the capability of our method in correlating the surface tension of mixtures even at high temperature like 373 K. The differences between σ_{EXP} and σ_{CAL} the present method for several ionic melts are shown in **Figure 4B.5** as a function of σ_{EXP}. It is interesting to note random scattering of deviations for these systems with APED as about 1 per cent. In the water - $(Ag, Tl)NO_3$ system, an addition of Ca^{2+}, Cd^{2+}, or Cs^{+} has caused substantial changes in the surface tension of those mixtures. The hydrating powers of these cations play vital role in such large variations.[37]

As a matter of fact the trend in relative values of adjustable parameters obtained in our study for water - $(Ag,Tl,Cs)NO_3$ -$(Ag,Tl,Cd)NO_3$, $(Ag,Tl,Ca)NO_3$ are in qualitative agreement with the hydration energies of these cations.[40] Besides studying aqueous systems, like shown above, molten

systems comprised of an organic salt with a non-aqueous solvent were also examined. Our Equation has resulted into excellent estimation of surface tension data for anisole - TP system to APED = 0.20 per cent at 373 K.[13] It is important to realize that the proposed equation is applicable to liquids with low dielectric constant (like anisole) and high dielectric constant (like water) with the same capability. Further it is equally capable in handling molten inorganic and organic salts.

The components constituting the mixtures studied and listed in **Table 4B.1** and **2** differ widely in their molar surface areas. A successful application of the currently proposed equation to the mixtures of components with a maximum difference in molar surface area of about 6 x 10^{-19} m^2 employed in this investigation show wide use in correlating the surface tension data of mixtures with their compositions. Further, it should be noted that the third term with a square of the composition $x_{2,b}$ on the right side of Equation (3) or Equation (4) is necessary to fit the surface tension data. Without this term, the derived working equation was noted to be unsuitable for correlating the surface tension data. An examination of **Table 4B.2** reveals an average APED of 0.63, where the range of APED for individual systems varies from 0.02 to 4.19. In general, the APED below 0.5 is seen in as many 60 per cent of the systems, while 11 per cent of them have APED in the range of 0.5 to 1. The systems with APED = 1 to 2 and 2 to 4 range of APED are about 7 to 8 per cent each.

In summary, we have derived a simple equation for correlating the surface tension data of liquid mixtures both at ambient and high temperatures. A successful extension of this equation to the fused salt solutions with a single liquid phase throughout the composition range is a major achievement. Use of the proposed equation in estimating the surface tension of a system with a large difference in the surface tensions of pure components renders our method as a powerful tool. Validity of the proposed equation to such multi-component systems with liquids of varying dielectric constants constituting a single liquid phase throughout the composition range lend confidence in the method described above. It should be noted that the proposed equation does not into account the solvation effects in the ionic melts. The primary objective of the above work was to present a correlation between the surface tension and composition of the solution. This objective has been achieved by writing equations for accounting the non-idealities of simple liquid mixtures and then extending the treatment to solutions of fused salts.

Literature cited:

1. Bertrand, G. L.; Acree, W. E. Jr.; Bruchfield, T. E. “Thermochemical Excess Properties of Multicomponent Systems: Representation and Estimation from Binary Mixing Data.” *J. Soln. Chem*. **1983**, 12, 327.
2. Acree, W. E. Jr.; Bertrand, G. L. “Viscosity, Refractive Index, and Surface Tension of Multicomponent Systems: Mathematical Representation and Estimation from Data for Binary Systems.” *J. Soln. Chem*. **1983**, 12, 755.
3. Flory, P .J. “Statistical Thermodynamics of Liquid mixtures.” *J. Am. Chem. Soc*. **1965**, 87, 1833.
4. Abe, A.; Flory, J. “The Thermodynamic Properties of Mixtures of Small, Non-polar Molecules.” *J. Am. Chem. Soc*.**1965**, 87, 1838.
5. Dhillon, M. S.; Chugh, H. S. “Surface Tension and Surface Heats of Mixing of Mixtures of o-dichlorobenzene with cyclohexane, benzene, o- xylene, m-xylene, and p-xylene at 293.15 and 303.15 K.” *Z. Phys. Chemie., Leipzig*. **1979**, 260, 497.
6. Carey, B. S.; Scriven L. E.; Davis, H. T. “Semiempirical Theory of Surface Tension of Binary Systems.” *AIChE J*. **1980**, 26, 705.
7. Goldsack, D. E.; Sarvas, C. D. “Volume Fraction Statistics and the Surface Tensions of Non-electrolyte Solutions.” *Can. J. Chem*. **1981**, 59, 2968.
8. Edmonds, B.; McLure, I. A. “Thermodynamics of n-alkane + dimethylsiloxanes Mixtures.” *J. Chem. Soc., Faraday Trans.1*, **1982**, 78, 3319.

9. Pandey, J. D.; Gupta, U. “Surface Tension of Binary Molten Salt Mixtures.” *J. Phys. Chem.* **1982**, 86, 5234.
10. Sprow, F. B.; Prausnitz, J. M. “Surface Tension of Simple Liquid Mixtures.” *Trans. Faraday. Soc*. **1966**, 62, 1105.
11. Guggenheim, E. A. “Statistical Thermodynamics of the Surface of a Regular Solution.” *Trans. Faraday. Soc*. **1945**, 41, 150.
12. Lebowitz, J. L.; Helfand, E.; Praestgaard, E. “Scaled Particle Theory of Fluid Mixtures.” *J. Chem. Phys.* **1965**, 43, 774.
13. Kumar, A. “Surface Tension, Viscosity, Vapor Pressure, Density and Sound Velocity for a System Miscible Continuously from a Pure Fused Electrolyte to a Nonaqueous Liquid with a Low Dielectric Constant: Anisole with Tetra-n-butylammonium Picrate.” *J. Am. Chem. Soc*.**1993**, 115, 9243.
14. Gibbs, J. W. *Collected Works*, **1978**,Vol I, Longmans.
15. Bakker, G. *Hand buch der Experimental Physik*, **1928**, 6, 378.
16. Vershaffelt, J. E. “The Thermomechanics of the Superficial Layer. I. Generalities. II. The Formula of Adsorption. III. Mixed Phases.” *Acad. Roy. Belgique, Bull. Classe sciences*, **1936**, 22, 373, 390, 402.
17. Guggenheim, E. A., “The Thermodynamics of Interfaces in systems of Several Components.” *Trans. Faraday. Soc*. **1940**, 36, 397.
18. Langmuir, I. “The Constitution and Fundamental Properties of Solids and Liquids: II. Liquids.” *J. Am. Chem. Soc*., **1917**, 39, 1883.
19. Frumkin, A. *Z. Physik Chem*. **1925,**116, 502.

20. Butler, J. A. V. “The Thermodynamics of the Surfaces of Solutions.” *Proc. Royal Soc.* **1932**, A135, 348.
21. Schuchowitzky, A. A. “Surface Tensions of Solutions. I.” *Acta Physicochim.* URSS, **1944**,19,176, 508.
22. Belton, J.W; Evans, M. G. “Studies in the Molecular Forces involved in Surface Formation. II. The Surface Free Energies of Simple Liquid Mixtures.” *Trans. Faraday, Soc*., **1945**, 41, 1.
23. Szyszkowski, B. V. *Z. Physik Chem*., **1908**, 64, 385.
24. Prigogine, I.; Sarolea, L. “The Surface Tension of Solutions of Molecules of Different Dimensions.” *J. Chim. Phys*. **1950**, 47, 807.
25. Legrand, D. G.; Gaines, G. L. jr. “Surface Tension of Mixtures of Oligomers.” *J. Polym. Sci. part C*, **1971**, 34, 45.
26. Aveyard, R. “Adsorption from Some n-alkane Mixtures at the Liquid / Vapor, Liquid / Water, and Liquid / Solid Interfaces.” *Trans. Faraday. Soc*. **1967**, 63, 2778.
27. Prigogine, I.; Bellemans, A.; Englert- Chwoles, A. “Statistical Thermodynamics of Solutions.” *J. Chem. Phys***. 1956,** 24, 518 and the references cited therein.
28. Bellemans, A. *J. Chim. Phys*. **1960,** 57, 40.
29. Brock, J. R.; Bird, R. B. “Surface Tension and the Principle of Corresponding States.” *AIChE J.* **1955**, 1, 174.
30. Eberhart, J. G. “The Surface Tension of Binary Liquid Mixtures.” *J. Phys. Chem*., **1966**, 70, 1883.

31. Bertozzi, G.; Sternheim, G. “Surface Tension of Liquid Nitrate Systems.” *J. Phys. Chem.*, **1964**, 68, 2908.
32. Evans, H. B.; Clever, H. L. “Surface Tensions of Binary Mixtures of Isooctane with Benzene, Cyclohexane, and n- Dodecane at 30^0 C.” *J. Phys. Chem.*, **1964**, 68, 3433.
33. Sanchez, I. C. “Liquids: Surface Tensions, Compressibility and Invariants.” *J. Chem. Phys*. **1983**, 79, 405.
34. Wilson, G. M. “Vapor- Liquid Equilibrium. XI. A New Expression for the Excess Free Energy of Mixing.” *J. Am. Chem. Soc*., **1914**, 86, 127.
35. Mayer, S. W. “Dependence of Surface Tension on Temperature.” *J. Chem. Phys*., **1963,** 38, 1803.
36. Reiss, H.; Frisch, H. L.; Helfand, E.; Lebowitz, J. L. “Aspects of the Statistical Thermodynamics of Real Fluids.” *J. Chem. Phys*., **1960**, 32, 119.
37. Abraham, M.; Abraham, M-C.; Ziogas, I “Surface Tension of Liquids from Molten Nitrate Mixtures to Water.” *J. Am. Chem. Soc*., **1991**, 113, 8583.
38. Hansen, R. S.; Soger, L. “Surface Tension of Binary Solutions of non-electrolytes.” *J. Colloid Interface Sci*. **1972**, 40, 424.
39. Defay, R.; Prigogine, I.; Bellemans, A.; Everett, D. H. *Surface Tension and Adsorption*, **1985,** John Wiley and Sons, New York.
40. Marcus, Y. *Ion Solvation*, Wiley-Interscience Publication, **1985,** John Wiley and Sons, Chinchester, Great Britain.

41. Kim, J. I. “A Critical Study of the Ph_4 As Ph_4 B Assumption for Single Ion Thermodynamics in Amphiprotic and Dipolar-Aprotic Solvents; Evaluation of Physical Parameters Relevant to Theoretical Consideration.” *Z. Phys. Chem. Frankfurt*, **1978**, 113, 129.
42. Iqbal, M. J.; Rauf, M. A.; Ijaz, N. S. “Surface Tension Measurements of Glycerol with Organic Cosolvents.” *J. Chem. Eng. Data.* **1992**, 37, 45.
43. Shipp, W. E. “Surface Tension of Binary Mixtures of Several Organic Liquids at 25^0C.” *J. Chem. Eng. Data*. **1970**, 15, 308.
44. Dhillon, M. S.; Mahl, B. S. “Surface Tensions of Mixtures of Chlorobenzene with cyclohexane, benzene, o- , m-, and p-xylenes.” *Z. Phys. Chem., Leipzig*, **1978**, 259, 249.
45. Suri, S. K.; Ramakrishna, V. “Surface Tension of Some Binary Liquid Mixtures.” *J. Phys. Chem.* **1968**, 72, 3073.
46. Agarwal, D. K.; Gopal, R.; Agarwal, S. “Surface Tension of Binary Liquid Mixtures 0f Some Polar and Non polar Liquids with dimethylsulfoxide.” *J. Chem. Eng. Data*. **1979**, 24, 181.
47. Swearingen, L. E. “Some Physical Properties of Phenol in Benzene.” *J. Phys. Chem.* **1928**, 32, 1346.
48. Lam, V. T.; Benson, G. C. “Surface Tension of Binary Liquid Systems. I. Mixtures of Non-electrolytes.” *Can. J. Chem*. **1970**, 48, 3773.
49. Siskova, M.; Secova, V. “Surface Tension of Binary Solutions of Non-electrolytes. V. Measurement of Surface Tension of Non-electrolyte

Solutions by Means of a Modified Capillary Rise Method." *Coll. Czech. Chem. Commun*. **1970**, 35, 2702.

50. Chand, K.; Ramakrishna, V. "Liquid-Vapor Interface of Some Binary Dioxane Solutions." *Indian J. Chem*. **1969**, 7, 698.
51. Devvapalli, H. S.; Kudchedkar, A. P. "Mixture Properties of the Water + γ-Butyrolactone + Tetrahydrofuran System. II. Visocities and Surface Tension of γ- Butyrolactone + Water at 303.15 – 343.15 K and γ-Butyrolactone + Tetrahydrofuran at 278.15 – 298.15 K." *J. Chem. Eng. Data*. **1989**, 34, 463.
52. Hoke, B. C.; Chen, J. C. "Binary Aqueous – Organic Surface Tension Temperature Dependence." *J. Chem. Eng. Data* **1991**, 36, 322.

5. VOLUMETRIC PROPERTIES

Before discussing the results on the volumetric properties of the fused salt solutions, it is worth reviewing the related work in both experimental and theoretical areas. It should be noted that the volumetric properties cover the density, speed of sound, thermal expansion coefficient, apparent molar volume and apparent molar compressibility.

5.1 Background:

The partial and apparent molar volumes of electrolyte solutions are very useful tool in elucidating the various structural interactions i.e. ion-ion, ion-solvent, and solvent-solvent interactions present in solutions. The partial molar volumes of electrolytes at infinite dilution can be used to study the ion-solvent and solvent-solvent interactions, while the knowledge on the ion-ion interactions can be gathered from the concentration dependence of the partial and apparent molar properties of electrolytes. The effect of pressure on ionic equilibria required for the process of engineering and oceanographic studies can be calculated by using the partial molar volumes and compressibilities of electrolytes. Further, the study of the concentration dependence of the partial and apparent molar volumes of electrolytes in different solvents, as a function of temperature can be very useful in examining the ion-ion interactions. The ion-solvent interactions can be appropriately studied using the knowledge of partial molar volumes of electrolytes at infinite dilution, where interactions between two ions vanishes.

The apparent molar volume, ϕ_v, of an electrolyte in solution was first calculated by Marignac as follows:[1]

$$\phi_v = (V - n_1 V_1^0) / n_2 \qquad (1)$$

where, V is the volume of the solution, $n_1 V_1^0$ is the volume of water in the solution, n_1 is the moles of water, n_2 is the number of moles of electrolyte in solution and V_1^0 is the molar volume of water. A regularity between the additivity of the densities or ϕ_v's of different salt solutions was observed by Favre and Valson.[2] They assumed that the volume change on adding a salt to water was the resultant of two opposing effects: (a) contraction in volume due to the adsorption of water on the dissolved salt and (b) expansion in volume due to the dissociation of salt. Later Arrhenius theory proved the observed additivity relationship found by Favre and Valson and Ostwald.[3,4]

A reasonable theoretical explanation of the solution volumes was provided by Tammann in his theory of internal pressure (π).[5] His theory was based on the observation that an increase in pressure and the addition of salt to water lowered the temperature of maximum density. Thus, a dissolved salt appears to cause the water to behave as if it were under a high external pressure. This theory was applied to solution volumes by attributing ϕ_v to (a) the change in volume of the salt due to changing the pressure from 1 atm. to π, (b) the change in volume of the solvent due to changing the pressure from 1 atm. to π, and (c) the change in volume when one mixes the salt and the solvent at π to give a solution at 1 atm. external pressure and π atm. internal

pressure.[6] Investigation of ϕ_v of organic non-electrolytes in organic solvents was found to be nearly independent of concentration and solvent. No general relationship between the ϕ_v values in solution and internal pressure was found. Another theory which was different from that of Tammann and Drude and Nernst was forwarded by Baxter, where he thought that the ϕ_v was due to (a) an expansion due to the freeing of the ions from crystalline restraints, (b) a smaller expansion due to repulsion of like charges, and (c) a contraction due to ion-water interactions mostly due to the contraction of water.[7,8]

After the advancement of Debye–Huckel theory and the work of Fajan on the refractivity of solutions and the Born model, new advances were made in the knowledge of solutions, as a result the need of a revision and reinterpretation of solution volumes became evident.[9,10] A theory for the volume change produced by electrostriction in the vicinity of an ion was put forth by Webb.[11] The electrosrtiction of a solvent is given by:

$$V^0(\text{elect}) = \int_{r_0}^{\infty} -(\Delta V_r / V)\, 4\pi r^2\, dr \qquad (2)$$

Where ΔV_r / V is the fractional change of volume at a distance r from the center of ion P_r and r_0 are the pressure and radius of ion, respectively. Later Masson put forward a valuable, empirical generalization on the change of the ϕ_v values the square root of molar concentration.[12]

$$\phi_v = \phi_v^0 + S_{v*} \sqrt{c} \qquad (3)$$

where ϕ_v^0 is the apparent molal volume at infinite dilution and S_{v*} is the experimental slope specific electrolyte. Scott and Geffcken examined the ϕ_v values of electrolytes using this equation and found that it adequately represents the concentration dependence of ϕ_v of electrolytes over a wide range of temperature and concentration range.[13,14]

The interionic theory of Debye and Huckel was applied to the concentration dependence of ϕ_v by Redlich and Rosenfeld.[15,16] They attributed the increase in ϕ_v of electrolytes with increasing concentration to the screening of the electrostriction of the ions by the approach of the counter ions. They also predicted that a constant slope should be obtained for a given electrolyte charge type at constant temperature and pressure if the Debye – Huckel theory is obeyed. A theoretical limiting slope was obtained as $S_v = k\, w^{3/2}$. The equations developed by Masson, and Redlich and Rosenfeld looks very similar but bears an entirely different meaning. The Masson equation can explain the concentration dependence of ϕ_v over a wide range, whereas, the Redlich equation can merely act as a limiting law for low concentration. The value of S_v in the Masson equation is treated as a variable while, a single value of k common to all electrolytes and depending only on the temperature and solvent properties has been postulated by Redlich.

Redlich and Meyer later derived the theoretical values of k (=1.868) in water as a function of temperature confirming with the experimental value of k = 1.86 at 298.15 K.[17,18]

Recently the studies on ϕ_v of tetraalkylammonium halides shows an abnormal behavior for the concentration dependence of ϕ_v. These salts shows a large negative deviation from the limiting law and are seen to be passing through several maximas and minimas with increasing concentrations. The effect of temperature on the deviation constant b_v is also seen to be different from that observed for the common electrolytes.[19] The behavior is attributed to ion-pairing, hydrophobic bonding, iceberg effects, micelle formation, salting -in effects and induced cation-cation interactions.[20-28] The ϕ_v values of tetraalkylammonium salts as reported in the literature at 298 K show that S_{v*} was negative for all the salts except Me_4NBr.[27]A plot of ϕ_v vs.$\sqrt{c}$ at high concentration for n-Bu_4NBr and n-Pr_4NBr passes through a minimum and then the ϕ_v values were seen to increase with concentration. These results have been discussed in terms of the solute-water interactions and formation of clathrate-like structures. Similar results were obtained by Conway et.al., the ϕ_v values of the tetraalkylammonium salts that they studied when fitted with the Redlich equation give negative values for the deviation constant b_v.[23] The main contribution for the deviation from the limiting law has been associated with long-range coulombic interactions, primary hydration of ions, mutual salting-out, and ion-pairing. The reason for the large negative values of b_v is attributed to a mutual salting-out and salting-in effect. The negative values of b_v obtained for various tetraalkylammonium bromide salts by Desnoyers and Arel was found to be approximately linear to the number of carbon atoms in the alkyl chain.[24] The deviations are interpreted in terms of mutual salting-in

effects. For the larger salts where the number of carbon atoms are 7 or more, a minimum in the plot of ϕ_v vs.$\sqrt{c}$ is observed. This behavior is attributed to micelle formation. They suggested that the ϕ_v values of all hydrophobic solutes behaved in a similar manner after the long-range coulombic interactions were considered. The concentration dependence of ϕ_v of these solutes are interpreted in terms of the true volumes of the solute and the competition between the increase in "ice-likeness" of the solvent and loss of free volume near the solute during hydrophobic hydration. A large negative deviation in the ϕ_v values was observed for the tetraalkylammonium bromide salts by Franks and Smith and that the deviation was more pronounced at low temperatures.[22] They interpreted the concentration dependence of ϕ_v in terms of cation-cation interactions, induced by cooperative ion-water interactions. A positive deviation from the limiting law was observed for the ϕ_E's of these salts. The ϕ_v values of these salts have also been examined using an ion-association model by Wirth.[21] The observed ϕ_v for Me_4Nbr from 0 to 5 M was explained with the value ion-pairing association constant K_A = 1.24. In addition to ion-pairing, the concentration dependence of ϕ_v's of other tetra alkyl salts has been explained by the formation of dimers and micelles.

Although, ion-association model can successfully explain the negative deviations from the limiting law, the ion-pair that is formed is not of the classical type since the volume change for most electrostatic ion-pairs is positive. The formation of ion-pair with a volume less than the free ions is possible, however, for large ions since smaller anion can penetrate the

aliphatic portion of the cation when the ion-pair is formed, causing the volume to decrease.

The ϕ_v values of the symmetrical salts $NaBPh_4$, and Ph_4AsCl at 273, 298 and 323 K in dilute aqueous solutions have been studied by Millero.[29,30] Negative deviation from the limiting law was observed for both the salts. These result shows the problems involved in attributing the causes of the deviations from the limiting law to a specific type of interaction. The negative deviations for these salts can be explained by cation-cation or anion-anion interactions. These results indicate the necessity of considering all the possible interactions, i.e. cation-cation, anion-anion, cation-anion and higher order triplet interactions while discussing the deviations from the limiting law.

It is noted that many salts like quaternary ammonium salts are generally fully ionized in several organic solvents, but some of them do exhibit strong ion-pairing in the dilute region.[31-37] Since the volumetric methods are known to give valuable information regarding solute-solute, solute-solvent and solvent-solvent interactions, the study of volumetric properties are of great importance in characterizing the structure and properties of solution. Unfortunately, systematic data on volumetric properties of these systems are not reported in the literature. Very recently some studies have been carried out for the fused sodium thiocyanate and lithium nitrate in aqueous methanol and the isentropic compressibility calculated therefrom.[38,39] The results are explained in terms of hydration phenomena. In an earlier paper, Rahman and Mahiuddin have discussed the temperature and concentration dependence of

the sound velocity in sodium nitrate and sodium thiosulphate solutions.[40] Temperature dependence of isentropic compressibilities is another interesting aspect of their studies.

5.2 Our Results on Experimental Volumetric Properties:

The volumetric properties of several systems comprising a fused salt completely miscible in organic solvent have been investigated at different temperatures in order to evaluate ion- solvent and ion-ion interaction parameters. Since the equation representing its behavior over the full range of composition must be on mole fraction basis rather than the molality basis, the data obtained out of such measurements have been analyzed using the mole fraction based equation of Petrenko and Pitzer.[41]

Three systems of TP with nitrobenzene, 1-butanol, and anisole were undertaken for the investigation. The reason to choose three solvents was based on wide difference in their relative permittivities. At 298 K nitrobenzene, 1-butanol and anisole are characterized with relative permittivity of 34.82, 17.51 and 4.33, respectively. At the 363 K (the m.p. of TP), the relative permittivities of nitrobenzene, 1-butanol and anisole are 24.80, 9.4 and 3.60, respectively. This difference in the relative permittivity is expected to give information on the changes of volumetric properties of TP on addition of solvents. Densities and speed of sounds were measured to obtain different volumetric properties. Due to limited experimental facilities, the density and speed of sound were measured independently rather than in the same solution.

In **Tables 5.1, 5.2 and 5.3** are given the experimental density, (ρ) values of the nitrobenzene-TP, 1-butanol-TP and anisole-TP systems at different temperatures. As a matter of fact, the density measurements were made up to the saturation limit at each temperature. The densities of TP were measured to be 1118.40, 1115.01 and 1107.59 kg m^{-3} at 363, 368 and 373 K, respectively.

For the sake of illustrations, variation of ρ with temperature at several specific compositions are plotted in **Figures 5.1, 5.2 and 5.3** for the nitrobenzene, 1-butanol, and anisole solutions containing TP systems.

Table 5.1: Densities, ρ (kg m^{-3}) of the nitrobenzene-TP system at different mole fractions and temperatures

x_2	ρ / (kg m^{-3})	x_2	ρ / (kg m^{-3})	x_2	ρ / (kg m^{-3})
293 K		303 K		313 K	
0	1205.04	0	1195.29	0	1185.37
0.1042	1211.58	0.0858	1200.11	0.0629	1189.96
0.2043	1213.42	0.1675	1202.98	0.1376	1193.32
0.3123	1212.48	0.2412	1202.98	0.2086	1194.30
		0.3047	1200.57	0.2865	1193.32
323 K		333 K		343 K	
0	1175.44	0	1165.52	0	1155.64

0.0666	1180.29	0.1078	1168.77	0.0964	1157.11
0.1483	1182.71	0.1894	1170.14	0.1747	1158.55
0.2375	1183.24	0.2978	1171.12	0.2823	1159.53
0.3537	1182.22	0.4161	1169.19	0.3945	1158.09
0.4947	1179.80	0.5015	1166.78	0.4796	1156.17
353 K		363 K		0.5724	1153.26
0	1145.76	0	1135.89	0.6839	1149.86
0.0743	1146.52	0.1044	1138.27	0.7956	1146.01
0.2006	1147.45	0.2006	1138.76	0.8849	1143.16
0.3271	1148.43	0.3085	1139.25	0.948	1140.28
0.4386	1146.01	0.3865	1138.76	368 K	
0.5055	1145.52	0.5203	1137.33	0	1130.94
0.6059	1142.16	0.6096	1134.42	0.1077	1133.44
0.7025	1139.25	0.7176	1131.02	0.1857	1134.42
0.7993	1136.35	0.8104	1127.66	0.3233	1134.42
0.8773	1132.05	0.8625	1124.76	0.4313	1134.42
0.9219	1129.59	0.9146	1122.83	0.5017	1134.42
373 K		0.9629	1120.41	0.6245	1130.57
0	1126.30			0.7063	1128.15
0.0927	1129.15			0.8104	1123.32
0.1819	1130.50			0.9074	1119.43
0.2711	1131.15			0.9591	1117.51
0.4072	1130.74				

0.4973	1129.43
0.6002	1126.96
0.7006	1123.45
0.8001	1119.04
0.911	1112.82
0.9521	1110.22

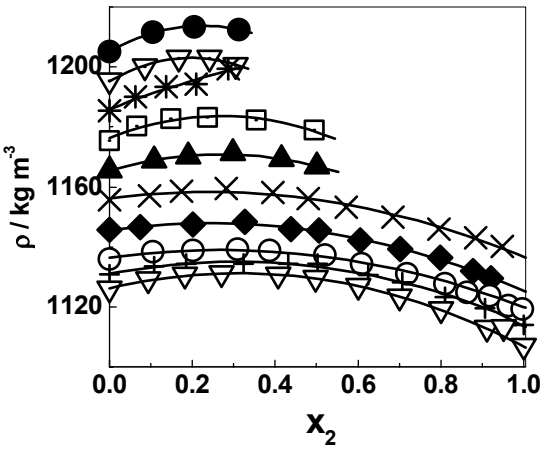

Figure 5.1: Isothermal plots of density (ρ) versus x_2 for the Nitrobenzene-TP system, ● 293, ▽ 303, ∗ 313, ❑ 323, ▲ 333, X 343, ◆ 353, O 363, + 368, ▼ 373K

Table 5.2: Densities (kg m^{-3}) of the 1-butanol-TP system at different mole fractions and temperatures

x_2	ρ / (kg m^{-3})	x_2	ρ / (kg m^{-3})	x_2	ρ / (kg m^{-3})	x_2	ρ / (kg m^{-3})
298 K		313 K		323 K		333 K	
0	803.76	0	795.23	0	787.54	0	780.9
0.104	808.12	0.0835	798.3	0.0522	789.68	0.1078	783.03
0.2043	809.35	0.1635	799.53	0.1461	791.53	0.1895	783.99
0.312	808.73	0.2538	799.22	0.2243	793.07	0.2975	784.65
						0.5017	781.74
343 K		353 K		363 K		368 K	
0	774.28	0	763.87	0	757.73	0	751.88
0.0964	775.26	0.0817	764.49	0.0886	758.03	0.0904	753.73
0.1747	776.23	0.1669	764.49	0.1825	758.63	0.1738	754.33
0.2823	776.88	0.2608	764.49	0.3286	758.34	0.2659	754.64
0.4796	774.63	0.4938	762.02	0.5042	756.18	0.4868	751.57
0.5722	771.87	0.5982	759.57	0.6225	752.79	0.5773	748.21
0.6817	768.79	0.7077	755.58	0.7043	749.11	0.6817	744.52
0.7964	764.18	0.8016	750.34	0.8103	743.28	0.7843	739.58
0.8852	759.88	0.866	746.04	0.9042	737.44	0.8660	735.59
0.9408	757.12	0.9181	742.65	0.9286	736.5	0.9355	730.66

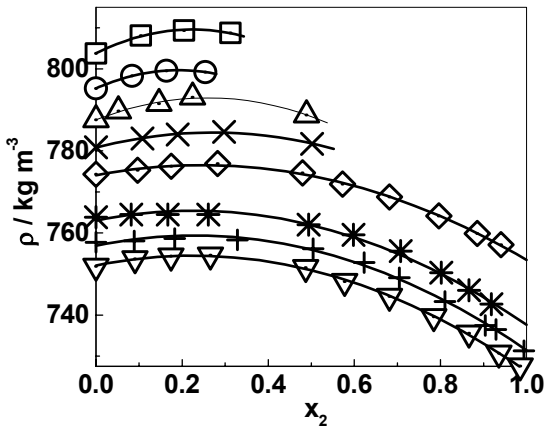

Figure 5.2: Isothermal plots of density (ρ) versus x_2 for the 1-butanol-TP system, ❑ 298, O 313, Δ 323, **x** 333, ◊ 343, ∗ 353, **+** 363, ∇ 368 K

Table 5.3: Densities, ρ (kg m^{-3}) of the anisole-TP system at different mole fraction and temperatures

	ρ / (kg m^{-3})			
x_2	298 K	308 K	318 K	328 K
0	1015.33	998.33	988.22	974.75
0.1052	1034.22	1022.23	1011.32	998.66
0.2121	1057.76	1045.01	1035.39	1024.22
0.3228	1076.45	1069.06	1057.39	1047.45

ρ / (kg m^{-3})

x_2	338 K	348 K	353 K	362 K
0	961.46	950.76	944.49	932.34
0.1052	979.54	979.65	972.34	961.54
0.2121	1016.32	1005.44	998.94	992.55
0.3228	1038.23	1032.97	1025.28	1014.43
0.4559	1061.11	1055.27	1048.92	1044.66
0.6013		1083.91	1072.83	1067.32
0.7095		1094.22	1087.44	1082.04
0.8259		1101.55	1098.34	1093.32
0.9444				1100.12
1				1105.33

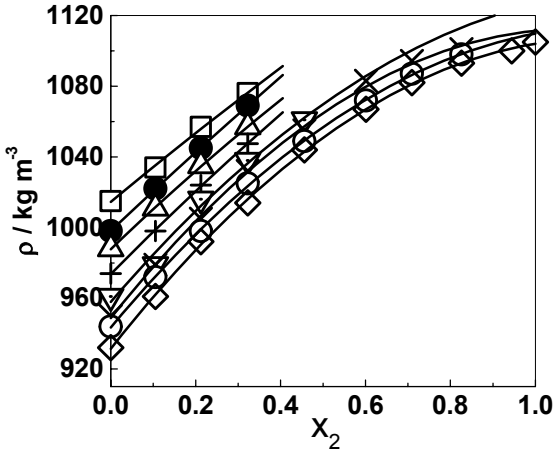

Figure 5.3: Isothermal plots of density (ρ) versus x_2 for the anisole-TP system, ❑ 298, ● 308, Δ 318, + 328, ∇ 338, X 348, O 353, ◊ 362 K.

The isothermal equation to correlate the ρ data with x_2 for all the three systems can be written as:

$$\rho = \rho^0 + q_1 x_2 + q_2 x_2^2 + q_3 x_2^3 \quad (4)$$

where ρ^0 is the density of pure solvent at a given temperature. The q_1, q_2 and q_3 are the adjustable parameters, whose values are determined by the least squares analysis. The average standard errors in q_1, q_2 and q_3 as estimated from the computer program varied as 2, 3 and 4%, respectively. The above parameters obtained at each temperature are listed together with rmsd of fits in **Tables 5.4, 5.5 and 5.6** for the systems studied.

Table 5.4: Adjustable parameters of isothermal equations correlating ρ with x_2 for nitrobenzene-TP system

T / (K)	q_1/ (kg m^{-3})	q_2 / (kg m^{-3})	q_3 / (kg m^{-3})	10^3 rmsd / (kg m^{-3})
293	1205.04	78.22	-175.2	9
303	1195.29	78.14	-197.31	10
313	1185.37	85.00	-200.26	2
323	1175.44	59.05	-103.85	3
333	1165.32	40.81	-75.41	7
343	1155.64	19.93	-39.11	3
353	1145.76	18.33	-38.7	2

363	1135.89	23.28	-41.28	4
368	1130.94	26.39	-42.83	6
373	1126.00	32.90	-52.06	5

Table 5.5: Adjustable parameters of isothermal equations correlating ρ with x_2 for 1-butanol-TP System

T / (K)	q_1/ (kg m^{-3})	q_2 / (kg m^{-3})	q_3 / (kg m^{-3})	q_4 / (kg m^{-3})	q_5 / (kg m^{-3})	10^3 rmsd / (kg m^{-3})
298	803.76	52.17	-116.7			6
313	795.23	46.30	-120.6			1
323	787.54	41.47	-79.6			8
333	780.90	21.57	-17.16	-44.8		2
343	774.28	14.81	-11.19	-53.19	29.56	8
353	763.87	5.610	-4.28	-27.67	-2.185	6
363	757.73	-0.175	44.64	-129.16	58.57	7
368	751.88	25.55	-62.65	18.36	-6.691	5

Table 5.6: Adjustable parameters of isothermal equations correlating ρ with x_2 for anisole-TP system

T / (K)	q_1/ (kg m^{-3})	q_2/ (kg m^{-3})	q_3/ (kg m^{-3})	q_4/ (kg m^{-3})	q_5/ (kg m^{-3})	10^3 rmsd / (kg m^{-3})
298	1015.0	194.87	-14.25			9
308	998.0	228.42	-26.48			8

318	988.0	228.37	-43.67			7
328	974.0	239.3	-34.06			5
338	961.0	255.48	-72.2			7
348	950.0	299.05	-229.05	299.68	-233.47	4
353	944.0	273.76	-52.89	-116.26	63.82	3
364	932.0	290.94	-67.10	-98.85	47.25	4

The speeds of sound u, were measured as a function of x_2 at constant temperature from 273 to 373 K. **Tables 5.7, 5.8 and 5.9** enumerate the speed of sound in the nitrobenzene-TP, 1-butanol-TP and anisole-TP systems with the limits of solubility of TP in these organic solvents.

Table 5.7: The speed of sound, u (m s^{-1}) as a function of x_2 at constant temperature for the nitrobenzene -TP system

$x_2 \longrightarrow$ 0	0.047	0.101	0.202	0.304	0.499	0.711	0.903	1
T/(K) $\downarrow$								
293 1480	1488	1512	1528	1544				
298 1464	1472	1496	1512	1528				
303 1440	1448	1472	1488	1508				
308 1416	1432	1448	1472	1480				
313 1400	1416	1424	1448	1464				
318 1384	1392	1416	1432		1488			
323 1368	1376	1384	1416	1432	1480			

333	1328	1336	1352	1392	1400	1448			
343	1304	1312	1320	1344	1368	1408	1464	1480	
353	1264	1272	1286	1320	1336	1376	1424	1456	
361									1440
363	1224	1240	1256	1296	1312	1344	1384	1424	1432
365	1216	1232	1240	1288	1304	1336	1360	1416	1424
367	1208	1224	1232	1280	1296	1328	1360	1400	1408
371	1200	1208	1232	1272	1288	1312	1336	1392	1400

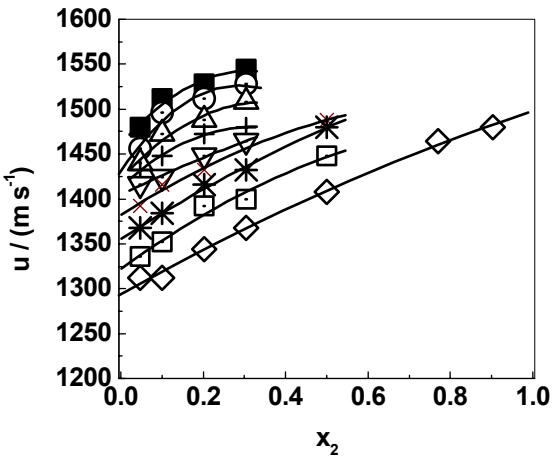

Figure 5.4: Speed of sound, u of the nitrobenzene-TP system at different concentrations and temperatures, ■ 298, **O** 308, Δ 318, **+** 328, ∇ 338, ✶ 348, ❒ 353, ◊ 362 K

Table 5.8: The speeds of sound, u (m s^{-1}) as a function of x_2 at constant temperature for the 1-butanol -TP system

$x_2 \rightarrow$ T/(K) $\downarrow$	0.0	0.052	0.096	0.22	0.406	0.605	0.703	0.897	1.0
293	1256								
298	1232								
303	1224								
308	1208								
313	1184								
314		1216							
318	1176	1200							
323	1160	1184	1208	1288					
328		1160	1200	1248					
333	1120	1152	1184	1232					
343	1088	1128	1152	1200	1324	1392			
348					1304		1440	1464	
353	1056	1096	1120	1168	1296	1368	1432	1448	
358					1272		1424	1424	
361									1440
363	1016	1064	1096	1160	1264	1344	1408	1416	1432
365	1008	1048	1088	1152	1252	1320	1400	1400	1424
367	1000	1036	1072	1144	1252	1320	1392	1392	1408
369									1400

371	992	1032	1056	1128	1220	1312	1384	1384	1400

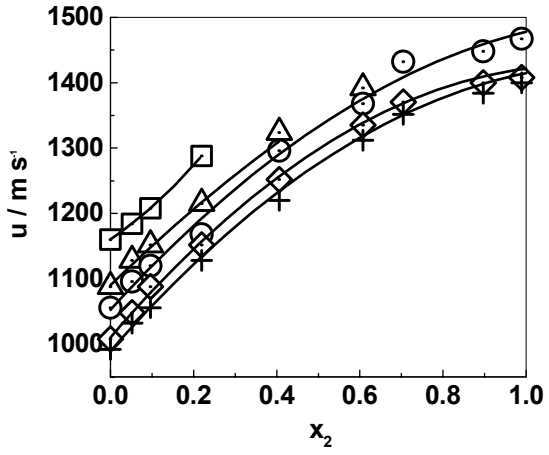

Figure 5.5: Speed of sound, u of the 1-butanol-TP system at different concentrations and temperatures, ❒ 323, Δ 343**, O** 363, ◊ 367, **+** 371 K

Table 5.9: The speeds of sound, u (m s^{-1}) as a function of x_2 at constant temperature for the anisole-TP system

$x_2 \rightarrow$	0.0	0.05	0.1	0.288	0.4	0.548	0.702	0.907	1.0
T/(K) $\downarrow$									
298	1408	1424	1448	1480					
303	1384	1400	1424	1464					
308	1368	1384	1408	1440	1488				
313	1344	1368	1376	1416	1472				
318	1320	1344	1356	1392	1456				
323	1304	1320	1344	1376	1440				

333	1264	1288	1304	1344	1408	1448			
343	1224	1256	1264	1312	1376	1416			
353	1184	1216	1224	1280	1344	1384	1432	1448	
358							1416	1432	
361									1440
363	1144	1168	1192	1248	1312	1360	1400	1416	1432
365	1128	1160	1176	1232	1304	1360	1392	1408	1424
367	1120	1152	1168	1224	1296	1352	1384	1400	1408
369									1400
371	1104	1144	1168	1216	1288	1344	1368	1400	1400

The representative plots of u versus x_2 at several temperatures are given in **Figures 5.4, 5.5 and 5.6** for these systems.

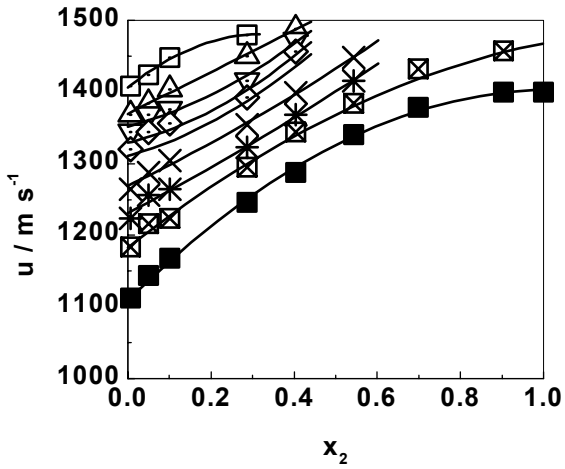

Figure 5.6: Speed of sound, u (m s^{-1}) of the anisole-TP system at different concentrations and temperatures, ❒ 298, Δ 308, ∇ 313, ◊ 318**, X** 333, ✷ 343, ☒ 353, ■ 371 K

The mole fraction dependence of the isothermal speeds of sound, u for these systems can be expressed as

$$u = u^0 + p_1 x_2 + p_2 x_2^2 + p_3 x_2^3 \ldots\ldots\ldots \quad (5)$$

where u^0 is the speed of sound of a solvent at a specific temperature. The p_1, p_2 and p_3 are the adjustable parameters obtained from the least squares analysis of the data tabulated in **Tables 5.10, 5.11 and 5.12**. Average standard errors in the adjustable parameters varied between 4 and 8%.

Table 5.10 Parameters of fitting of u vs. x_2 for the nitrobenzene-TP system

Param. →	u_0 /	p_1 /	p_2 /	p_3 /	rmsd /
T / (K) ↓	(m s^{-1})	(m s^{-1})	(m s^{-1})	(m s^{-1})	(m s^{-1})
293	1480	224.9	0	0	6
298	1464	223.9	0	0	6
303	1440	233.3	0	0	5
308	1416	238.6	0	0	8
313	1400	221.9	0	0	4
318	1384	215.3	0	0	6
323	1368	220.2	0	0	4
333	1328	246.7	0	0	7
343	1304	201.5	0	0	4
353	1264	250.5	-46.74	0	4

363	1224	436.0	-596.1	393.1	4
365	1216	452.9	-697.3	481.1	1
367	1208	420.1	-546.4	346.6	8
371	1200	477.6	-817.2	573.6	9

Table 5.11: Parameters of fitting of u vs. x_2 for the 1-butanol-TP system

Param. $\rightarrow$	u_0 /	p_1 /	p_2 /	σ / (m s^{-1})
T / (K) $\downarrow$	(m s^{-1})	(m s^{-1})	(m s^{-1})	
323	1160	563.9	0.0	6
333	1120	537.7	0.0	5
343	1088	639.2	-210.2	4
353	1056	689.9	-267.7	7
363	1016	780.8	-364.1	2
365	1008	756.0	-341.9	6
367	1000	778.1	-369.2	4
371	992	734.5	-321.1	6

Table 5.12: Parameters of fitting of u vs. x_2 for the anisole-TP system

Param.$\rightarrow$	u_0 /	p_1/	p_2/	p_3 /	σ /
T / (K) $\downarrow$	(m s^{-1})	(m s^{-1})	(m s^{-1})	(m s^{-1})	(m $s^{-1)}$
298	1408	267.5	0.0	0.0	10
303	1384	267.5	0.0	0.0	10

308	1368	287.8	0.0	0.0	9
313	1344	298.8	0.0	0.0	10
318	1320	312.9	0.0	0.0	13
323	1304	312.9	0.0	0.0	13
333	1264	335.8	0.0	0.0	10
343	1224	354.4	0.0	0.0	10
353	1184	470.2	0.0	-135.9	10
363	1144	493.1	-204.6	0.0	10
365	1128	521.1	-224.7	0.0	13
367	1120	527.8	-236.3	0.0	14
371	1104	555.4	-255.4	0.0	14

Both ρ and u can be employed to calculate the isentropic compressibility κ_s of the solutions by using $1/u^2 \rho$.

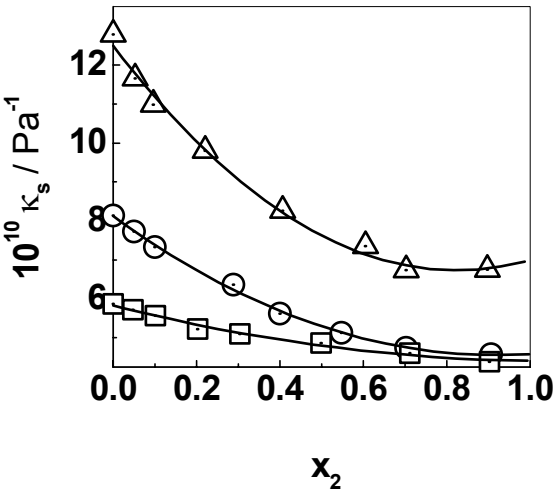

Figure 5.7 Isentropic compressibility, κ_s of the solutions of TP with ❒ nitrobenzene, **O** anisole and Δ 1-butanol in full composition range at 363 K.

In **Figure 5.7** are plotted the κ_s values as a function of x_2 in the full composition range. It is interesting to observe that the κ_s is the largest for the 1-butanol- system followed by anisole- and nitrobenzene-TP system. When TP is added to 1-butanol, a sharp change in κ_s is observed till the state of fused TP. However, mild decrease in κ_s is noted on addition of TP in anisole. The κ_s values for nitrobenzene-TP system decrease very slowly. The number of the free 1-butanol molecules decrease quite sharply when TP is added. This is however not the case with anisole and nitrobenzene. Note that T^+ cation is large with 4 Bu groups attached on it, there is no question that such a cation will solvate in these conditions.

This is supported by apparent molar volume and compressibility data collected for these systems. The details of these properties will follow in the subsequent lines. However, in order to give an approximate idea, one can consider for example; ϕ_v values for TP in nitrobenzene, 1-butanol and anisole at 364 K are very close to each other suggesting that the nature of solvent has no role to play in the solvation of T^+. This means that the solvent molecule cannot approach T^+ in order to solvate it owing to steric effect. Similarly, ϕ_K^0 values are very close to zero or positive indicating that T^+ is not compressed in the presence of these solvents, which is true from the examination of data collected here. However, the effect of 1-butanol is still puzzling. The sharp decrease in the κ_s values might be due to the breaking in the hydrogen bonding in 1-butanol. This might result into the sharp decrease in κ_s values. From this logic, it is understood that the solvation may be

stronger if methyl groups are attached to N^+ of T^+ because methyl group offers lesser steric hindrance than ethyl and butyl. This is indeed a case in water as evidenced from the work of Wen.[42]

The densities and speeds of sound can be converted into apparent molar volumes ϕ_v and compressibilities, ϕ_k by using the following relationship:

$$\phi_v = [(\rho^o - \rho) / m \rho \rho^o] + M / \rho \quad (6)$$

$$\phi_k = [(\kappa_s \rho^o - \kappa_s^o \rho) / m \rho \rho^o] + M \kappa_s / \rho \quad (7)$$

where M stands for the molecular mass of TP. κ_s^o is the isentropic compressibility of pure solvent and is calculated from the density and speed of sound of pure solvent at a given temperature.

$$\kappa_s^o = 1/u_o^2 \rho^o \quad (8)$$

In **Figures 5.8, 5.9 and 5.10** are shown the variation of ϕ_v with x_2 for all the three systems at constant temperatures.

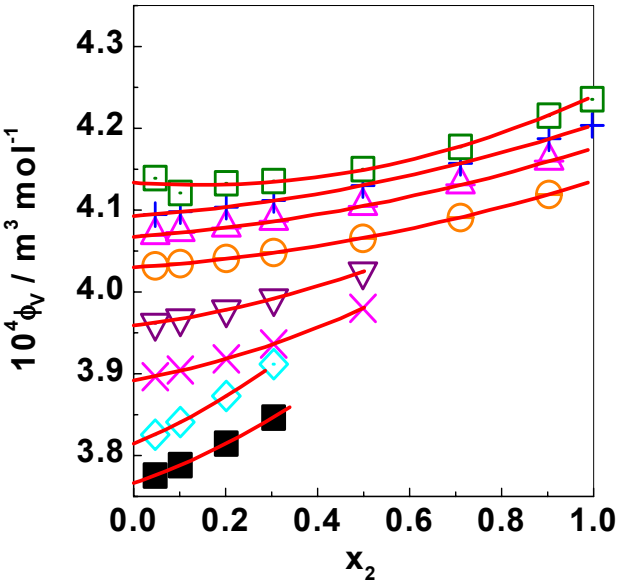

Figure 5.8: Plots of of ϕ_v versus x_2 for the nitrobenzene-TP system at different temperatures. ■ 293, ◊ 313, **X** 323, ▽ 333, **O** 343, Δ 353, **+** 363, ❑ 371 K

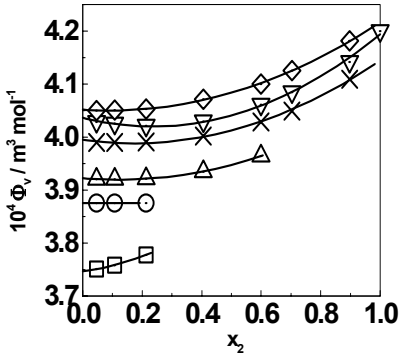

Figure 5.9: Plots of ϕ_v versus x_2 for the 1-butanol-TP system at different temperatures. ❑ 298, **O** 313, Δ 323, **X** 343, ∇ 363, ◊ 368.

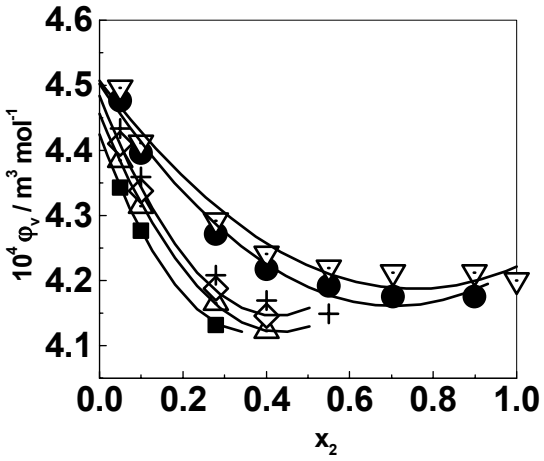

Figure 5.10: Plots of ϕ_v versus x_2 for the anisole-TP system at different temperatures. ■ 298, Δ 308, ◊ 328, + 338, ● 353, ∇ 362 K

At all the temperatures, ϕ_v of TP in nitrobenzene increases with increase in its concentration. This increase is steeper at low temperatures. In general, the $\phi_v - x_2$ plots show monotonous variation at all the temperatures. This monotonous variation in ϕ_v in fused salt solution is similar to what one sees in the strong electrolyte solutions. Therefore, the changes in ϕ_v can be explained in terms of Debye-Huckel theory. Though ion-pairing in such system has been observed on the basis of conductance data,[31] the $\phi_v - x_2$ plots do not show any evidence of ion-pairing throughout. In earlier chapter on vapor pressure, it was seen that the activity model was effective even without consideration of ion-pair formation. However, ion-pairing should be built in the model for a rigorous set of equations applicable for any systems. The similar situation is true here. It appears that TP acts as a strong electrolyte in

nitrobenzene through the composition range, though the relative permittivity of nitrobenzene is 24.80, sufficiently lower as compared to a polar solvent like water, in which NaCl, KCl, etc act as strong electrolytes. Another point in this connection is that the ϕ_v values of TP in solution are quite large and do not differ from its values in pure fused form at different temperature at and above the m.p. of TP. This indicates that solvents like nitrobenzene have less effective role to play towards the solvation of T^+ in the solution phase.

The similar trend is seen in the case of solution of TP in 1-butanol. The reason that this observation is not different from the one made in nitrobenzene is also supported by Pitzer and Simonson.[41]It is interesting that TP acts as a strong electrolyte in 1-butanol at 363 K with its relative permittivity being 9.4.

Anomalous behavior in ϕ_v was seen in the case of anisole-TP system at different temperatures. In this case, ϕ_v decreases with increasing concentration of TP up to x_2 = 0.6 and then enhances towards pure TP. This behavior is not expected in the case of an electrolyte acting as a strong electrolyte. However, such a trend has been observed by Wen[27,28] in aqueous quaternary ammonium salts, where ϕ_v first decreases and then increases owing to the caging effect. We are not sure of this effect taking place in this system. It is surprising to note that increase in temperature does not effect the shape of $\phi_v - x_2$ plots indicating the effect of caging, if any is not temperature-dependent. This is unlikely as the caging in such salts below their m.p. has been shown to be dependent on temperature. The ϕ^o_v values if obtained from

very dilute solution data might throw some light on this behavior. However, since our interest was to look at the full miscibility range, we have not chosen to give priority to such measurements.

The apparent molar compressibilities, ϕ_K calculated from density and speed of sound data are shown in **Figures 5.11, 5.12** and **5.13** for nitrobenzene-, 1-butanol- and anisole-TP systems, respectively. Though the $\phi_K - x_2$ plots can also be explained on the same lines as given above, it is interesting to know that anomalous behavior of $\phi_v - x_2$ plots of the anisole-TP system is not present in the case of $\phi_K - x_2$ plots at any temperatures. In order to confirm the $\phi_v - x_2$ plots, density measurements were repeated several times to ensure the reliability of data.

Aqueous Tetra-n-butyl ammonium cation is a strong hydrophobic in nature. It seems that it remains so in nitrobenzene and 1-butanol and thus repels the solvent molecules away causing the volume to increase with concentration. The decreasing ϕ_v in the anisole system indicates that cation shows opposite effect on anisole. However, in any case the solvation numbers if computed using density and speed of sound data vary between –2 to 1 for the nitrobenzene and 1-butanol systems, respectively, indicating that no solvent molecules are available around the cation. However, earlier and current studies show that the anisole system is characterized with a solvation number of 3.

TP has a disordered ionic lattice with alternative positive and negative charges. The pattern of lattice is lost on addition of a solvent and the ions

move in a random motion. The Debye-Huckel theory describes this phenomenon. But as the TP concentration increases, the relative strength of ion-solvation energies as compared to the sum of direct anion-cation attraction and intermolecular attraction in pure solvent becomes more dominant and a governing criteria of ion-solvent and ion-ion interactions. If ion solvation energies are stronger, negative departure from ideal behavior is seen. In the current cases, the ion solvation energies weaker as shown by poor or zero solvation, the positive deviations from the ideal behavior are seen in all these three systems.

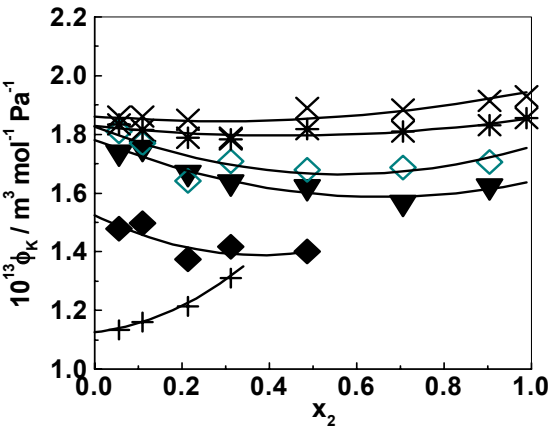

Figure 5.11: Mole fraction dependence of ϕ_K for the nitrobenzene-TP system at different temperatures. **+** 308, ◆ 323, ▼ 343, ◊ 353, ✷ 365, **X** 371 K.

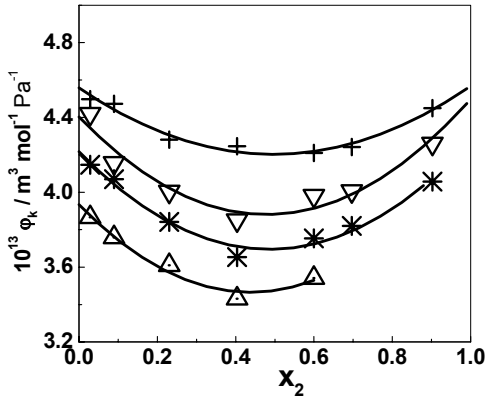

Figure 5.12: Mole fraction dependence of ϕ_K for the 1-butanol-TP system at different temperatures. Δ 343, ✷ 363, ∇ 367, + 371 K.

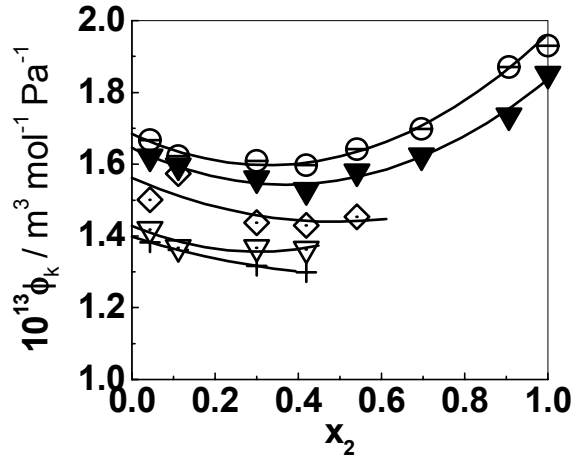

Figure 5.13: Isothermal plots of ϕ_K versus x_2 for the anisole-TP system. + 313, ∇ 323, ◊ 343, ▼ 365, O 371 K.

5.3 Analysis of Volumetric Data :

As described in earlier chapters, the Pitzer formalism has proven to be an important tool to analyze the thermodynamic properties of pure and mixed

salt solutions.[43] In fact, the basic Pitzer equations are built on the molality scale. However, since the concept of molality does not hold good in the case of fused salts, Petrenko and Pitzer later developed volumetric equations on the mole fraction basis and analyzed the apparent molar volumes of aqueous NaOH up to 523 K and 400 M Pa.[41]

An attempt was to extend the Petrenko- Pitzer model (PPM) to the fused TP systems in the nitrobenzene, 1-butanol and anisole. Though the relative permittivity of the above organic liquids is not high, the Debye- Huckel term was still retained as done in the treatment of solvent activities of these systems.

The PPM equations in the current context of ϕ_v and ϕ_k can be written as :

$$\phi_v = V_2^0 + f^v + (x_2 / 2)\, B^V_{TP}\, g\, (\alpha\, I_x^{1/2}) - 2\, x_2\, (W^V_{1,TP} - x_1\, U^V_{1,TP}) \qquad (9)$$

and analogous equation for ϕ_k is :

$$\phi_k = K_2^0 + f^k + (x_2 / 2)\, B^k_{TP}\, g\, (\alpha\, I_x^{1/2}) - 2\, x_2\, (W^k_{1,TP} - x_1\, U^k_{1,TP}) \qquad (10)$$

Both equations 9 and 10 are developed with pure TP liquid reference state. V_2^0, K_2^0 are partial molar volume and compressibility of TP at infinite dilution. The function of f^v and f^k denote the Debye- Huckel terms for volume and compressibility, respectively. These are defined as:

$$f^{v} = (A_v / \rho) \ln (1 + \rho I_x^{1/2}) \quad (11)$$

and

$$f^{k} = (A_k / \rho) \ln (1 + \rho I_x^{1/2}) \quad (12)$$

where A_v and A_k are the limiting slopes for volume and compressibility, respectively. ρ is related to the "closest – approach" distance for the ions. While the value of ρ could be different for different salts, the choice of a single ρ value for all the salts has been recommended in the PPM.

The B^{V}_{TP} and B^{k}_{TP} are the second virial coefficients for the volume and compressibility, respectively and are estimated by the non-linear squares fits. These coefficients denote the effects in dilute solutions of fused salts.

g is defined as:

$$g(y) = 2 [1 - (1 + y) \exp(-y) / y^2] \quad (13)$$

In equations 1 and 2, the parameters $W^{V}_{1,TP}$, $U^{V}_{1,TP}$, $W^{k}_{1,TP}$ and $U^{k}_{1,TP}$ are the adjustable parameters for volume and compressibility, respectively.

All the computations were performed using a software called as Origin v 5.0 supplied by M/S Microcal Inc.

5.3.1 Nitrobenzene-TP system:

The ϕ_v and ϕ_k values at different temperatures were subjected to non-linear least squares analysis in all the three cases for evaluating the parameters of equations (9) and (10). **Table 5.13** lists the $W^V_{1,TP}$ (average standard error= 3%) and $U^V_{1,TP}$

(average standard error=4%) parameters for ϕ_v data of nitrobenzene-TP system at different temperatures.

Table 5.13: Adjustable Parameters of Eq.(9) of PPM for correlating ϕ_V versus x_2 for nitrobenzene-TP systems at different temperatures

T/(K)	$10^6 V_2^0$ / (m^3 mol^{-1})	$10^6 B_{TP}$ / (m^3 mol^{-1})	α	$10^6 W^V_{1,TP}$ / (m^3 mol^{-1})	$10^6 U^V_{1,TP}$ / (m^3 mol^{-1})
293	380	9.034	13	0	0
298	380	9.935	13	0	0
303	380	10.00	13	0	0
308	380	8.019	13	0	0
313	380	10.00	13	0	0
318	390	6.346	13	0	0
323	390	6.082	13	0	0
333	390	9.512	13	9.409	0

343	400	10.00	13	20.00	0
353	410	0.022	13	-5.343	-3.392
363	410	-0.192	13	-5.907	-3.689
365	420	-10.00	13	-30.00	-6.375
367	420	-10.00	13	-30.00	-7.246
371	410	-1.825	13	-9.193	-7.320

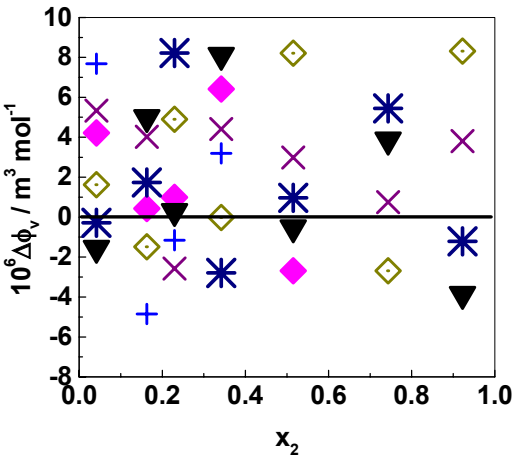

Figure 5.14: $\Delta\phi_v$ values for the nitrobenzene-TP system at different mole fractions of TP and at several temperatures. Differences obtained using PPM. **+** 308, ◆ 323, ▼ 343, ◊ 353, ✳ 365, **X** 371 K.

The values of V_2^0 were handled in two ways. First, V_2^0 was treated as an adjustable parameter and its best value was obtained from the least squares analysis. As discussed earlier, V_2^0 values were also obtained from the linear extrapolation of ϕ_v plots. Then these values were treated as fixed

input parameters and other parameters allowed to vary. It was interesting to observe a good agreement of about 2% between both the methods. Thus V_2^0 was thus treated as a fixed parameter obtained from the experimental ρ data. The same was found true in the case of K_2^0 obtained from speed of sound with an agreement in K_2^0 of about 4%.

A test of successful application of PPM involves a plot of differences, Δ between the experimental and correlated ϕ_v values as a function of x_2 at different temperatures (see: **Figure 5.14**). The differences or deviations are random in nature, thus rendering confidence in the correlating capability of PPM for nitrobenzene-TP system at different temperatures. In general, the ϕ_v values of nitrobenzene-TP systems can be correlated with PPM to within 2% from 293 to 371 K. The densities of above solutions can therefore be correlated to within 0.2% in the above temperature and concentration ranges. One notes in **Figure 5.14** that the PPM correlate the volume data in full composition range with good accuracy.

The ϕ_k data for nitrobenzene -TP system were also analyzed using PPM. The results of regression exercise are summarized in **Table 5.14** whereas K_2^0 was treated an input parameter as described above. B^k_{TP} $W^k_{1,TP}$ and $U^k_{1,TP}$ were the adjustable ones. The errors in $W^k_{1,TP}$ and $U^k_{1,TP}$ were noted to be 3 and 5%, respectively. **Figure 5.15** demonstrates the experimental ϕ_k in contrast to the correlated ones using equation (2) at several temperatures. An examination of the plot shows the fitting power of PPM in analyzing the ϕ_k values in a wider temperature range. Of the particular interest

is to examine the fitting ability of PPM in full composition range of nitrobenzene-TP system.

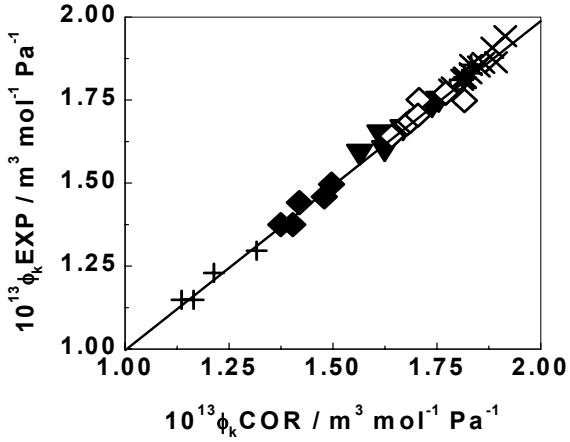

Figure 5.15: Experimental versus correlated ϕ_k values of the nitrobenzene-TP system at different mole fractions and temperatures, for symbols see: **Figure 5.11**

Table 5.14: Adjustable parameters of Eq. (10) for correlating ϕ_k versus x_2 for nitrobenzene-TP systems at different temperatures

T/(K)	$10^{11}\ \phi_K^0$ / ($m^3\ mol^{-1}\ Pa^{-1}$)	$10^{11}\ B_{TP}$ / ($m^3\ mol^{-1}\ Pa^{-1}$)	α	$10^{11}\ W^k_{1,TP}$ / ($m^3\ mol^{-1}\ Pa^{-1}$)	$10^{11}\ U^k_{1,TP}$ / ($m^3\ mol^{-1}\ Pa^{-1}$)
293	1.370	-5.128	13	-10.763	-3.392
298	1.409	-5.286	13	-11.095	-3.496
303	1.465	-5.497	13	-11.536	-3.636
308	1.517	-5.680	13	-11.925	-3.757
313	1.547	-5.782	13	-12.141	-3.834
318	1.594	-5.978	13	-12.539	-3.965

323	1.356	-2.517	13	-5.337	-0.699
333	1.495	-2.796	13	-5.926	-0.778
343	0.045	0.935	13	1.794	0.131
353	0.099	0.930	13	1.764	0.143
363	0.142	0.944	13	1.772	0.156
365	0.180	0.918	13	1.707	0.163
367	0.161	0.967	13	1.810	0.164
371	0.193	0.948	13	1.759	0.171

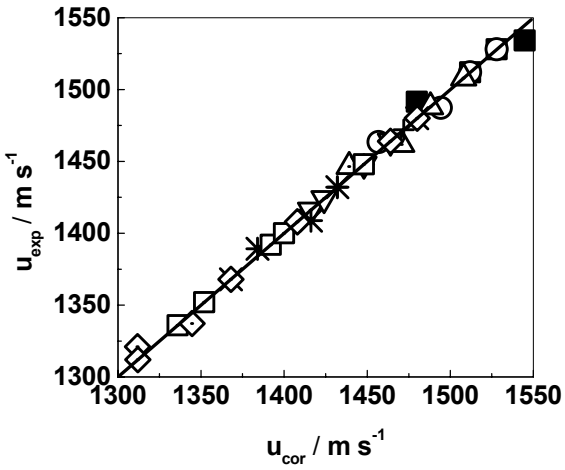

Figure 5.16: Contrast of u_{exp} and u_{cor} as obtained by PPM for the nitrobenzene-TP system at different temperatures. See **Figure 5.4** for symbols

A critical examination of the correlated ϕ_k values shows that PPM can correlate ϕ_k of the nitrobenzene-TP system up to 371 K in the full composition range to within 3%. The speeds of sound for the nitrobenzene system can

therefore be correlated over a wide range of temperature to within 4%. **Figure 5.16** demonstrates the experimental and correlated speeds of sound for the nitrobenzene-TP system at a few representative temperatures. In the fitting of the anisole-TP system, the standard error was estimated to be higher than noted in two earlier systems. For ϕ_v, $W^V_{1,TP}$ and $U^V_{1,TP}$ showed average errors of 5 and 7%, respectively. Similarly, 7 and 9% errors in $W^K_{1,TP}$ and $U^K_{1,TP}$, respectively were noted in the case of fitting of ϕ_K.

5.3.2 1-butanol-TP system

The ϕ_v and ϕ_k data of the above system were fitted to Eqs. (9) and (10) and adjustable parameters obtained with the procedure followed exactly as in the nitrobenzene-TP system. The results are listed in the **Table 5.15** for ϕ_v and in **Table 5.16** for ϕ_k at different temperatures.

Table 5.15: Adjustable Parameters of Eq.(9) for correlating ϕ_V versus x_2 for 1-butanol-TP systems at different temperatures

T(K)	10^6 V_2^0 / (m^3 mol^{-1})	10^6 B_{TP} / (m^3 mol^{-1})	α	10^6 $W^V_{1,TP}$ / (m^3 mol^{-1})	10^6 $U^V_{1,TP}$ / (m^3 mol^{-1})
298	590	2.606	13	0	0
313	600	-0.177	13	0	0
323	600	1.584	13	-7.854	-10
333	620	-9.002	13	-30	-20
343	620	1.934	13	-7.632	-20

353	570	-180	13	-340	-60
363	620	50	13	90	-0.138
368	620	60	13	110	4.659

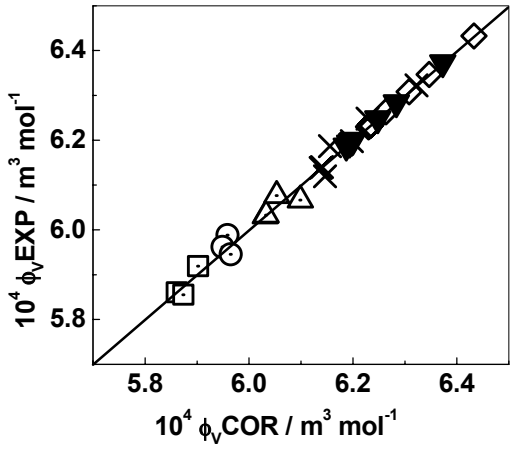

Figure 5.17: Experimental versus correlated ϕ_V values for the 1-butanol-TP system at several temperatures, for symbols see: **Figure 5.9**.

Table 5.16: Adjustable parameters of Eq.(10) for correlating ϕ_k versus x_2 for 1-butanol-TP systems at different temperatures

T/(K)	$10^{13}\,\phi_K^0$ / (m^3 mol^{-1} Pa^{-1})	$10^{13}\,B_{TP}$ / (m^3 mol^{-1} Pa^{-1})	α	$10^{13}\,W^k_{1,TP}$ / (m^3 mol^{-1} Pa^{-1})	$10^{13}\,U^k_{1,TP}$ / (m^3 mol^{-1} Pa^{-1})
298	4.346	-1.368	13	0	0
313	3.310	15.85	13	21.10	0
323	4.710	-31.34	13	-59.33	-21.20
333	1.305	-3.12	13	-3.887	-4.53

343	2.413	-6.74	13	-11.98	-3.68
353	3.074	-9.39	13	-17.76	-3.12
363	4.593	0.53	13	0.802	-0.934
368	0.680	5.48	13	12.49	-0.437

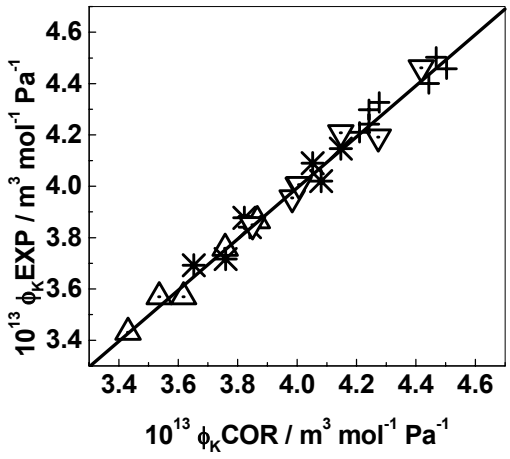

Figure 5.18: Plots of experimental and correlated of ϕ_K values at different temperatures for the 1-butanol-TP systems. For symbols see **Figure 5.12**

Figure 5.17 depicts the experimental and correlated ϕ_v as a function of x_2 at different temperatures. A look at the plots of **Figure 5.17** suggests that ϕ_v of the 1-butanol-TP system can be represented with the help of PPM. Similar plots are shown for verifying the correlation of ϕ_K of the 1-butanol-TP system in **Figure 5.18**. PPM can be seen to correlate both the ϕ_v and ϕ_K values of the 1-butanol- TP system throughout the x_2 range with good accuracy.

The PPM can correlate the ϕ_v values of 1-butanol-TP system throughout the miscibility of system to within 2.5% in the temperature studied. The solution densities in turn can be calculated with an average rmsd of 0.3%.

The adjustable parameters obtained for ϕ_k for this system were used to calculate the ϕ_k values at different mole fractions and temperatures. The ϕ_k of the 1-butanol-TP system can be predicted with 3% on an average. However, as high as 7% deviation were also witnessed at high temperatures. The sound speeds of the system can therefore be correlated to within 3% on an average basis up to 368 K.

5.3.3 Anisole-TP system

The density and speed of sound data for the anisole-TP system were subjected to Eqs. (9) and (10). The adjustable parameters for ϕ_v from Eq. (9) and for ϕ_k from Eq. (10) are listed in **Tables 5.17** and **5.18**, respectively.

Table 5.17: Adjustable Parameters of Eq.(9) for correlating ϕ_v versus x_2 for anisole-TP systems at different temperatures

T/K	$10^6 V_2^0$ / (m^3 mol^{-1})	$10^6 B_{TP}$ / (m^3 mol^{-1})	α	$10^6 W^V_{1,TP}$ / (m^3 mol^{-1})	$10^6 U^V_{1,TP}$ / (m^3 mol^{-1})
298	440	-20	13	0	0
303	440	-30	13	0	0
308	460	-10	13	0	0
313	440	80	13	160	0
318	440	80	13	170	0

323	440	90	13	170	0
333	450	80	13	160	0
343	450	90	13	170	0
353	470	20	13	40	-10
363	470	20	13	30	-10

Table 5.18: Adjustable Parameters of Eq.(10) for correlating ϕ_k versus x_2 for anisole-TP systems at different temperatures

T/ (K)	$10^{13}\ \phi_K^0$ / ($m^3\ mol^{-1}\ Pa^{-1}$)	$10^{13}\ B_{TP}$ / ($m^3\ mol^{-1}\ Pa^{-1}$)	α	$10^{13}\ W^k_{1,TP}$ / ($m^3\ mol^{-1}\ Pa^{-1}$)	$10^{13}\ U^k_{1,TP}$ / ($m^3\ mol^{-1}\ Pa^{-1}$)
313	1.438	-3.557	13	-5.254	0.0
318	1.500	-4.033	13	-6.069	0.0
333	1.268	-2.379	13	-3.342	0.0
343	1.528	-2.730	13	-52.44	-2.134
353	1.572	-2.517	13	0.304	0.0262
363	1.616	0.824	13	0.824	1.374

The agreement is shown in **Figure 5.19** where experimental ϕ_v are plotted against the correlated ones at different temperatures. The difference between the experimental and correlated ϕ_K values ($\Delta\ \phi_K$) for the anisole-TP system is demonstrated in **Figure 5.20** at several temperatures.

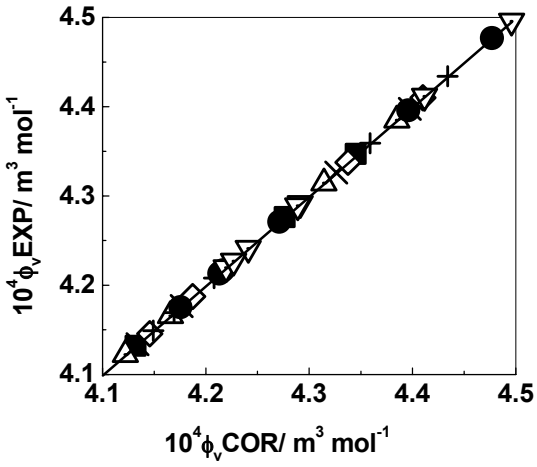

Figure 5.19: Plot of experimental versus correlated ϕ_v for the anisole-TP system at different mole fractions and temperatures. For symbols see: **Figure 5.10**

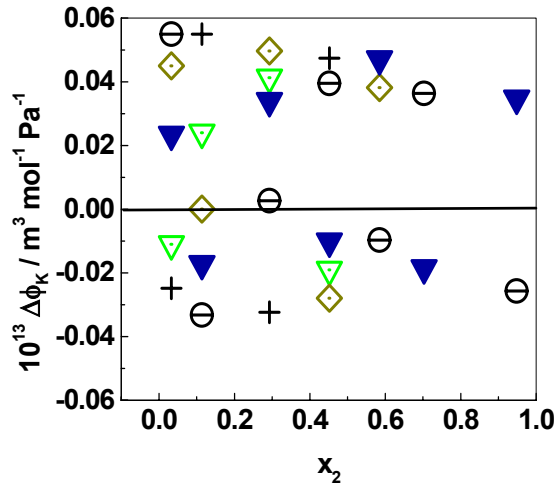

Figure 5.20: $\Delta\varphi_K$ (difference between experimental and correlated φ_K values) for the anisole-TP system at different temperatures. For symbols see: **Figure 5.13**

In summary, both the volume and compressibility of the fused salt solutions in the solvents of varying relative permittivities can be successfully correlated by PPM from fused salt to dilute solutions.

5.3.4 The Limiting Slopes for volume and compressibility

The limiting slopes, A_v and A_x for volumes and compressibilities were observed to be a function of temperature. **Table 5.19** enlists the required parameters used to compute A_v and A_x parameters.

Table 5.19: The fitting parameters of A_v and A_k in the temperature ranging up to 373 K; Equation: $A = a^0 + a_1 T + a_2 T^2$

Parameter	a^0	a_1	a_2
		Nitrobenzene	
A_v	7.88×10^{-5}	-8.069×10^{-8}	-3.756×10^{-10}
A_k	4.621×10^{-9}	-3.220×10^{-11}	5.397×10^{-14}
		1-butanol	
A_v	6.14×10^{-3}	-3.85×10^{-5}	6.046×10^{-8}
A_k	1.42×10^{-10}	-9.174×10^{-13}	1.471×10^{-15}
		Anisole	
A_v	-27.81×10^{-3}	17.024×10^{-5}	-25.975×10^{-8}
A_k	2.671×10^{-10}	-1.608×10^{-12}	2.407×10^{-15}

5.3.5 Temperature dependence of the W parameter of PPM:

In order to expand the role of PPM to elevated temperatures, $W_{1,TP}$ for volume and compressibility were fitted against temperature. **Figure 5.21**

shows the variation of $W_{1,TP}$ for volume with temperature. Though a quadratic equation was suffice to explain the curvature, the trend could not be improved in spite using global fitting program. On the other hand, temperature dependence of $W_{1,TP}$ for compressibility is reasonably simple as shown in **Figure 5.22**. Both these plots belong to the nitrobenzene-TP system. The worse situation was however noted in 1-butanol-TP and anisole – TP systems.

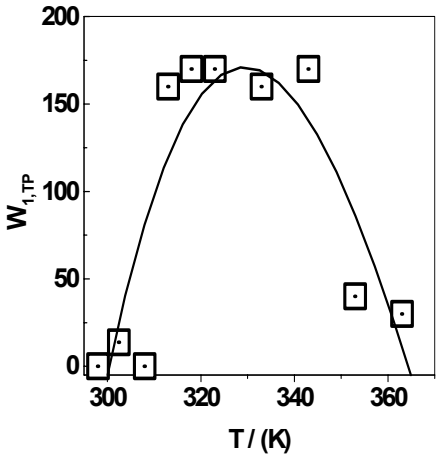

Figure 5.21: Temperature dependence of $W_{1,TP}$ for volumes of the nitrobenzene-TP system.

From the above fitting program used for the analysis of our data, it is strongly believed that though PPM is proven to be effective in dealing with the thermodynamics of aqueous NaOH up to high temperatures and pressures, we are not certain of its success in the case of organic fused salt when dissolved in organic solvents preferably of low relative permittivity.

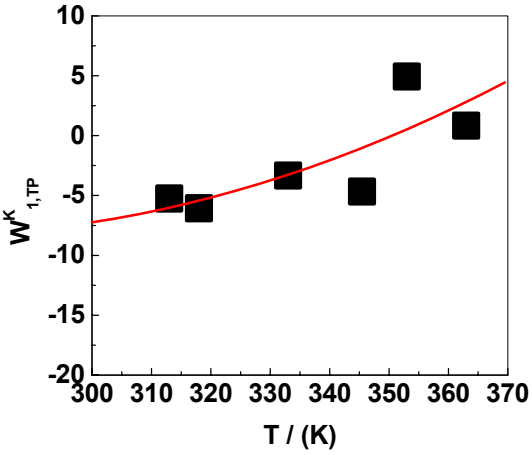

Figure 5.22: Temperature dependence of $W^{K}_{1,TP}$ for compressibility of the nitrobenzene-TP system.

5.4: Thermal Expansion of the systems:

The temperature dependence of density can be used to obtain the thermal expansion coefficients as:

$$\alpha = - 1 / \rho \, (\partial \rho / \partial T) \qquad (14)$$

The thermal expansion coefficients of these systems are listed in **Tables 5.20, 5.21** and **5.22** for nitrobenzene-, 1-butanol and anisole-TP systems, respectively. In **Figure 5.23** are shown the variation in α at 363 K in the full composition range of the nitrobenzene-, 1-butanol- and anisole-TP systems.

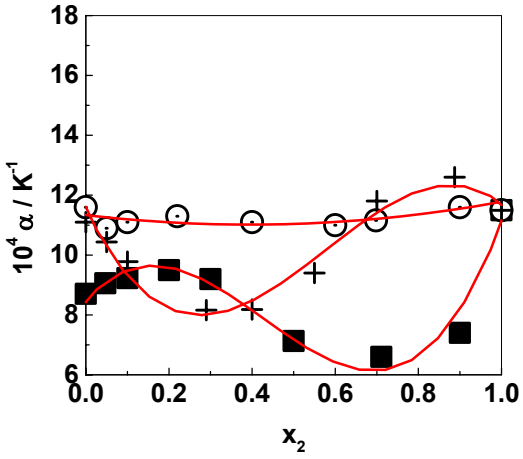

Figure 5.23: Dependence of α on mole fraction in full composition range for nitrobenzene-, 1-butanol- and anisole-TP system at 363 K. ■ nitrobenzene, **O** 1-butanol and **+** anisole

Addition of TP in nitrobenzene decreases the α values after x_2 = 0.3, which further enhances towards the pure TP molten phase. This effect and the effect noted in the case of 1-butanol are also seen in the density data measured at different temperatures. Again, the anisole-TP system shows anomalous behavior. No appreciable change in α is seen throughout the composition. TP was noted to have α as 10.21 x 10^{-4} K^{-1} at its m.p.

Our efforts to correlate apparent molar expansibility from α by PPM failed due to large errors incurred in the calculation of temperature dependence of density data. We therefore obviated such a fitting from the present work.

Table 5.20: Thermal expansion coefficient,α of the nitrobenzene-TP system at various mole fractions and temperatures

	$10^4\,\alpha$ / (K^{-1})							
$x_2 \rightarrow$	0	0.047	0.101	0.202	0.303	0.499	0.711	0.903
T/(K) $\downarrow$								
293	8.206	8.524	8.669	8.898	8.658			
298	8.239	8.557	8.701	8.932	8.694			
303	8.272	8.593	8.741	8.977	8.744			
308	8.307	8.633	8.781	9.017	8.772			
313	8.342	8.663	8.809	9.042	8.803			
318	8.377	8.709	8.861	9.101	8.851			
323	8.412	8.743	8.895	9.128	8.869	11.00		
333	8.485	8.825	8.984	9.226	8.968	10.07		
343	8.556	8.902	9.073	9.325	9.066	9.119	9.591	9.183
353	8.630	8.983	9.152	9.408	9.148	8.140	8.132	8.423
363	8.705	9.059	9.228	9.482	9.211	7.128	6.625	7.636
365	8.720	9.078	9.241	9.498	9.228	6.925	6.324	7.479
367	8.736	9.094	9.258	9.515	9.244	6.720	6.020	7.320
371	8.766	9.126	9.290	9.544	9.276	6.307	5.409	7.000

Table 5.21: Thermal expansion coefficient, α of 1-butanol-TP system at different mole fractions and temperatures

$10^4 \alpha$ / (K^{-1})

$x_2 \rightarrow$	0	0.052	0.096	0.22	0.406	0.605	0.703	0.897
T/ (K) ↓								
323	8.809	10.47	10.68	10.80	10.64	10.64	5.259	2.223
333	9.486	10.57	10.79	10.90	10.74	10.72	7.256	4.504
343	10.17	10.68	10.90	11.02	10.85	10.82	9.297	6.826
353	10.92	10.79	11.02	11.14	10.97	10.94	11.39	9.187
363	11.63	10.92	11.15	11.27	11.10	11.08	13.56	11.61
365	11.81	10.94	11.17	11.30	11.12	11.11	14.00	12.11
367	11.96	10.97	11.20	11.33	11.15	11.14	14.45	12.61
371	12.27	11.02	11.26	11.38	11.21	11.20	15.36	13.62

Table 5.22 : Thermal expansion coefficient, α of the anisole-TP system at various mole fractions and temperatures

$10^4 \alpha$ / (K^{-1})

$x_2 \rightarrow$	0	0.05	0.1	0.288	0.4	0.548	0.702	0.907
T /(K) ↓								
298	13.87	13.1392	12.48	10.21	9.309	8.489	8.026	9.429
303	13.68	12.9564	12.30	10.07	9.230	8.557	8.292	9.950
308	13.49	12.7694	12.11	9.928	9.149	8.625	8.561	10.47
313	13.30	12.5782	11.91	9.779	9.067	8.694	8.834	11.01

318	13.10	12.3829	11.72	9.628	8.984	8.764	9.111	11.56
323	12.90	12.1834	11.52	9.474	8.900	8.835	9.391	12.11
333	12.49	11.7721	11.10	9.159	8.727	8.979	9.962	13.25
343	12.05	11.3444	10.67	8.834	8.549	9.126	10.55	14.44
353	11.60	10.9003	10.23	8.500	8.366	9.276	11.15	15.67
363	11.13	10.4401	9.776	8.157	8.178	9.430	11.78	16.96

Literature cited:

1. Marignac, C., *Ann. Chim (Paris)*, **1871**, 22, 415.
2. Favre., P. A.; Valson, C. A., *C. R. Acad. Sci*., **1872**, 75, 1000.
3. Arrhenius, S. *Z. Phys. Chem*. **1887**,1.631.
4. Ostwald , W., *J Prakt. Chem*., **1878**, 18, 328. Also see: " *Lehrbuch der alleimeinen Chemie." 2nd Ed*., 1890.; section on solutions translated in English in 1891.
5. Tammann, G., *Z. Phys. Chem*., **1893**, 11, 676.
6. Tammann, G., *Z. Phys. Chem*., **1895**, 16, 91, 139.
7. Drude, P.; Nernst, W., *Z. Phys. Chem*., **1894**, 15, 79.
8. Baxter, G. P. "Changes in Volume upon Solution in Water of the Halogen Salts of the Alkalis." *J. Am. Chem. Soc*., **1911**, 33, 922.; Also see (a) Baxter, G. P. *ibid*, **1918**, 40, 192.; (b) Baxter G. P.; Wallace, C. C., *ibid*., **1916**, 38, 70.
9. Fajans, K., *Z. Phys. Chem. (Leipzig)*, **1934**, 34, 125.; ibid., **1935**, 29, 153.
10. Born, M. "Volumes and Heat of Hydration of Ions" *Z. Phys*., **1920**, 1, 45.
11. Webb, T. J. "The Free Energy of Hydration of Ions and the Electrostriction of the Solvent." *J. Am. Chem. Soc*., **1926**, 48, 2589.
12. Masson. D. O. "Solute Molecular Volumes in Relation to Solvation and Ionization." *Phil. Mag*., **1929**, 8, 218.
13. Scott, A. F. "The Apparent Volumes of Salts in Solutions. I. A Test of the Empirical Rule of Masson." *J. Phys. Chem*., **1931**, 35, 2315.; II. The Problem of their Interpretation. *J. Phys. Chem*. **1931**, 35, 3379.

14. Geffcken, W. “The Apparent Molecular Volume of Dissolved Electrolytes. I.” *Z. Phys. Chem., Abt. A*, **1931**, 155, 1.
15. Redlich, O.; Rosenfeld, P. “The Theory of the Molal Volume of a Dissolved Electrolyte.” *Z. Elektrochem.*, **1931**, 37, 705.
16. Redlich, O.; Rosenfeld, P. “The Partial Molar Volume of Dissolved Electrolyte*.” Z. Phys. Chem., Abt. A*. **1931**, 155, 65.
17. Redlich, O.; Meyer, D. M. “The Molal Volumes of Electrolytes.” *Chem. Rev.*, **1964**, 64, 221.
18. Redlich, O. “Molal Volumes of Solutes. IV.” *J. Phys. Chem.*, **1940**, 44, 619.
19. Frank, F.; Smith, H. T. “Apparent Molal Volumes and Expansibilities of Electrolytes in Dilute Aqueous Solution.” *Trans. Faraday Soc.*, **1967**, 63, 2586.
20. Hepler, L. G.; Stokes, J. M.; Stokes, R. H. “Dilatometric Measurements of Apparent Molar Volumes of Dilute Aqueous Solution.” *Trans. Faraday Soc.*, **1965**, 61, 20.
21. Wirth H. E. “Equilibria in Solutions of Tetraalkylammonium bromides*.” J. Phys. Chem.*, **1967**, 71, 2922.
22. Frank, F.; Smith, H. T. “The Association and Hydration of Sodium Dodecyl Sulphate in the Submicellar Concentration Range.” *J. Phys. Chem.*, **1964**, 68, 3581.
23. Conway, B. E.; Verall, R. E.; Desnoyers, J. E. “Partial Molal Volumes of Tetraalkylammonium Halide and Assignment of Individual Ionic Contributions.” *Trans. Faraday Soc.*, **1966**, 62, 2738.

24. Desnoyers, J. E.; Arel, M. “Apparent Molal Volumes of n-Alkylamine Hydrobromides in Water at 25^0 C.” *Can. J. Chem.*, **1967**, 45, 359.
25. Conway, B. E.; Verall, R. E. “Ion-Solvent Size Ratio as a Factor in the Thermodynamics of Electrolytes.” *J. Phys. Chem.*, **1966**, 70, 1473.
26. Conway, B. E.; Verall, R. E. “Partial Molar Volumes and Adiabatic Compressibilities of Tetraalkyammonium and Aminium Salts in Water. I. Compressibility Behavior." J. Phys. Chem., **1966**, 70, 3952.
27. Wen, W. Y.; Saito, S. “Apparent and Partial Molal Volumes of Five Symmetrical Tetraalkylammonium Bromides in Aqueous Solutions” *J. Phys. Chem.*, **1964**, 68, 2639.
28. Wen, W. Y.; Saito, S. “Activity Coefficients and Molal Volumes of Two Tetraethanolammonium Halides in Aqueous Solutions at 25^0.” *J. Phys. Chem.*, **1965**, 69, 3569.
29. Millero, F. J. “Apparent Molal Volumes of Aqueous Sodium Tetraphenyl boron Solutions from 0^0 to 60^0 C.” *J. Chem. Eng. Data*. **1970**, 15, 562.
30. Millero, F. J., “Apparent Molal Volumes of Aqueous Tetraphenyl Arsonium Chloride Solutions at 0^0, 25^0, and 50^0 C.” *J. Chem. Eng. Data*. **1971**, 16, 229.
31. Bien, G. S.; Kraus, C. A.; Fuoss, R. M. “Properties of Electrolytic Solutions. X11. The Influence of Temperature on the Conductance of Electrolytes in Anisole.” *J. Am. Chem. Soc*. **1934**, 56, 1860.

32. Seward, R. P. “Electrical Conductance and Viscosity in the System Tetra-n-butylammonium Picrate- n-Butyl Alcohol at 91^{0}C.” *J. Am. Chem. Soc*. **1951**, 73, 515.
33. Seward, R. P. “The Electrical Conductance and Viscosity of Solutions of Tetra-n-butylammonium Picrate in Anisole, Nitrobenzene and Ethylene Carbonate.” *J. Phys. Chem*. **1958**, 62, 758.
34. Kumar, A. “Surface Tension, Viscosity, Vapor Pressure, Density, and Sound Velocity for a System Miscible Continuously from a Pure Fused Electrolyte to a Nonaqueous Liquid With a Low Dielectric Constant: Anisole with Tetra-n-butylammonium Picrate.” *J Am. Chem. Soc*. **1993**, 115, 9243.
35. Yao, N. P.; Bennion, D. N. “Transport Behavior in Dimethyl Sulfoxide. 111. Conductance-Viscosity Behavior of Tetra-n-amylammonium Thiocyanate from Infinite Dilution to molten Salt at 55^{0}C.” *J. Phys. Chem.* **1971**, 75, 3586.
36. Davies, C. W.; “*Ion Association*”. Chapter 10, **1962**, Butterworths, London.
37. Pitzer, K S.; Simonson, J. M. “Ion-Pairing in a System Continuously Miscible from the Fused Salt to Dilute Solution” *J. Am. Chem. Soc*. **1984**, 106, 1973.
38. Rahman, N.; Dass, N. N.; Mahiuddin, S. “Isentropic Compressibility of Aqueous and Methanolic Sodium Thiocyanate Solutions.” *J. Chem. Eng. Data*., **1999**, 44, 465.

39. Rahman, N.; Mahiuddin, S.; Dass, N. N. “Speed of Sound in Aqueous and Methanolic Lithium Nitrate Solutions.” *J. Chem. Eng. Data*., **1999**, 44, 473.

40. Rahman, N.; Mahiuddin, S. “Concentration and Temperature Dependence of Ultrasonic Velocity and Isentropic Compressibility in Aqueous Sodium Nitrate and Sodium Thiosulphate Solutions.” *J. Chem. Soc. Faraday Trans*. **1997**, 93, 2053.

41. Petrenko, S. V.; Pitzer, K. S., “Thermodynamics of Aqueous NaOH over the Complete Composition range and to 523 K and 400 M Pa.” J. Phys. Chem. B., 1997, 101, 3589.

42. for summary on this topic, Wen, W-Y. “Aqueous Solutions of Symmetrical Tetraalkylammonium Salts” Chapter 15, in *Water and Aquous Solutions,* Horne, R. A. Editor, Wiley-Interscience, New York, 1972.

6. Conclusions

In the above dissertation, the following objectives have been achieved:

1. Vapor pressure and volumetric properties of fused salt - organic solvent have been measured.
2. Though vapor pressure data of the nitrobenzene-TP systems showing positive deviation from Raoult's law have been analyzed by the Pitzer-Simonson model, new set of equations have been developed to effectively analyze the strong negative and positive deviation from the Raoult's law for a variety of systems.
3. For the first time, simple working equations have been proposed to correlate the surface-tension data of the fused salt solutions. The non-ideality arising out of mixing of two components in a single liquid phase has been accurately described.
4. The measured volumetric properties presented in this dissertation of TP containing salts have been analyzed by the mole fraction based equation of Petrenko and Pitzer.

In summary, the quantitative information on the experimental vapor pressure and volumetric properties has been the main focus of this dissertation.

As the planned work was highly focused, it has not been possible to examine anomalous viscosity behavior of fused organic salt on addition of a solvent. Similarly, conductance and surface tension data could not be parts of this dissertation.

List of Publications:

Sr. No.	Authors	Title	Journal
1.	**Pramod D. Sonawane** and Anil Kumar.	Vapor Pressures of Nitrobenzene + Tetrabutylammonium Picrate at 373 K.	*J. Chem. Eng. Data* **1998**, 43, 97-100
2.	**Pramod D. Sonawane** and Anil Kumar.	A New Equation for the Correlation of Surface Tension-Composition data of Solvent-Solvent and Solvent-Fused Salt Mixtures.	*Fluid Phase Equilibria.* **1999**, 157, 17-28.
3.	**Pramod D. Sonawane**, Somnath Nandi, Sanjeev S. Tambe, Anil Kumar, and Bhaskar D. Kulkarni.	Solvent Activity Prediction of Electrolyte Solutions Using Neural Networks.	Proceedings of the 54th Annual Session of Indian Institute of Chemical Engineers. Chemcon **2001** Chemie.
4.	**Pramod D. Sonawane** and Anil Kumar	The Solvent Activity-Composition Correlation for Systems Continuously Miscible from Molten Salt to Dilute Solution	*Indian J. Chem.* **2002**, 41 A, 1112-1119.

NOTE: **3 more papers** on the volumetric properties are being written at the time of submission of this thesis.